STUDIES OF MOLECULAR INTERACTIONS BY VIBRATIONAL SPECTROSCOPY

A Thesis submitted to the
University of Southampton
for the degree of

Doctor of Philosophy

by

Alan James Woodward, B.Sc. (Hons.), M.Phil.

Department of Chemistry,
The University,
Southampton.

October, 1970.

A C K N O W L E D G E M E N T S

The investigations described in this thesis were carried out between October 1968 and October 1970 under the supervision of Dr. N.B.H. Jonathan. I wish to express my sincere thanks to him for his constant interest and encouragement throughout the work.

Gratitude is also extended to Dr. D.E. Rogers for his help with the normal coordinate analysis calculations and to Mr. J. Hawkins for building the i.r./adsorption cell.

The award of a Research Studentship by the Science Research Council is gratefully acknowledged.

The research has been sponsored in part by the Air Force Cambridge Research Laboratories through the European Office of Aerospace Research (OAR), United States Air Force, under contract AF61(052)-69-C-0032.

ABSTRACT

FACULTY OF SCIENCE

CHEMISTRY

Doctor of Philosophy

STUDIES OF MOLECULAR INTERACTIONS BY VIBRATIONAL SPECTROSCOPY

by Alan James Woodward

Vibrational spectroscopy has been used to study two phenomena arising from molecular interactions.

Firstly, rotational isomerism: Infrared and Raman spectra are reported for the acid chloride derivatives of difluoroacetic acid and dibromoacetic acid. Data are given for vapour liquid and solid state spectra. It is concluded that two molecular forms exist in the vapour and liquid phases of the acid chlorides and that the more polar form is present in excess in the solid state. The nature of these stable conformations is discussed with the help of a) a vibrational analysis based on a Urey-Bradley potential function, and b) calculations of the conformational potential energy as a function of the internal rotation angle. It is concluded that in the less polar forms the oxygen atom is approximately in the cis position with respect to the hydrogen atom. The more polar forms are obtained from these forms by an internal rotation about the C-C axis of between 90 and 135°.

Secondly, molecular adsorption: An apparatus is described for infrared spectroscopic studies of gas adsorption on evaporated alkali halide films. Spectra are reported for NO adsorbed on films of NaCl, NaBr, NaI, KCl and CsCl. Sharp absorptions are observed whose relative intensities are strongly dependent on coverage. They are assigned to different adsorption sites and orientations of the NO molecules on the surface. The spectra provide conclusive evidence that dimerisation accompanies adsorption on certain surface sites. This contradicts an earlier interpretation of adsorption isotherms and heats determined for these systems.

C O N T E N T S

Page

PART 2. Infrared Spectra of NO Adsorbed on Alkali Halide Films

PART 1

A SPECTROSCOPIC STUDY OF ROTATIONAL ISOMERISM IN DIHALOACETYL CHLORIDES

1.1 INTRODUCTION

The phenomenon of rotational isomerism arises from the hindered rotation of one part of a molecule with respect to another about a single chemical bond. The forces hindering the internal rotation are dipole-dipole, dipole-induced dipole, dispersion and repulsion interactions occurring between the non-bonded atoms and bonding electrons of the molecule. These interactions vary continuously during the rotation so that, although there is an infinite number of conformations which the molecule may assume during one complete internal rotation, these conformations do not have the same potential energy. The probability of the molecule assuming a particular conformation A at any given time is determined by the exponential term of the Maxwell-Boltzmann distribution law, viz. $\exp.(-E_A/kT)$ where

E_A = the energy difference between conformation A and the most stable conformation

k = the Boltzmann constant

T = the absolute temperature.

The conformations of minimum potential energy are therefore favoured. If one of these relatively stable conformations, or rotational isomers as they are called, is to convert by means of an internal rotation into another stable conformation the molecule must pass through conformations of higher energy, i.e. there is a barrier to internal rotation. The magnitude of this rotational barrier will govern the rate of inter-conversion (isomerisation) of the isomers. If the barrier is very small

compared with the available thermal energy kT then rotation will be almost completely free and isomerisation will be very fast. Molecules with larger rotational barriers will show slower rates of isomerisation, and in the extreme case when the barrier is greater than kT the rate is so slow that geometrical isomers may be separated.

The two main applications of rotational isomerism are to conformational analysis in organic stereochemistry and to theories concerning the structures of macromolecules. Several physical techniques have been used to study the phenomenon, the earliest of these being the determination of entropy and specific heat values and the measurement of electric dipole moments. The development of X-ray and electron diffraction techniques, nuclear magnetic resonance and, of particular interest in view of the present work, infrared and Raman spectrometers has considerably widened the scope of such studies.

The limiting value of the rates of isomerisation in fast conformational equilibria is ca. $10^{11} - 10^{12}$ sec^{-1}. The time constant for the interaction of electromagnetic radiation with the molecular dipole, which gives rise to the absorption of infrared radiation is ca. $10^{-13} sec^{-1}$. The lifetime of each rotational isomer is therefore sufficient to allow its detection by infrared absorption spectroscopy. Provided the concentration of the isomer in the conformational equilibria is a few per cent of the total[1] it should be possible to determine its vibrational frequencies.

The techniques for assigning each observed vibrational frequency to its parent rotational isomer are well established. Infrared and

Raman spectra are recorded for the compound in the vapour, liquid and solid states. Solid samples are produced by cooling either the vapour or the liquid of the compound, and if this cooling is not too rapid then, theoretically (provided the energy difference between the isomers is not zero) complete conversion of the sample to the more stable isomer will occur. A comparison of the spectrum of this one-isomer solid with that of the liquid or vapour, and a process of elimination then gives the vibrational frequencies of each isomer. These assignments may be supported by data from solution spectra. Assuming that the rotational isomers have significantly differing dipole moments, the more polar isomer will be stabilised with respect to the less polar isomer with increasing solvent polarity. This effect will be manifest in an increase in intensity of spectral bands due to the more polar isomer at the expense of those of the less polar isomer. Additionally, for some cases, e.g. 1,2-dichloroethane, symmetry considerations enable a determination of the nature of the stable conformations from the infrared and Raman activity of their vibrational frequencies.

An analysis of the above type is fairly straightforward for small molecules. However, for a macromolecule where there is more than one bond about which internal rotation can occur, and each of the possible conformations of the molecule is executing 3N-6 normal modes of vibration, the vibrational spectra are extremely complex and prevent analysis.

One of the first applications of i.r. and Raman spectroscopy to the study of rotational isomerism was in fact an investigation of

isomerism in structural units of a polypeptide chain.[2] From an understanding of these repeating units the structure of the complete molecule was proposed. Since then, many papers have reported vibrational spectra of rotational isomers and the investigations have tended to become an academic exercise.

In 1958, Mizushima et al.[3] reported a spectroscopic study of dichloroacetyl chloride and concluded that two molecular forms coexist in the vapour and liquid phases of the compound. With the angle of internal rotation (azimuthal angle) θ defined as indicated in Fig.1.1 (i.e. θ is taken to be zero when the carbon-hydrogen and carbon-oxygen bonds are eclipsed), the results of a normal coordinate analysis of $CHCl_2COCl$ indicated that the less polar of these isomers is the conformation $\theta = 0^\circ$, and for the more polar isomer $\theta \approx 90^\circ$. It was stated that an electron diffraction analysis of gaseous dichloroacetyl chloride could also be explained in terms of conformations having azimuthal angles of 0° and 90°. Following this work, it was considered of interest to study the two series of compounds involving $CHCl_2COCl$, i.e. the dichloroacetyl halide series and the dihaloacetyl chloride series, to see if the data for these compounds could be explained in a similar manner. Infrared and Raman spectra have been recorded for each compound, and normal coordinate analyses and calculations of the potential energy of each molecule as a function of θ have been made to assist the interpretation of data. The results for the dichloroacetyl halide series have been given elsewhere.[4] It was

concluded that the acid fluoride, chloride and bromide all exhibit rotational isomerism. The less polar isomers of $CHCl_2COCl$ and $CHCl_2COBr$ were found to be the conformations $\theta = 0^\circ$. While for the more polar isomers θ was considered to be in the range $90^\circ - 135^\circ$. The data for $CHCl_2COF$ could only be explained in terms of a less polar conformation $\theta \approx 90^\circ$ and a more polar conformation $\theta \approx 180^\circ$. This was found to be somewhat surprising, and the need for a further investigation of this compound using a different technique was emphasised.

Data are now given for difluoroacetyl chloride and dibromoacetyl chloride, and in order that the final discussion of the experimental data may proceed in a logical manner it has been considered necessary to describe the theoretical aspects of the work first.

The definition of the azimuthal angle θ given in Fig.1.1 will be assumed throughout the subsequent discussion.

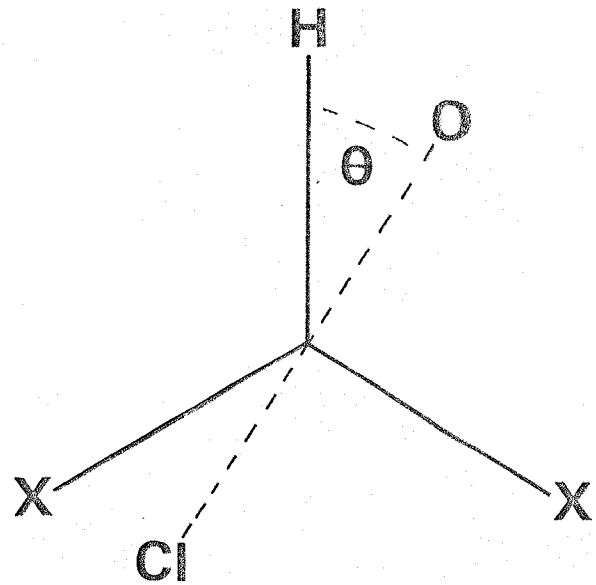

FIG. 1·1 Definition of the Azimuthal Angle θ

1.2 THE CONFORMATIONAL POTENTIAL ENERGY CALCULATIONS

1.2.1 Introduction

Ideally a theoretical analysis of the energy and geometry of a molecule should rely on quantum-mechanics and would be accomplished by solving the appropriate Schrödinger equation for the desired molecular system. Such calculations are, however, extremely complex and, although progress has been made in this field in recent years, alternative approaches have, to date, proved more satisfactory. In particular, the following have been employed: a) simplified quantum-mechanical treatments; b) calculations of an empirical nature based on a model obeying classical mechanics; and c) combinations of these two approaches. The calculations to be described here fall into the second of these categories, and it is perhaps worthwhile to discuss briefly the basis of these semi-empirical treatments. For this purpose, it is useful to consider the inexact concept of "strain". "Strain-free" molecules have structures and energies taken to be "normal"; compounds whose geometries differ significantly from these values are observed to have higher energies and are said to be "strained". If the geometry of a molecule is defined by four types of structural parameters bond lengths r, bond angles α, torsional angles θ, and non-bonded distances q, the "strain energy" in a strained molecule, i.e. its energy excess over that of a normal molecule, may be thought of as the sum of four components:

$$S.E. = E_r(r) + E_\alpha(\alpha) + E_\theta(\theta) + E_{nb}(q) \quad . \ . \ . \quad (1.1)$$

The actual geometry of the molecule will be that for which this strain energy is a minimum (though this does not necessarily imply maximum stabilisation with respect to any one given parameter). The equation has an obvious appeal to the non-theoretical chemist who always seems to demand the additivity of terms having physical significance. Consequently, most empirical calculations of conformational potential energies have used Equation (1.1) as a starting point. The equation does, however, have serious deficiencies. For example, the partitioning of energy on which it is based is obviously a crude idealisation of the actual situation in a molecule, since the internal coordinates r, α, θ and q are not independent. Furthermore, the equation requires a set of "normal" or "strain-free" structural parameters from which magnitudes of deformations are measured. Several such sets have appeared in the literature, but since, in the strict sense, no molecule is really strain-free, the choice of model and parameters is arbitrary.

Assuming that a suitable set of potential energy functions and parameters can be obtained, the terms in Equation (1.1) may be evaluated to give the strain energy in the assumed structure. Minimisation of this energy with respect to molecular geometry will then give the geometry and relative energy (relative to that of the "normal" molecule) of the most stable conformation of the molecule. In the case of the dihaloacetyl chlorides where there is only one torsional degree of freedom θ it would be necessary to increase θ step-wise and minimise the strain energy with respect to the other three sets of parameters for each value of θ in order to build up the required

curve of the potential energy as a function of the rotation angle. Several highly complex mathematical procedures have been programmed for these minimisation processes, but the problem is still immense. One requires to find the point of lowest energy on a surface generated in a many-dimensional space though local minima, valleys and saddle points are also likely to be present. Hence great care must be taken to ensure that the computer will lock into the correct molecular configuration.

Several workers have simplified the above problem by neglecting some of the terms in Equation (1.1), e.g. by requiring constant bond lengths[5] and angles[6] in systems where such constraints could be assumed to have but little effect on energy differences. The assumption of constant bond lengths is perhaps justified in systems where the strain energy is small. The results of vibrational analyses indicate that the force constant for an angle bend is considerably smaller than that for a bond stretching mode; therefore, relief of strain in a molecule will primarily involve bond angle deformations. In 1965 R.A. Scott and H.A. Scheraga published data obtained from a potential function which assumed both bond lengths and bond angles to be held fixed[7] i.e. the equation used took the form

$$S.E. = E_{\theta}(\theta) + E_{nb}(q) \qquad (1.2)$$

This approach proved amazingly successful in predicting the internal rotation barriers in substituted ethanes, though not surprisingly it

tended to break down for molecules with a very high degree of substitution. The more general treatment outlined above should obviously be used in these cases, provided one can be certain of finding a correct energy minimum. Despite this limitation of the Scott/Scheraga model, its application to the dichloroacetyl halide series proved extremely helpful when discussing the nature of the stable conformations of the molecules.[4] Calculations have now been made to assist the analysis of the dihaloacetyl chlorides.

1.2.2 The Scott/Scheraga Potential Function

Any semi-empirical calculation of an internal rotation barrier must include a term arising from non-bonded interactions in the molecule. Calculations for ethane indicate that non-bonded H • • • H repulsions contribute ca. 50% to the barrier.[8] Valence bond calculations and potential functions based on intermolecular interactions show a contribution of 15% or less. Scott and Scheraga therefore conclude that "a calculation of the barrier must include a contribution of at least 50%, and probably more, from a source other than non-bonded interactions". The origin of this other source has been the subject of some controversy though traditionally it has been accounted for by including a torsional strain term of the form $E_\theta(\theta) = \frac{1}{2} U_0 (1 + \cos 3\theta)$ where U_0 is the barrier height in the absence of non-bonded interactions. Scott and Scheraga use such a term and, following the theory proposed by Pauling[9] attribute its origin to exchange interactions of the electrons in bonds adjacent to

the bond about which internal rotation occurs (e.g. the CH bonds in ethane).

Simple quantum-mechanical treatments of the ethane problem, based only on s and p electrons, predict a barrier which is too low and has no contribution from exchange interactions. Pauling therefore introduced an additional 4% d and 2% f character into the carbon bond orbitals. This results in a greater concentration of the bond orbitals in the bond direction and an increase in bond strength of 38%. Additionally, it produces an estimated barrier height of 3kcal/mole and predicts greatest stability for the staggered conformation. This is in agreement with experimental data. A more interesting result of the theory is that, for molecules having orbitals of similar hybrid character, the barrier height should be a constant fraction of the bond energy, excluding non-bonded interactions due to bulky substituent groups. This again is found to be true experimentally, since most of the substituted ethanes have barriers of the order of 3kcal/mole, and the barriers are lower for molecules containing the weaker carbon-silicon, carbon-germanium and silicon-silicon bonds. As orbitals containing unshared electron pairs do not have the d and f character, they do not contribute to the barrier; the theory therefore predicts that the barrier in CH_3NH_2 should be two-thirds that in ethane and the barrier in CH_3OH should be one-third that in ethane. This again has been found to be true. To explain rotation about single bonds next to double bonds Pauling considers bonds such

as C=C and C=O as two bent single tetrahedral bonds. This allows consideration of molecules such as CH_3CHO, or in this case CHX_2COCl, in analogy with the ethanes. The potential function would be three-fold and the minima would occur in the staggered conformation, i.e. the bent bonds and CH bond of the CHO group would be staggered with respect to the CH bonds of the methyl group. Because the bent bonds are distorted to some extent the barrier height should be lower. Molecules such as CH_3CHO, CH_3CFO and CH_3CClO have barrier heights of the order of 1 kcal./mole. Scott and Scheraga suggest that the concept of a sigma-pi bond could be retained in these situations if one assumed that there is no exchange interaction between the double bond and the CH bond orbitals of the methyl group. The three-fold potential can then be attributed to interactions of the CX orbital on the carbonyl group with methyl CH orbitals, suggesting a barrier about one-third of that in ethane. This then is the basis for the torsional strain term in Scott and Scheraga's treatment of internal rotation barriers.

For the non-bonded interaction term a modified Buckingham or "6-exp" function is used. This is one of many non-bonded potential functions which have appeared in the literature and, apart from empirical success, there would appear to be no compelling reason for choosing one function rather than any other. Practically all of them are derived from inter- rather than intra-molecular interactions, and this leads to one of the major assumptions of conformational analysis, viz., that intermolecular potentials provide a quantitative

model for intramolecular interactions. It is thus assumed that the chemical environment between atoms or groups may be neglected. Maintaining this analogy between intra- and intermolecular interactions it is customary to separate the non-bonded interaction energy into two components: a short-range repulsive component resulting from the interpenetration of electron densities, and an attractive component, operative at longer range and attributed to London forces. Pairwise additivity of these components is assumed for all the atom-atom interactions within the molecule, though this has been found to be unrealistic in some cases[10]. In the "6-exp" potential function, the attractive component is represented by an inverse sixth power term $- c_k /(r_k)^6$ where r_k is the non-bonded distance for a particular interaction k, and c_k is a constant. This is the induced dipole - induced dipole term in the multipole expansion of the dispersion energy between two polarisable systems. The repulsive component is represented by the exponential term $a_k \exp(- b_k r_k)$ where a_k and b_k are constants. Even for intermolecular energies this functional form is not precisely correct. Kestner and Sinanoglu[11] have found that for He-He interactions at small distances, calculated repulsion energies were approximated to only within 10% by an exponential in r_k. Also, the coefficient c_k in the attractive term was found to decrease for values of r_k less than the van der Waal's minimum distance, and beyond this distance terms in r_k^{-8} and r_k^{-10}, corresponding to higher induced multipole-induced multipole interactions, become

significant. Nevertheless, the function has been of considerable assistance in conformational analysis.

Scott and Scheraga modify the 6-exp function by adding a Coulombic component of the form d_k/r_k, where d_k is a constant. This is included for molecules such as hexafluoroethane to take into account electrostatic interaction between residual changes considered to be centred on the fluorine atoms.

The complete Scott/Scheraga equation takes the form:

$$U(\theta) = \frac{1}{2} U_o \left[1 + \cos 3 (\theta + 60)^o \right] + \sum_{k=1}^{m} \left\{ a_k \exp(- b_k r_k) - \left[c_k/(r_k)^6 \right] + (d_k/r_k) \right\} \qquad (1.3)$$

The exchange interaction term has been modified to fit the definition of θ being used here.

1.2.3 Application of the Scott/Scheraga potential to CHX_2COCl

The Molecular Model

The use of Equation(1.3) requires a molecular model having a rigid geometry except for one rotational degree of freedom about the (HX)C - C(OCl) bond. A problem arises however when considering what rigid structural parameters to use for the molecule. It has been mentioned previously that in the more general approach (when

bond angles and bond lengths are allowed to vary) the choice of a set of "strain-free" parameters is somewhat arbitrary. Here the problem is even more acute. Does one use an arbitrary set of "strain-free" parameters; an arbitrary set of parameters for an eclipsed conformation; an arbitrary set for a staggered conformation ....? For the present calculations the set listed in Table 1.1 have been used. The CHX group is assumed to be tetrahedral and the angles for the CClO group are taken from data for acetyl chloride.[12]

Exchange Interactions

The work of Scott and Scheraga has shown that when the overall non-bonded interaction energy, calculated by the modified 6-exp potential, is subtracted from the experimental rotation-barrier of a molecule the energy remaining is constant within a given class of molecules. This is in agreement with Pauling's theory. It is assumed that this remaining energy varies cosinusoidally as a function of the azimuthal angle θ. This may be true in the case of a totally symmetric molecule such as ethane, but for asymmetric molecules a more complex function may be more appropriate. Previous workers have paid little attention to this possibility since they have only been concerned with the difference in energy between the maxima and minima of the function. In cases where non-bonded interactions are small, this difference will be little affected by the nature of the torsional function. The present calculations have been made with the intention of determining the stable conformations of the molecule, and in cases where the

overall non-bonded interaction energy is small, or where non-bonded energy is invariant over a particular region of the internal rotation, these conformations will be determined by the nature of the torsional function.

The application of a cosine function to CHX_2COCl must be a poor representation of the actual situation, since it assumes a) that the -CHX group is tetrahedral; b) that in terms of exchange interactions, -COCl may be considered to act either as a tetrahedral arrangement of single bonds, or simply as -C-Cl; and c) that the energy of a particular interaction is independent of the two bonds involved. However since the adoption of an alternative function would be intuitive, calculations have been made with the cosine function. The interpretation of the resultant conformational potential energy plots will be made with reference to the above arguments.

The value U_o = 1·11 kcal./mole has been used in the function, this being the value given by Scott and Scheraga for molecules of this type. It is the average value of U_o obtained by substituting experimental barrier heights ΔE (taken from microwave data) for CH_3CHO, CH_3CFO and CH_3CClO in the equation:

$$\Delta E = E_\theta(0^\circ) - E_\theta(60^\circ) = U_o + \sum_{k=1}^{m}\left[a_k \exp(-b_k r_k) - \frac{c_k}{(r_k)^6} + \frac{d_k}{r_k}\right]_{\theta = 0^\circ} - \sum_{k=1}^{m}\left[a_k \exp(-b_k r_k) - \frac{c_k}{(r_k)^6} + \frac{d_k}{r_k}\right]_{\theta = 60^\circ} \quad \ldots\ldots \quad (1.4)$$

TABLE 1.1

STRUCTURAL PARAMETERS[a,b]

Bond lengths (Å)		Bond angles	
C–H	= 1·09	∠ O–C–C	= 125°
C–C	= 1·54	∠ Cl–C=O	= 125°
C–Cl	= 1·76	∠ Cl–C(O)–C	= 110°
C=O	= 1·22		
C–F	= 1·35	Other angles	= 109° 28'
C–Br	= 1·90		

[a] S.Mizushima et al. Spectrochim Acta 13, 161 (1958)

[b] Tables of interatomic distance and configuration in molecules and ions (The Chemical Society, London).

Non-bonded interactions

Evaluation of c_k

The coefficients c_k are derived from the Slater-Kirkwood equation[13] which for a pair of unlike atoms, A and B, may be written

$$E_{sk} = \frac{3\hbar e}{2m^{\frac{1}{2}}} \cdot \frac{1}{r^6} \cdot \frac{\alpha_A \alpha_B}{(\alpha_A/N_A)^{\frac{1}{2}} + (\alpha_B/N_B)^{\frac{1}{2}}} \quad \ldots (1.5)$$

where

E_{sk} = interaction energy

$\alpha_A \alpha_B$ = atomic polarisabilities of A and B

e = electronic charge

$\hbar$ = $h / 2\pi$, h being Planck's constant

m = electronic mass

N_A, N_B = effective value of N for A and B.

c_k is therefore given by

$$c_k = \frac{3\hbar e}{2m^{\frac{1}{2}}} \cdot \frac{\alpha_A \alpha_B}{(\alpha_A/N_A)^{\frac{1}{2}} + (\alpha_B/N_B)^{\frac{1}{2}}} \quad \ldots (1.6)$$

In the original Slater-Kirkwood expression, N is the number of electrons in the outer shell of the atom of a rare gas, it being assumed that these electrons contribute equally to the polarisability, and that the contribution from inner electrons is negligible. Pitzer[14], however, suggested that the inner shell contribution is significant, and by replacing N by an "effective" value of N, N_{eff} (on which he put an error bar of about 20%), he obtained better results for the

interaction energy of rare gas atoms. To extend equation (1.6) to other atoms, the N_{eff} values of the rare gases have been plotted against the atomic number, Z (Fig.1.2). N_{eff} values for the required atoms are taken from this curve and used with atom polarisability data taken from Ketelaar[14] to calculate values of c_k.

Evaluation of b_k

Amdur et al.[15] have measured the collision cross sections for He and Ne atoms with energies between 500 and 2100 eV. Analysis of the results led to expressions for the interaction potentials and from these b_k values of 4·55 and 4·61 have been extracted for He and Ne respectively. Other values of this parameter for A, Kr and Xe have been given by Westheimer[16] as 3·60, 2·80 and 2·50 respectively. Fig. 1.3 shows a plot of these b_k values against atomic number Z. From such a plot, b_k values have been obtained for other like pairs of atoms. For an unlike pair of atoms A and B, $b_{A,B}$ was taken as the geometric mean of $b_{A,A}$ and $b_{B,B}$ following the procedure of Hendrickson[17].

Evaluation of a_k

This parameter was obtained by minimising the 6-exp potential at the van der Waal's minimum distance. Differentiation of the 6-exp potential gives

$$\frac{dE}{dr_k} = - a_k b_k e^{-b_k r_k} + \frac{6\, c_k}{r_k^{7}} \qquad \ldots \quad (1.7)$$

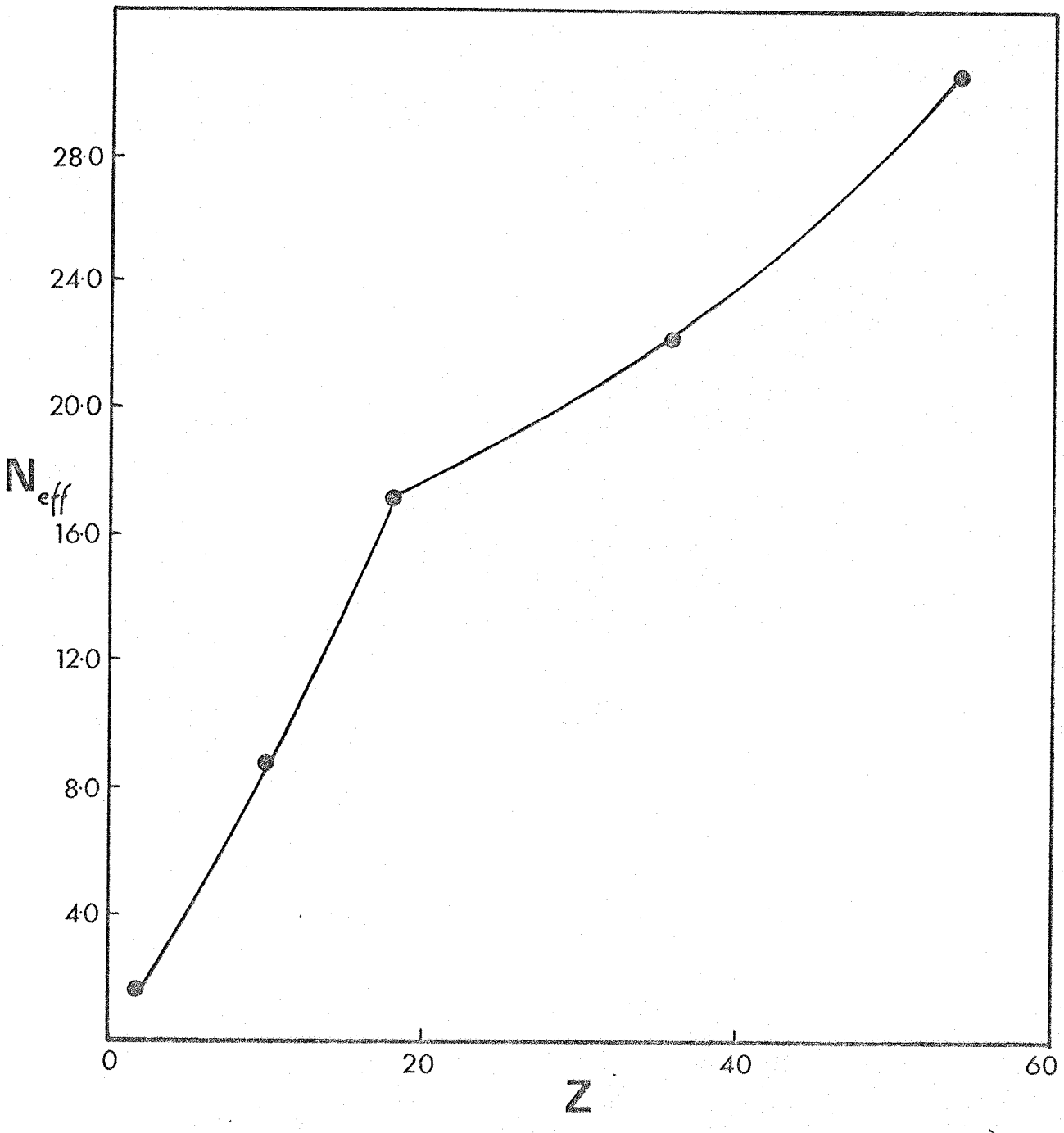

FIG. 1·2 Plot of Neff vs. Z (Neff values are taken from Pitzer)

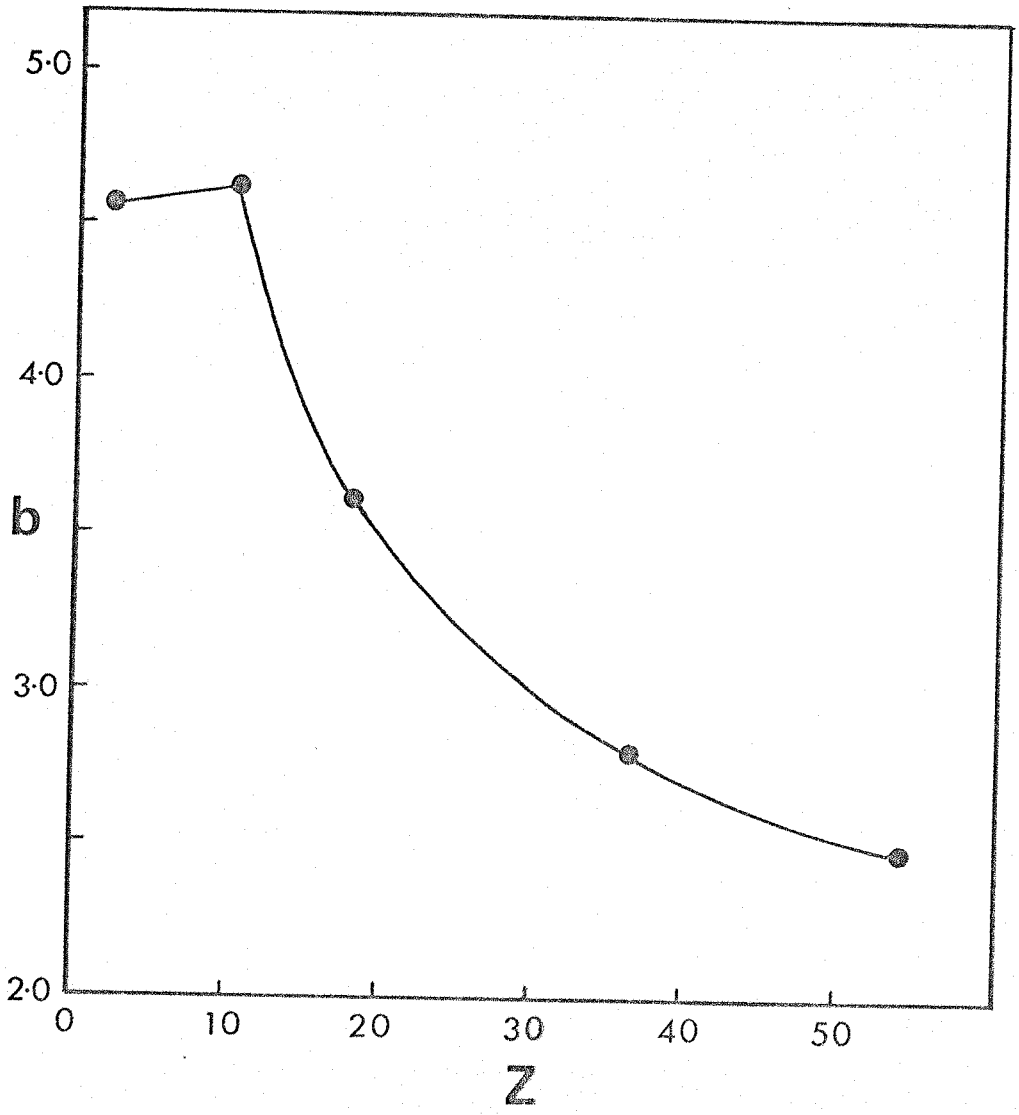

FIG. 1·3 Dependence of the parameter b on Z

TABLE 1.2

PARAMETERS FOR THE NONBONDED, 6-exp POTENTIAL FUNCTION

Interaction	a	b	c	d
O . . . H	$3{\cdot}46 \times 10^4$	4·57	121	0
O . . . F	$1{\cdot}11 \times 10^5$	4·60	202	0
O . . . Br	$7{\cdot}59 \times 10^4$	3·57	1370	0
Cl. . . H	$4{\cdot}68 \times 10^4$	4·13	322	0
Cl. . . F	$1{\cdot}35 \times 10^5$	4·15	526	4·09
Cl. . . Br	$9{\cdot}55 \times 10^4$	3·23	3603	0

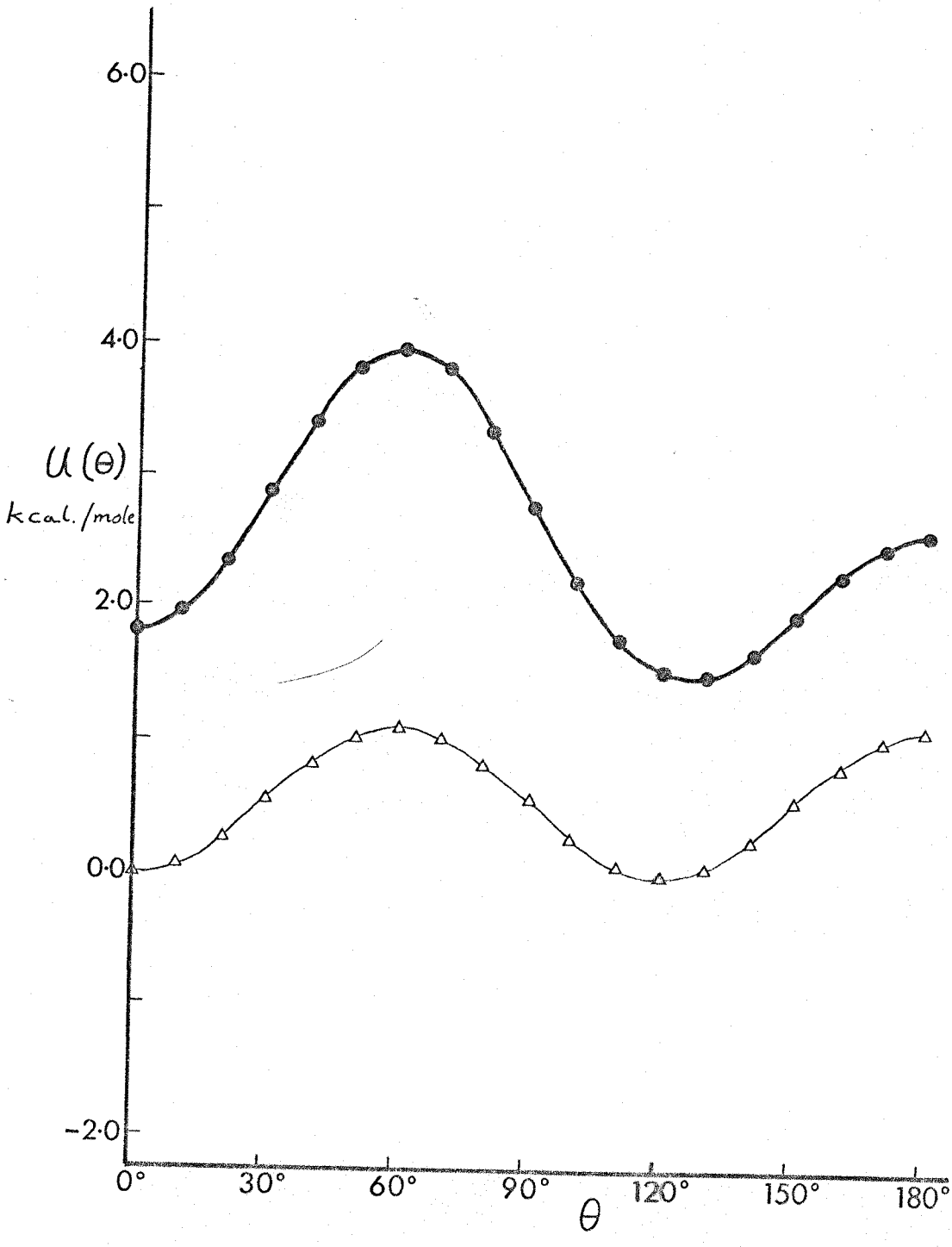

FIG. 1·4 Computed Conformational Potential Energy for CHF_2COCl

△ — exchange interaction contribution

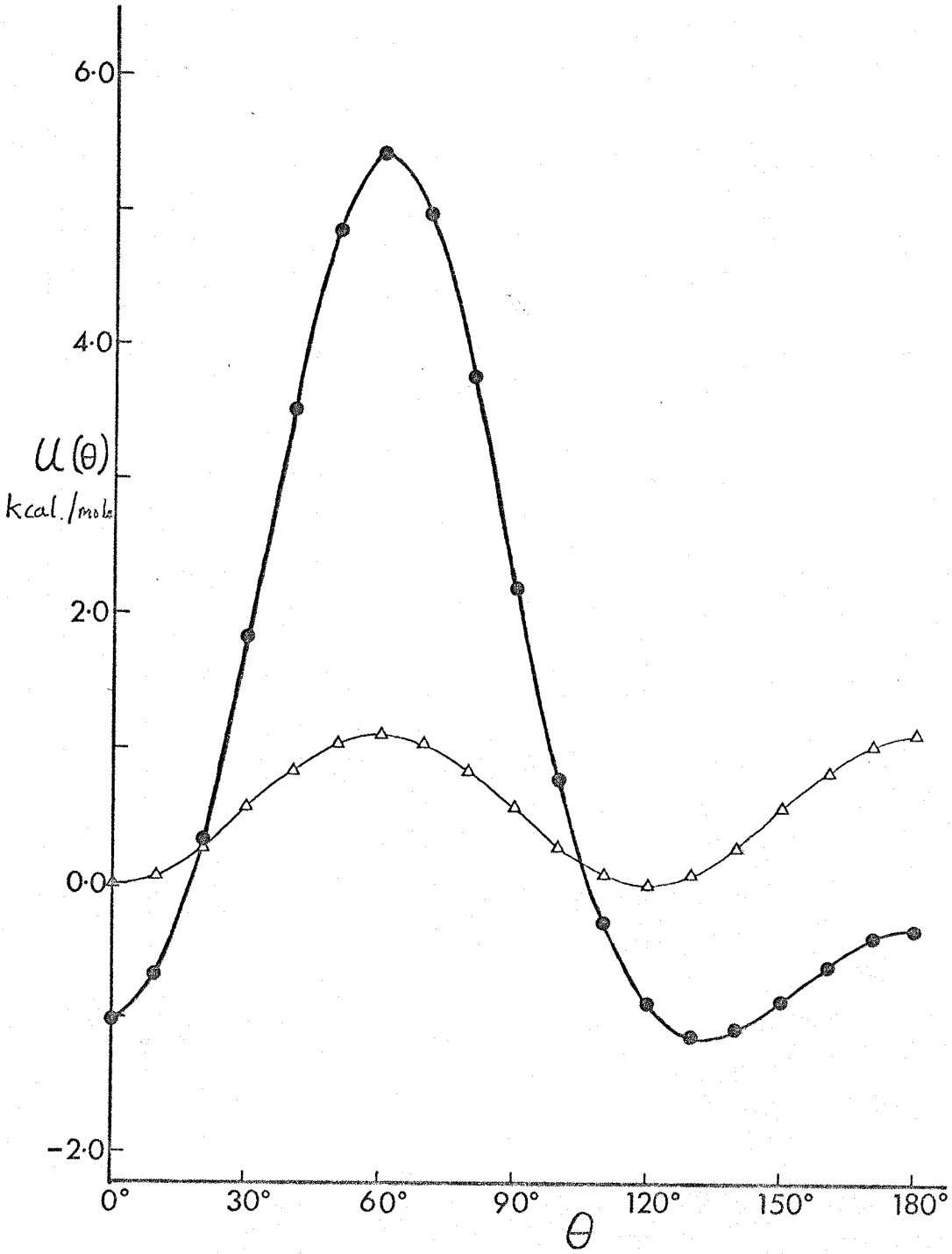

FIG 1.5 Computed Conformational Potential Energy for $CHCl_2COCl$

△ — exchange interaction contribution

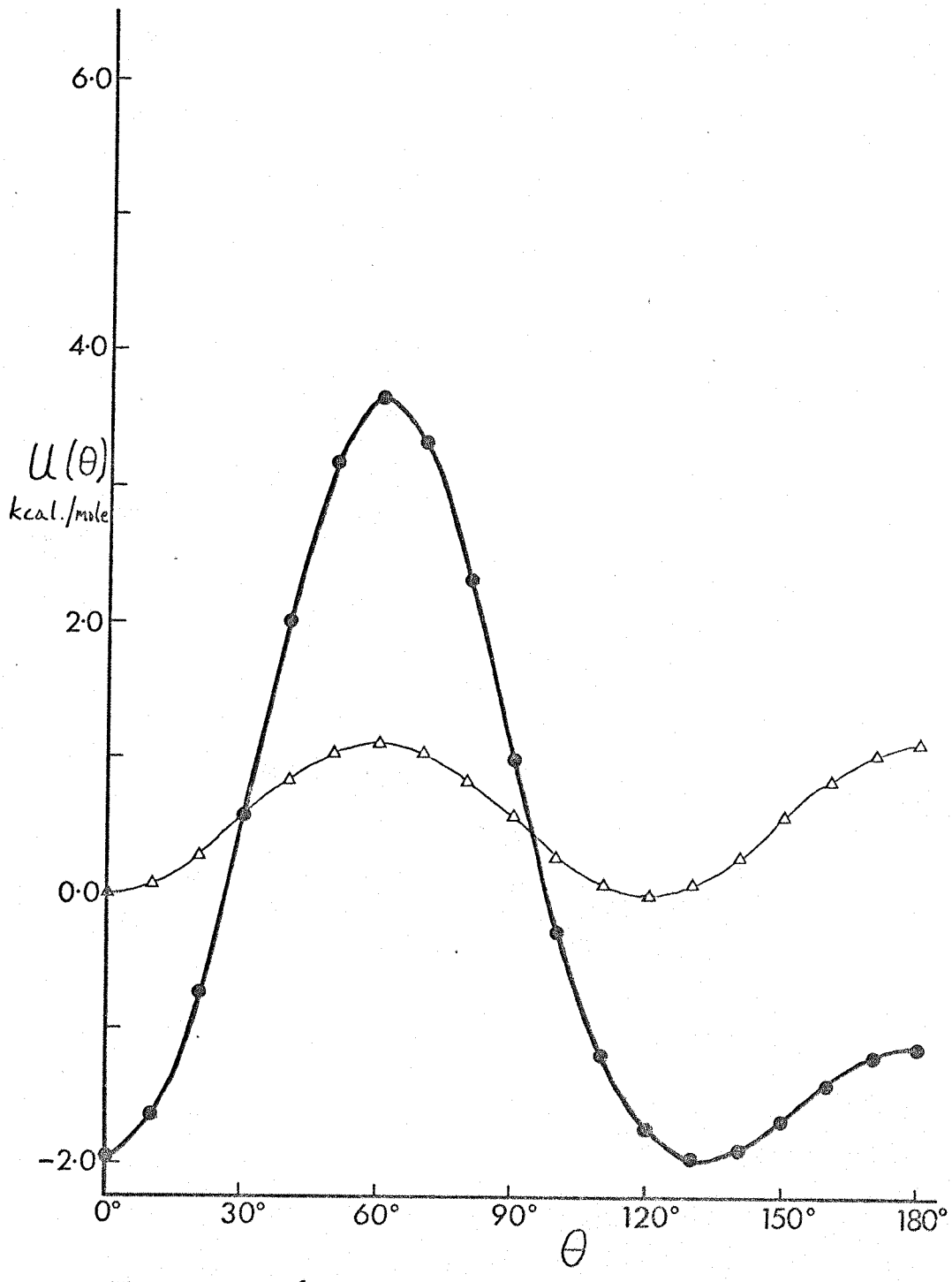

FIG. 1·6 Computed Conformational Potential Energy for $CHBr_2COCl$

△ — exchange interaction contribution

Equating this with zero when $r_k = r_o$, the sum of the van der Waal's radii of the interacting atoms,

$$a_k = \frac{1}{b_k} \frac{6C_k}{r_o^7} \cdot e^{b_k r_o} \quad \ldots \quad (1.8)$$

van der Waal's radii were taken from Bondi[18].

Evaluation of d_k

This parameter, which is a measure of the charge on the halogen atom, is obtained by dividing the bond dipole by the bond distance. For C-F the bond dipole was taken as the difference in the electronegativities of carbon and fluorine in C_6F_6. Scott and Scheraga assume all d_k, except $d_{F...F}$, $d_{Cl..Cl}$ and $d_{F...Cl}$ to be zero. $d_{F...Cl}$ is taken as the geometric mean of $d_{F...F}$ and $d_{Cl...Cl}$.

Table 1.2 gives the complete set of parameters used in the non-bonded potential function. A few slight errors were found in Scott and Scheraga's parameters and these were corrected. A computer programme, CONPOT, was written for the analysis and used on an I.C.L. 1907 system.

1.2.4 Results and Discussion

The computed potential energy curves for CHF_2COCl, $CHCl_2COCl$ and $CHBr_2COCl$ are shown in Figs. 1.4, 1.5 and 1.6 respectively, together with a plot of the exchange interaction component. Unfortunately,

no experimental barrier height data are available for checking the accuracy of the potential functions. The data available for halogen substituted ethanes, however, indicate that the barriers calculated here are of the right order. Woodward and Jonathan[4] have determined the energy difference between the rotational isomers of $CHCl_2COCl$ in the vapour phase and found it to be in the range 100 - 500 cals./mole. No values are available for the difluoro- and dibromo-compounds, but the spectroscopic data of the present study suggest that the energy difference is also small for these compounds. These results could indicate that the computed potential energy curves are fairly accurate in the regions of potential energy minima.

Figs. 1.4 to 1.6 show that the non-bonded interaction component is dominant in the region $\theta = 0^\circ$ to $\theta \approx 110^\circ$ of the potential energy curves. In the region $\theta \approx 110^\circ$ to $\theta = 180^\circ$ this component is almost invariant, the shape of the curve being determined by the exchange interaction component. It is interesting to consider to what extent the assumptions implicit in the functional form of these components have dictated the shape of the computed curves.

Firstly, the assumption of a rigid geometry. The calculations have shown that with the assumed geometries the distances between the centres of eclipsed halogen atoms are far less than the sum of their van der Waal's radii. Therefore when an actual molecule passes through an eclipsed conformation the bond angles will relax to relieve the immense repulsive strain as far as possible, i.e. the molecule will

be flexing continuously during the internal rotation. Recent calculations by Veillard[19] have shown that such flexing of bond angles is probably significant even in the case of ethane. The removal of the constraint on bond angles would therefore be expected to decrease to some extent the non-bonded potential barrier, although the overall shape of the non-bonded potential would probably be retained.

Secondly, the imprecise nature of the 6-exp part of the non-bonded potential. Any increase in the accuracy of this function either by changing the parameters of the present function or by using a more precise functional form would also be expected to affect predominantly the barrier height. This has been found using the modified sets of parameters a_k, b_k and C_k recently proposed by Abraham and Parry.

Thirdly, consider the Coulombic term $\sum_{k=1}^{m} d_k/r_k$. Scott and Scheraga's neglect of Coulombic terms for halogen-halogen interactions other than those involving fluorine and chlorine is unreasonable since the C-F, C-Cl and C-Br bond dipoles, which are measures of the charge separation in these bonds, are almost identical (see following section). Abraham and Parry include d_k parameters for all halogen-halogen interactions. However, the overall Coulombic term has no effect on the shape of the potential curves since it remains constant as θ varies due to the slow variation of the $1/r_k$ function.

Finally, consider the assumption of a cosine function for the exchange interaction component. Since the non-bonded component is almost invariant in the region $\theta \approx 110^{\circ}$ to $0 = 180^{\circ}$ this function determines the position of the second potential energy minimum. The use of a more realistic function than the cosine function would result in a shift in the position of this minimum.

From the above considerations it is concluded that the compounds CHF_2COCl, $CHCl_2COCl$ and $CHBr_2COCl$ each have at least two stable conformations. One of these conformations has $\theta = 0^{\circ}$ while the other(s) lie(s) in the range $\theta = 90^{\circ} - 180^{\circ}$. One is scarcely justified in defining the second angle more accurately than this.

Dipole Moment Considerations

Mizushima et al., have calculated the dipole moment of $CHCl_2COCl$ for various azimuthal angles. Their data are plotted in Fig.1.7. Since the bond dipoles for C-F, C-Cl and C-Br are very similar (C-F, 1·4D; C-Cl, 1·5D; and C-Br, 1·4D (C-H, 0·4D)[20]), a similar curve will also apply to CHF_2COCl and $CHBr_2COCl$, i.e. of all the possible conformations that with $\theta = 0^{\circ}$ will be the least polar.

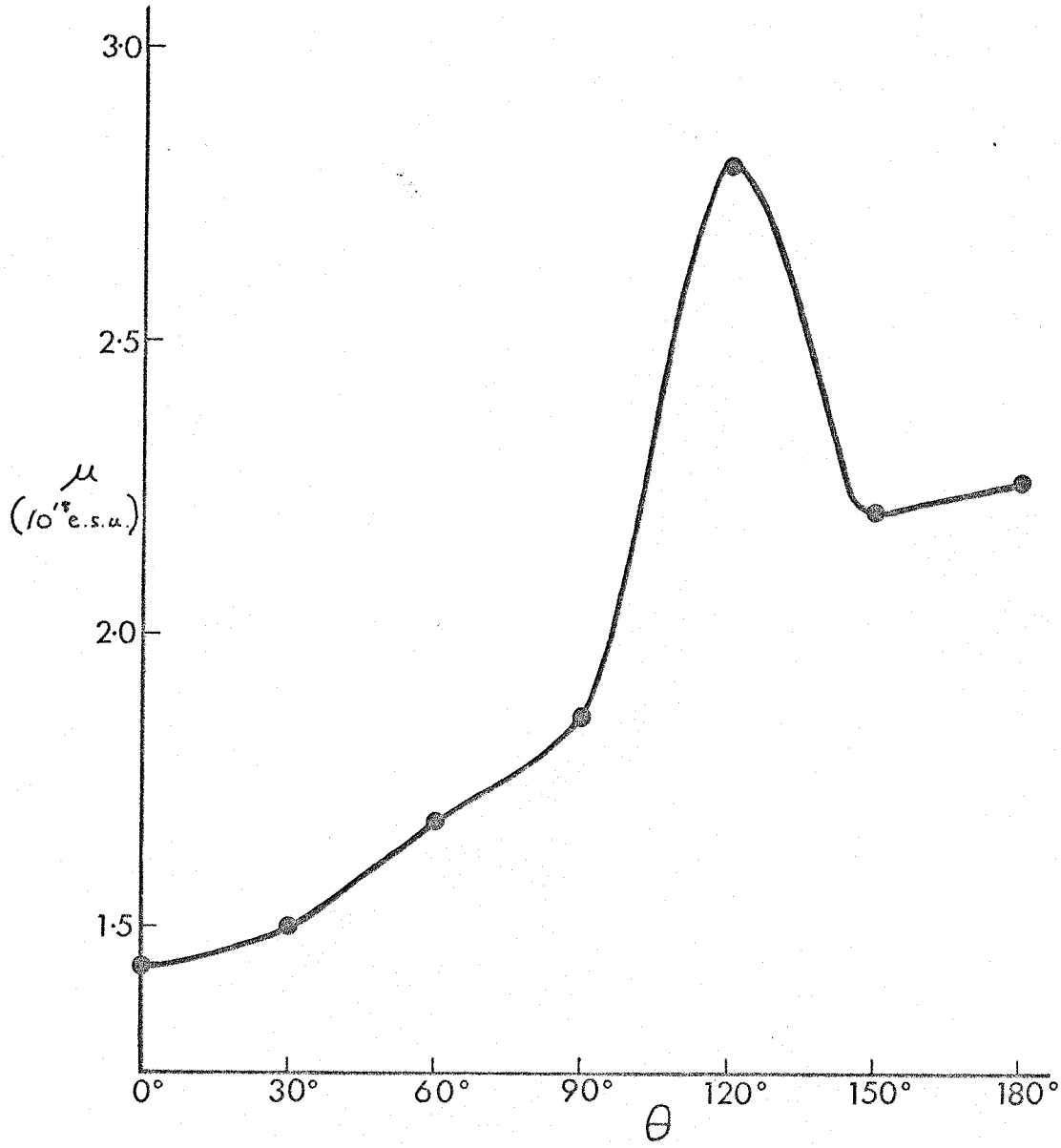

FIG. 1·7 Calculated Dipole Moment of $CHCl_2COCl$
Data taken from Mizushima et al.[3]

1.3 THE NORMAL COORDINATE ANALYSES

Vibrational analyses of CHF_2COCl and $CHBr_2COCl$ have been included in this work a) to assist the assignment of observed vibrational frequencies, and b) to provide additional information regarding the conformations of the rotational isomers. Thirteen of the fifteen fundamental frequencies have been calculated for five different conformations of each molecule. A brief outline of the principles involved in the calculations will now be given; fuller details may be found in books on the subject[21,22] and many research papers (eg. 23,24).

1.3.1 Normal Vibrations

If coordinates (called normal coordinates) Q_i can be found such that the potential energy V (assumed to be quadratic) and the kinetic energy T of the molecule are given by

$$2V = \sum_i \lambda_i Q_i^2 \qquad (1.9)$$

$$2T = \sum_i (\dot{Q}_i)^2 \qquad (1.10)$$

then in terms of these coordinates the molecular motion is separated into modes that are mathematically independent of one another. This can be seen as follows.

Consider some general coordinates and velocities q_i and $\dot{q}_i$. In this system Newton's equations of motion can be written as

$$\frac{d}{dt}\frac{\partial T}{\partial \dot{q}_i} - \frac{\partial T}{\partial q_i} + \frac{\partial V}{\partial q_i} = 0 \qquad (1.11)$$

For the special coordinates giving Equations (1.9) and (1.10), Equation (1.11) becomes

$$\ddot{Q}_i + \lambda_i Q_i = 0 \qquad \ldots (1.12)$$

That is

$$\frac{\partial^2 Q_i}{\partial t^2} = -\lambda_i Q_i$$

This can be integrated directly, giving

$$Q_i = A_i \cos (\lambda_i^{\frac{1}{2}} t + \epsilon_i) \qquad \ldots (1.13)$$

where A_i is an amplitude, $\lambda_i^{\frac{1}{2}}$ is a frequency and ϵ_i is an arbitrary phase. Thus, each normal coordinate undergoes its harmonic motion independently of all the other normal coordinates and with a frequency ν_i given by $\lambda_i^2 = 4\pi\nu_i^2$. (The resulting motion is harmonic because it was assumed that the potential energy could be expressed in a quadratic form.)

To determine the normal coordinates and the normal vibration frequencies it is therefore necessary to derive expressions for the potential and kinetic energies of the molecule in a suitable coordinate system and then transform these expressions to the space of normal coordinates.

1.3.2 The Potential Energy Function

If we define 3N-6 internal displacement coordinates R_i, $i = 1,2,3 \ldots 3N-6$, in order to describe small vibrations of a molecule,

then the potential energy of the molecule may always be expanded as a Taylor series in these coordinates about the equilibrium configuration e[25].

$$V = V_e + \sum_i \left(\frac{\partial V}{\partial R_i}\right)_e R_i + \frac{1}{2} \sum_{ij} \left(\frac{\partial^2 V}{\partial R_i \partial R_j}\right)_e R_i R_j + \text{higher terms} \quad \ldots \quad (1.14)$$

The term V_e in this equation simply defines the zero of the energy scale and is therefore trivial. The second term may be set equal to zero if the coordinates R_i are independent, because derivatives are taken at the equilibrium position. Terms in R of order higher than R^2 may be neglected in the case of small vibrations for the motions are then basically harmonic. The potential function thus reduces to:

$$V = \frac{1}{2} \sum_{ij} F_{ij} R_i R_j \quad \ldots \quad (1.15)$$

where the harmonic force constants F_{ij} are defined as

$$F_{ij} = \left(\frac{\partial^2 V}{\partial R_i \partial R_j}\right)_e \equiv \left(\frac{\partial^2 V}{\partial R_j \partial R_i}\right)_e$$

In this form the function is of no use. Consider, for example, the case of acetyl chloride. Fifteen internal coordinates are needed to describe the system and therefore 225 force constants are required to define the potential energy of the molecule.

In the so-called Simple Valence Force Field (SVFF), the number of force constants is drastically reduced by the assumption that constants other than the F_{ii}'s are zero, i.e.

$$V = \frac{1}{2} \sum_i F_{ii} R_i^2 \qquad \ldots (1.16)$$

A further reduction usually occurs as a result of symmetry in the molecule.

The Modified Valence Force Field (MVFF) adds certain of the cross terms $F_{ij}R_iR_j$ to the SVFF to take into account non-bonded interactions in the molecule. The exact physical significance of the F_{ij}'s is however difficult to comprehend and the decision as to which terms are to be included is not easy.

The Urey-Bradley Force Field (UBFF)[26] attempts to surmount this difficulty by expanding the potential energy of a molecule in terms of the internal displacement coordinates Δr_i, $\Delta \alpha_{ij}$ and Δq_{ij}, which represent a change in bond length, bond angle, and the distance between non-bonded atoms, respectively. These coordinates are not independent, and therefore, referring back to Equation (1.14), linear terms must be included in the expansion. The function is written:

$$V = \sum_i \left[K_i' r_{io} (\Delta r_i) + \frac{1}{2} K_i (\Delta r_i)^2 \right] + \sum_{ij} \left[H_{ij}' r_{io} r_{jo} (\Delta \alpha_{ij}) + \frac{1}{2} H_{ij} r_{io} r_{jo} (\Delta \alpha_{ij})^2 \right] + \sum_{ij} \left[F_{ij}' q_{ijo} (\Delta q_{ij}) + \frac{1}{2} F_{ij} (\Delta q_{ij})^2 \right] \qquad \ldots (1.17)$$

where the equilibrium values r_{io}, r_{jo} and q_{ijo} are inserted to reduce all force constants to the same dimensions. Once again the number of force constants involved is large, but by expressing the coordinates

Δq_{ij} in terms of the coordinates Δr_i and $\Delta \alpha_{ij}$ the function reduces to an expression in what are now independent variables and the linear terms may be equated to zero. (This is not strictly true. There is often an interdependence of some of the $\Delta \alpha_{ij}$ coordinates and these terms must be removed by substituting the appropriate redundancy relationship.) A further reduction in the number of force constants is obtained by making the now standard assumption that $F_{ij}' = -\frac{1}{10} F_{ij}$, which has proved to be satisfactory for many molecules[27].

The UBFF is the potential function which has been applied to the analysis of difluoroacetyl chloride and dibromoacetyl chloride. The general validity of the function to this type of molecule has been demonstrated[28], and force constants, which are readily available in the literature have been shown to be transferable[29].

1.3.3 The Kinetic Energy Function

Having chosen a suitable potential energy function, the next step in the normal coordinate analysis of a molecule is to derive an expression for the kinetic energy of the molecule in the same coordinate system. In practice, it is more convenient to express the kinetic energy in Cartesian coordinates x_i and then transform the equation to the space of the internal coordinates R_i used in the potential energy function. The Wilson s-vector method[21] is used to construct the transformation B from Cartesian to internal coordinates, i.e.

$$R = Bx \qquad \ldots \quad (1.18)$$

where R and x represent column vectors of internal and Cartesian coordinates respectively. The inverse kinetic energy matrix G in internal coordinates is then computed from

$$G = BM^{-1} B' \qquad \ldots \quad (1.19)$$

where M is a diagonal matrix of the reciprocal masses of the atoms and B' is the transpose of the B matrix (ref.(2) gives a proof of this relationship). The kinetic energy T of the molecule is given by

$$2T = \dot{R}' G^{-1} \dot{R} \qquad \ldots \quad (1.20)$$

$\dot{R}$ being a column vector of the derivatives of the internal coordinates with respect to time. In the same notation the potential energy V can be expressed as

$$2V = R'F R \qquad \ldots \quad (1.21)$$

where F is the matrix of coefficients in the Urey-Bradley function.

1.3.4 The Transformation to Normal Coordinates

The transformation matrix L is such that it diagonalises the F matrix and simultaneously diagonalises the kinetic energy matrix to an identity matrix. It is defined as follows:

$$R = L Q \qquad \ldots \quad (1.22)$$

Expressing potential and kinetic energy in terms of the normal

coordinates

$$2V = R'FR = Q' (L'FL) Q = Q'\Lambda Q \quad \ldots (1.23)$$

$$2T = \dot{R}'G^{-1}\dot{R} = \dot{Q}'(L'G^{-1}L)\dot{Q} = \dot{Q}'E\dot{Q} \quad \ldots (1.24)$$

where E is the identity matrix, Λ a diagonal matrix, and

$$L'FL = \Lambda \quad \ldots (1.25)$$

$$L'G^{-1}L = E \quad \ldots (1.26)$$

The transformation L must therefore satisfy the equation

$$L'(F - G^{-1}\lambda)L = \Lambda - \lambda E \quad \ldots (1.27)$$

where λ is a variable scalar.

From this it can be shown that

$$|L|^2 . |F - G^{-1}\lambda| = |\Lambda - \lambda E| \quad \ldots (1.28)$$

and since $|L| \neq 0$, the roots of $|\Lambda - \lambda E| = 0$ are also the roots of $|F - G^{-1}\lambda| = 0$. Solution of the secular equation

$$|F - G^{-1}\lambda| = 0 \quad \ldots (1.29)$$

therefore gives the values λ_i from which the normal vibration frequencies ν_i are obtained ($\lambda_i^2 = 4\pi^2\nu_i^2$). Having found the values λ_i the corresponding eigenvectors can be found and then the transformation L can be formed from these. Finally, normal coordinates can be calculated from Equation (1.22).

1.3.5 The Analysis of CHF_2COCl and $CHBr_2COCl$

Vibrational frequencies have been computed for the conformations $\theta = 0^\circ$, 45°, 90°, 135° and 180°. The rigid geometries given in Table 1.1

have been assumed for each conformation. This is an obvious over-simplification of the actual situation in the molecules for the equilibrium geometries will vary with θ. In fact the structural parameters which have been used probably fail to describe any of the conformations precisely. It has however been found that small changes in bond angles and bond lengths have an almost negligible effect on the calculated frequencies[30].

Table 1.3 gives the values and the origins of the force constants used in the Urey-Bradley force field. Following the procedure of previous workers[3,31] the complexity of the analyses have been reduced by neglecting non-bonded force constants for interactions between different rotating groups. This must give a poor representation of the molecular system, for the very fact that the molecules exhibit rotational isomerism indicates that these interactions are significant. As a result of this simplification the potential energy of the system remains constant as θ varies and changes in the computed frequencies are a result of changes in the inverse kinetic energy G matrix with θ.

In view of these factors, any conclusions based on a comparison of observed and calculated frequencies can only be regarded as tentative.

The computer programmes were written by J.H. Schachtschneider[32] and used on an I.C.L. 1907 computer.

TABLE 1.3

FORCE CONSTANTS USED IN CALCULATIONS

Force constants (mdyn/Å)[a-e]

K (C-C) = 2·8	H (H-C-F) = 0·1	F (F ... H) = 1·1
K (C-H) = 3·9	H (F-C-F) = 0·45	F (F ... F) = 1·3
K (C=O) = 11·0	H (C-C-F) = 0·13	F (F ... C) = 1·3
K (C-F) = 4·0	H (H-C-Br) = 0·06	F (Br ... H) = 0·6
K (C-Cl) = 1·75	H (Br-C-Br) = 0·06	F (Br ... Br) = 0·5
K (C-Br) = 1·5	H (C-C-Br) = 0·13	F (Br ... C) = 0·7
	H (C-C-H) = 0·15	F (C ... H) = 0·4
	H (C-C=O) = 0·4	F (O ... C) = 0·4
	H (Cl-C=O) = 0·3	F (Cl ... O) = 1·0
	H (C-CO-Cl) = 0·1	F (Cl ... C) = 0·6
		F' = $-(1/10)F$
		$\bar{K}$ = 0·3 (CHF_2COCl)
		$\bar{K}$ = 0·1 ($CHBr_2COCl$)

a S.Mizushima et al. Spectrochim.Acta 13, 161 (1958)
b Nakagawa et al. J.Chem.Phys. 20, 1723 (1952).
c T. Simanouti, J.Chem.Phys. 17, 848 (1949).
d J. Aldons and I.Mills, Spectrochim.Acta 19, 1567 (1963).
e J. Overend and J.R. Scherer, J.Chem.Phys. 32, 1296 (1960).

1.3.6 Results and Discussion

The computed data are given in Section 1.4 where they are discussed in conjunction with the interpretation of the spectroscopic data. Table 1.5 compares observed and computed vibrational frequencies of CHF_2COCl and $CHBr_2COCl$. Tables 1.6 and 1.7 show the computed distribution of potential energy among the force constants used in the analysis of CHF_2COCl and $CHBr_2COCl$ respectively.

1.4 SPECTROSCOPIC STUDIES OF THE DIHALOACETYL CHLORIDES

1.4.1 Sample Preparation

Difluoroacetyl chloride was prepared by reaction of difluoroacetic acid with excess benzoyl chloride (b.p. 28°C; lit. b.p. 28°C [33]).

Dibromoacetyl chloride was prepared by reaction of parent acid and excess thionyl chloride (b.p. 65° - 70°C at ~5 mm.Hg; lit. b.p. 60° - 64°C at 4 mm.Hg [34]).

All samples were fractionally distilled two or three times before use.

1.4.2 Spectroscopy - instruments and cells

Infrared spectra were recorded in the range 200 - 4000 cm^{-1} with Grubb-Parsons (Model GS2A) and Perkin-Elmer (Model 225) spectrometers. Liquid-phase Raman spectra were measured with a Spex Raman spectrometer (Model 1400) equipped with an argon ion laser. A brief description of these instruments and the cells used for obtaining vapour, liquid and solid spectra is given below.

Grubb-Parsons Model GS2A Double Beam Grating Spectrometer[35]

This instrument is designed to cover the range 2μ to 25μ, but for all practical purposes the useful range is 2μ to 20μ. The grating is ruled at 1200 lines per inch and blazed to give maximum energy at 9μ. A potassium bromide fore-prism is used in the first order of the grating (5-25μ) and a calcium fluoride prism for the second (3·5-5μ), third (2·5-3·75μ) and fourth (2-2·5μ) orders. The

source of infrared radiation is a Nernst filament and the detector a thermocouple. A slit programme is provided in order to keep the energy reasonably constant throughout the range. Manual operation of the slits is also possible. The limiting resolution of the GS2A is 1·5 cm^{-1}, but under normal operating conditions is approximately 4 cm^{-1}. The wavelength accuracy obtainable between 5-15μ is 0·004μ.

Perkin-Elmer Model 225 Spectrometer[36]

This is a double-beam infrared instrument with automatic optical null, built-in electronics and drum recorder. It covers the region 5000 - 200 cm^{-1} in four ranges, 5000 - 2000 cm^{-1}, 2500 - 1000 cm^{-1}, 1000 - 400 cm^{-1} and 450 - 200 cm^{-1}. Two gratings with 150 lines/mm. and 30 lines/mm. are installed for the whole range. Both gratings are used in first and second orders. A potassium bromide fore-prism is used for first, second and third ranges and a filter in the fore-monochromator for the fourth range. The infrared source is a Globar which is air cooled and has a photoelectric radiation control. The detector employed is a pneumatic Golay cell. Programmed and manual operation of the slits is possible. The resolution at different frequencies is 0·33 cm^{-1} at 2400 cm^{-1}, 0·16 cm^{-1} at 1034 cm^{-1} and better than 0·41 cm^{-1} at 286 cm^{-1}. The scale is linear in wave-number and its expansion at any point of the individual range is possible. An adjustable automatic suppression ensures that spectral regions free from bands are rapidly scanned and the regions of spectral absorption are reproduced with maximum possible accuracy.

Spex Model 1400 Laser-Raman Spectrometer[37]

This is a double monochromator-spectrometer of 0·75 metre focal length covering the spectral range 3100 cm^{-1} to 10,000 cm^{-1}. The two gratings, which are ruled at 1200 lines/mm and blazed at 5000Å are ganged in the Czerny-Turner manner. Such an arrangement reduces scattered light to a minimum. The three slits are bilaterally adjustable to 3 mm. wide by 50 mm. long. There is a shutter on the exit slit. Electrical and manual scanning of the instrument is possible with several speeds in the range 0·4 to 1000 cm^{-1}/min. The wave-number is output on two five-digit counters, one reading wave-number; the second can be set to zero at any excitation frequency and displays the frequency shift (Δ cm^{-1}). The accuracy is quoted to be $\pm$ 1 cm^{-1} over a 5000 cm^{-1} interval direct reading from the counter. The resolution of the instrument is given as 0·2 cm^{-1} at 15802 cm^{-1} (half-width measurement).

For the present work the Spex was equipped with a Spectra-Physics 141 r.f. excited argon ion laser (excitation wavelength 4880Å).

Gas Cell

Infrared spectra of CHF_2COCl and $CHBr_2COCl$ in the vapour phase were recorded at room temperature using a standard 10 cm. path-length glass cell equipped with potassium bromide windows. The windows were attached to the cell with a Teflon adhesive[38].

Liquid Cells

The infrared spectrum of liquid $CHBr_2COCl$ was obtained from a

film held between potassium bromide discs (25 mm diam. x 5 mm.). I.r. spectra of solutions of $CHBr_2COCl$ in solvents of varying polarity were recorded using a matched pair of standard commercial cells; Teflon spacers being used to obtain cells of the required thickness.

Infrared spectra were not recorded for the liquid phase of CHF_2COCl because of the high volatility of this compound.

Raman spectra of the liquids and solutions were obtained with a Spex liquid cell. This is simply a glass tube (8 mm. i.d. x 20 mm.) with an optically flat base and cover. The cell was aligned in the sampling region of the spectrometer with the incident laser radiation falling normally on the base.

The Low Temperature Cell

Solid state spectra have been obtained using the glass cell shown diagrammatically in Fig.1.8. The cell has the advantage that a film of solid may be obtained either by cooling a liquid film between KBr or NaCl discs held in the copper block, or by allowing the vapour of the compound to condense on a pre-cooled disc. The second procedure is usually more convenient. Continuous evacuation of the cell prevents condensation of water and carbon dioxide on the central KBr disc, while a heating jacket can be used to prevent similar condensation on the outer windows.

Irrespective of the method of solid formation, the film produced is still usually a mixture of rotational isomers. This is a result of the sample being cooled too rapidly, thus preventing complete equili-

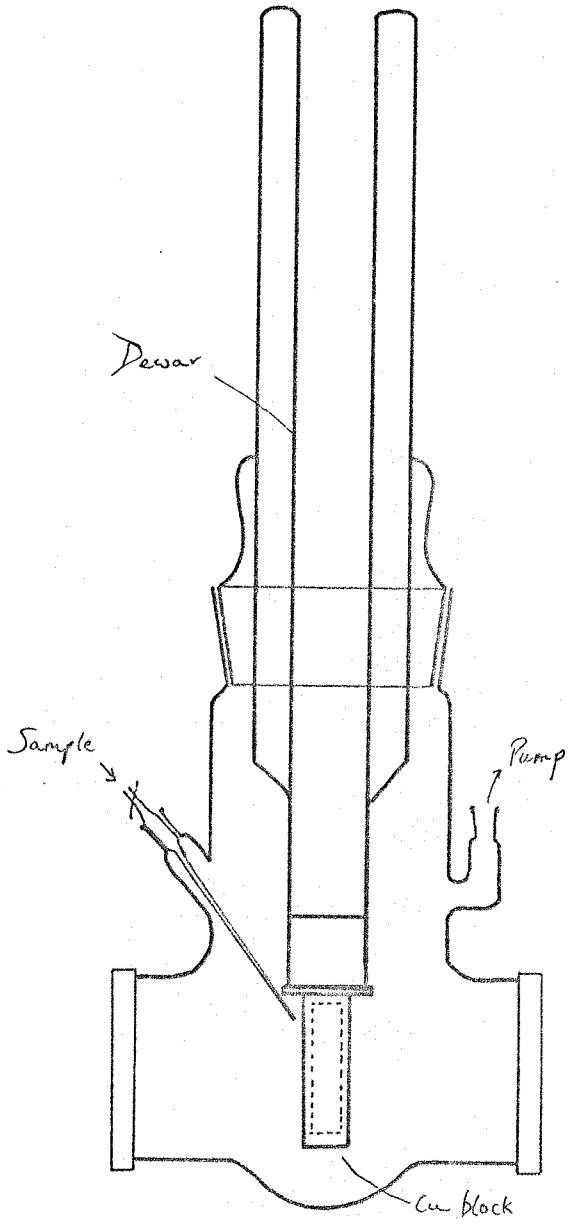

FIG. 1·8 The Low Temperature Cell

bration to the more stable isomer. The one-isomer solid can usually be obtained from this film by the process of repetitive 'annealing'[39]. The film is allowed to warm slowly until it becomes opaque, and is then immediately recooled. In the case of a frozen vapour the transition from the transparent to the opaque state cannot be seen, and a trial and error method must be adopted to anneal the film.

1.4.3 Group Theory Treatment of CHX_2COCl

The conformation $\theta = 0^{\circ}$ of CHX_2COCl has only a plane of symmetry and therefore belongs to the C_s point group. Of the fifteen possible fundamental vibrations of this conformation, ten are found to be of the A' symmetry class and the remaining five are of the A" symmetry class. All of them are allowed in the infrared and Raman. Also, the combinations and overtones of the species A' and A" are allowed in the i.r. and Raman. All other conformations of CHX_2COCl are without any element of symmetry and therefore belong to the C_1 point group. The fundamental vibrations for these conformations are of the A symmetry class and are i.r. and Raman active. Appendix 1.1 gives a more complete group theory treatment of the molecules.

1.4.4 Results and Discussion

The observed infrared spectra of difluoroacetyl chloride in the vapour and solid states and dibromoacetyl chloride in the liquid and solid states are shown in Figs. 1.9 and 1.10 respectively. Complete spectral data for the two compounds are given in Table 1.4.

TABLE 1.4

Spectral Data (cm^{-1})

CHF_2COCl					$CHBr_2COCl$				
Vapor	Infrared Solid A [a]	Solid B [a]	Raman Liquid	Assignment [b]	Vapor	Infrared Liquid	Solid	Raman Liquid	Assignment [b]
2976				M,L ν(C-H)		3003			M,L ν(C-H)
1946 w	1961 w				1942 w	1950 w			
~1810 sh, 1802 vs	1808 ssh, 1786 vs	1805 msh, 1783 s	~1793 (1)	L, M ν(C=O)	1815 vs, 1786 vs	1795 s, 1770 ssh	1786 s, 1761 msh	~1794 (1), ~1766 (1)	M, L ν(C=O)
1361 msh, 1348 s	1368, 1342 mw	1361 w, 1351 wsh	~1347 (1)	M, L δ(C-H)	1232 mw, 1212 wsh	1225 mw, 1210 wsh	1225 mw, 1206 wsh	1232 (1)	M, L δ(C-H)
1170 vs	1163 msh		~1167 (?)	L, M ν(C-F_2)	1155 msh, 1143 m	1149 mwsh, 1131 mw	1149 wsh, 1125 mw	1150 ($\frac{1}{2}$), 1136 (1)	L, M δ(C-H)
	1145 s	1145 ms			1070 ms	1064 m	1064 mw		L, M ν(C-C)
1117 vs		1106 vs		M, L ν(C-F_2)	976 s	976 s	978 s	979 ($\frac{1}{2}$)	
	1099 vs	1093 msh			752 m	748 m	752 m	751 (2)	M, L ν(C-Br_2)
1083, 1075, 1060 msh	1071 msh				738 m	735 msh	736 m		M, L ν(C-Br_2)
980 s	985 vs	996 m	976 (1)	L, M ν(C-C)	719 s	714 s	714 s	716 (2)	M, L ν(C-Br_2)
					662 m	658 s	660 s	660 (1)	
835, 829, 822 s	822 s	833 wsh, 814 s	827 (4)	L, M δ(C-F_2)		553 m	554 mw, 532 mw	552, 534 (2)	L, M ν(C(O)-Cl)
658, 651 m	637 m	630 m	635 (6)	M, L ν(C(O)-Cl)		483 w, 456 w		487 (2), 460 ($2\frac{1}{2}$), 340 (4), 253 (10), 223 (2), 179 (5), 163 (5), 148 (3)	L, M, L δ(C-Cl), δ(C-Br), M, M, L, M, L δ(C=O)
602 s	602 m		610 (9)						
542 w									
525 ?	538 m	528 m							
503 w	503 m		505 (8)	L, M, L, M δ(C-F), L δ(C-Cl), M δ(C=O), M, L					
	460 mw	458 mw	463 (10)						
			405 (2)						
			353 (1), 343 (1)						
			233 (1)						
			211 (5)						

a. These spectra show different degrees of conversion to the more polar isomer (see text)

b. See text.

M denotes the more polar form and L the less polar form

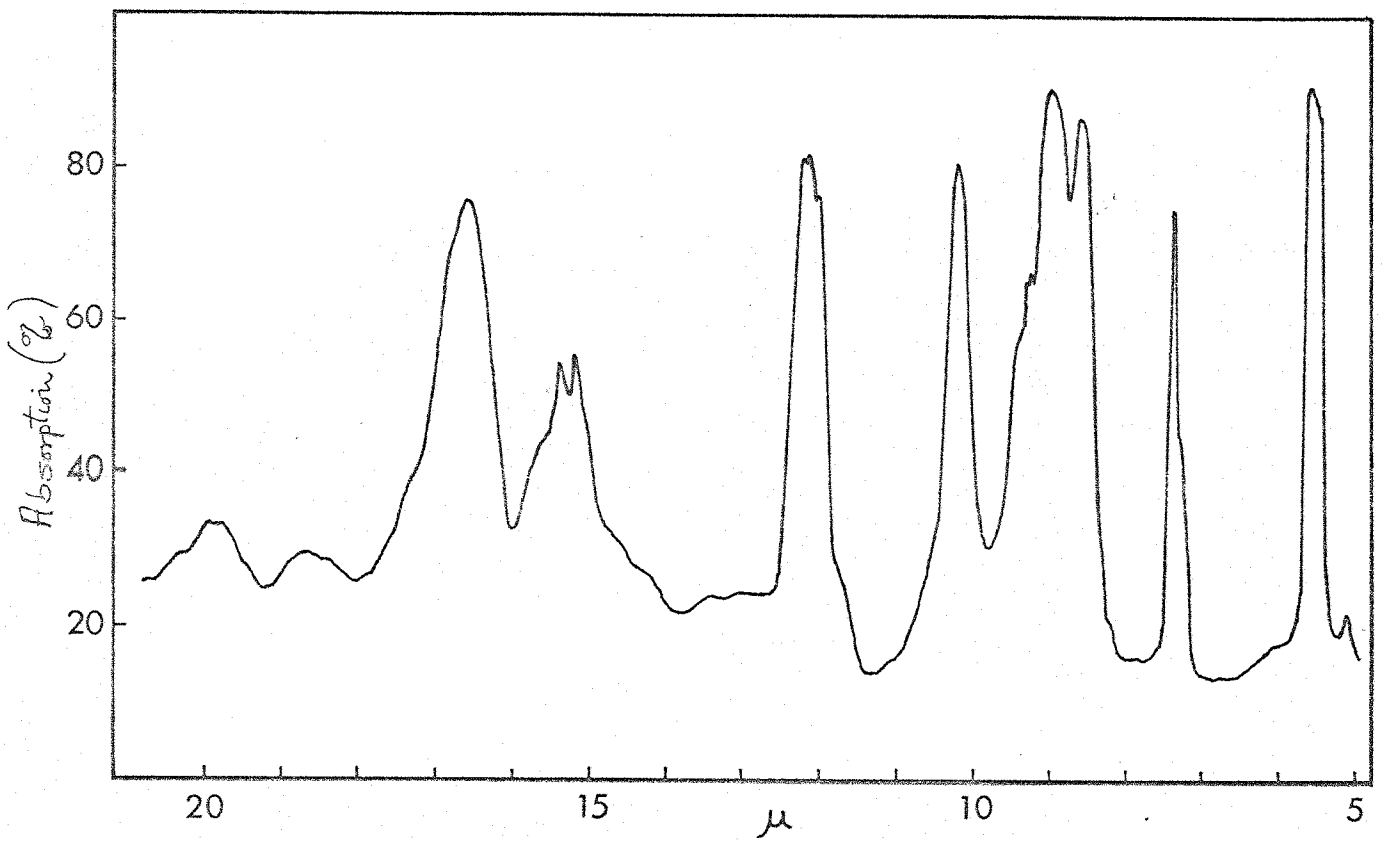

FIG. 1·9a. Infrared spectrum of CHF_2COCl – vapour

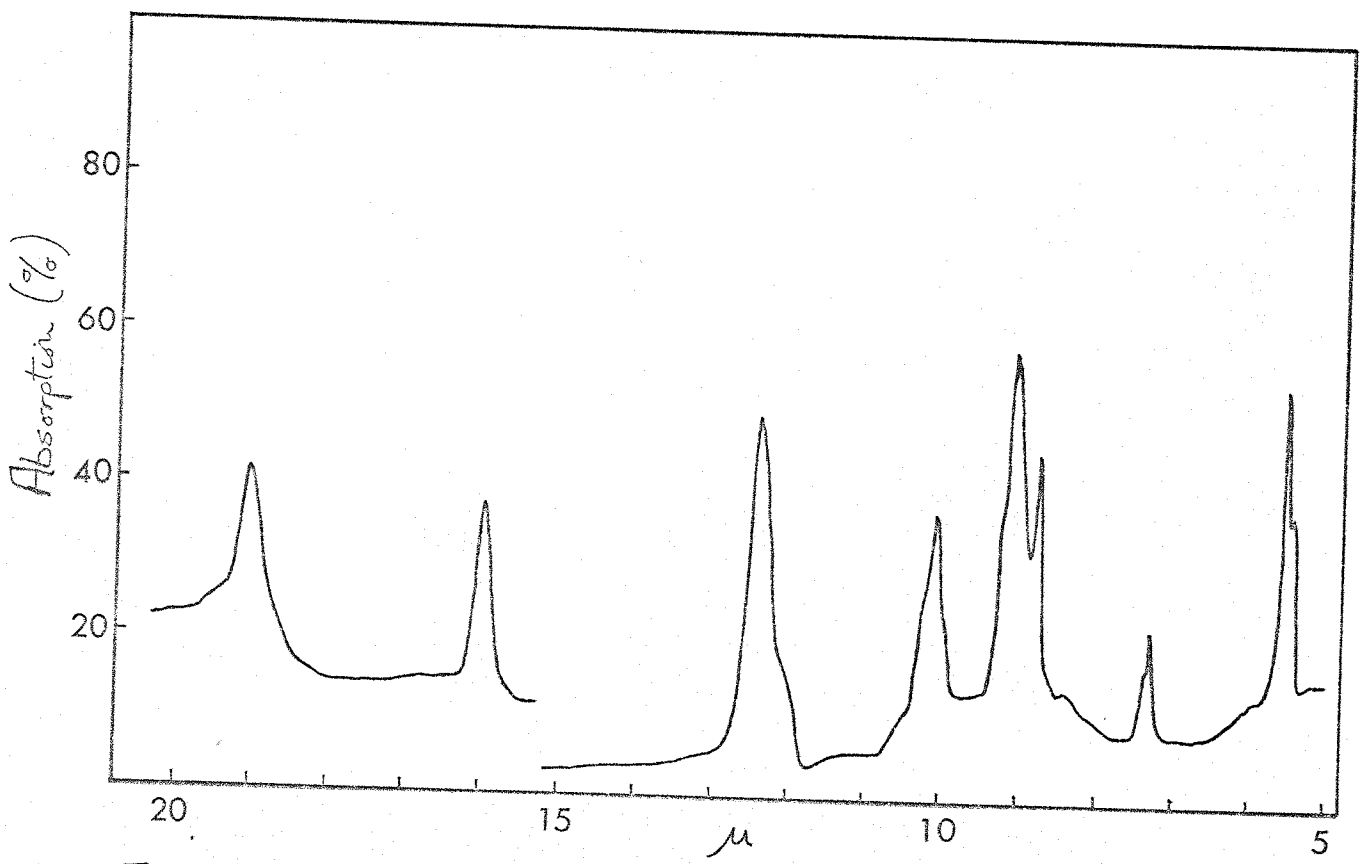

FIG. 1·9b. Infrared spectrum of CHF_2COCl — solid

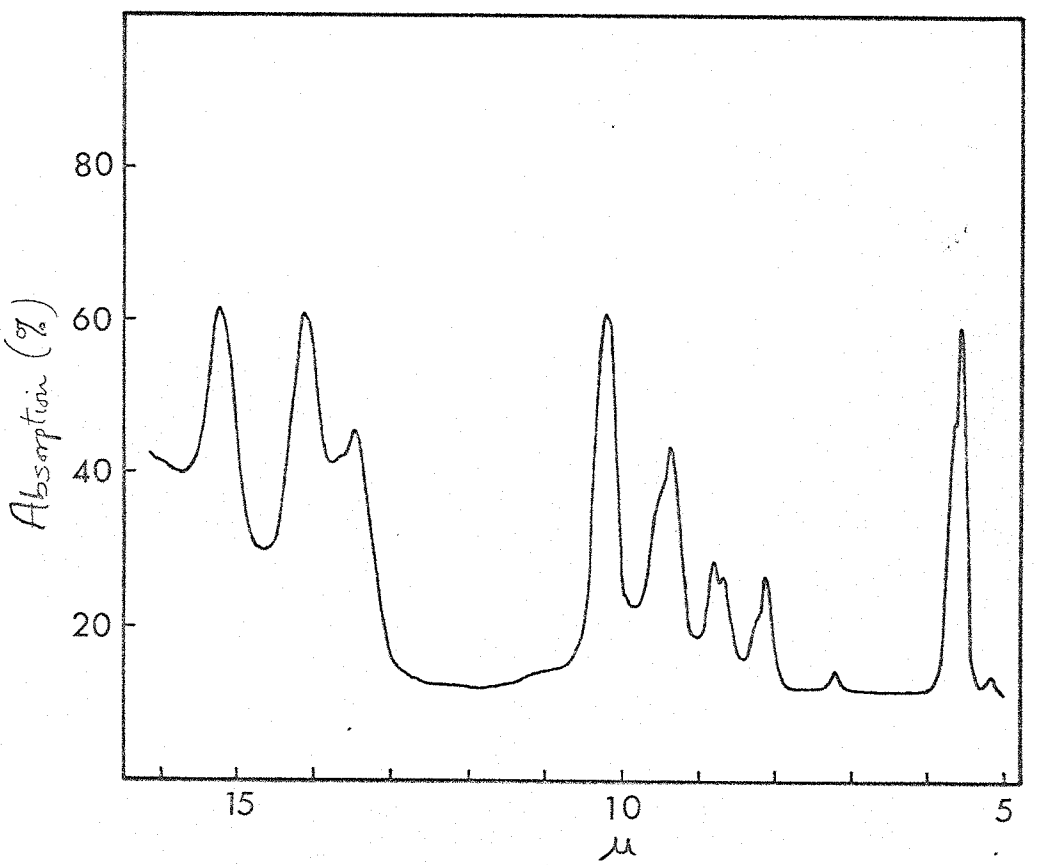

FIG. 1·10a. Infrared spectrum of $CHBr_2COCl$ - liquid

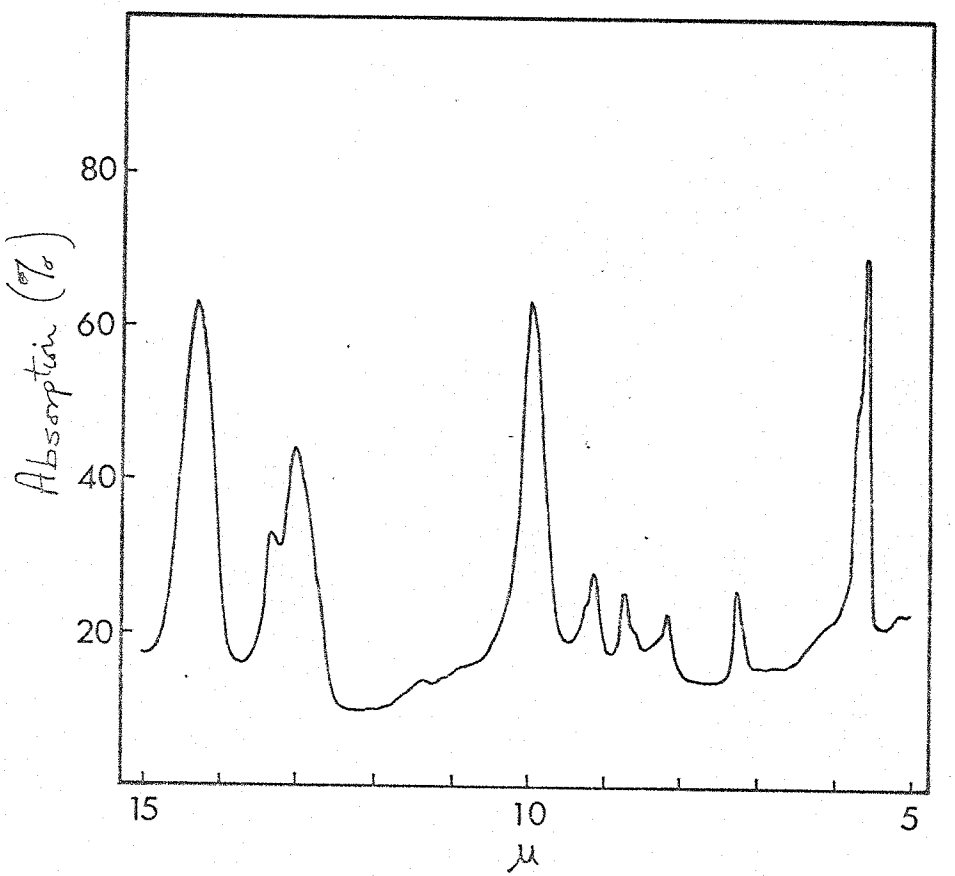

FIG. 1·10 b Infrared spectrum of $CHBr_2COCl$ – solid

TABLE 1.5

FREQUENCIES CALCULATED FOR VARIOUS VALUES OF THE AZIMUTHAL ANGLE

	Calculated frequencies				Observed frequencies	
(°): 0	45	90	135	180	More polar form	Less polar form
			CHF_2COCl			
3075	3074	3074	3074	3075	2976	2976
1769	1768	1765	1758	1751	1802	1810
1490	1490	1497	1500	1494	1361	1348
1293	1293	1295	1297	1297	-	-
1140	1173	1182	1168	1160	1145	1170
1127	1100	1100	1118	1140	1117	1099
1100	1096	1075	1056	1045	980	1075
709	705	748	794	813	822	835
635	681	678	655	635	655	602
549	539	534	521	502	525	542
498	445	426	451	492	463	503
415	416	380	359	357	349	405
211	207	209	243	258	233	211
			$CHBr_2COCl$			
2877	2876	2875	2876	2876	3003	3003
1749	1750	1751	1748	1745	1815	1786
1133	1131	1145	1153	1151	1232	1212
1115	1124	1117	1111	1110	1143	1155
1076	1071	1064	1049	1041	976	1070
741	768	785	772	754	752	738
680	664	674	686	681	719	662
575	584	583	613	653	534	553

/contd.over

Table 1.5 contd.

	Calculated frequencies					Observed frequencies	
(°):	0	45	90	135	180	More polar form	Less polar form
	519	516	510	499	489	460	489
	352	335	328	333	351	-	-
	334	301	251	246	250	253	340
	171	173	171	184	211	223	179
	138	130	125	162	157	163	148

Table 1.5 makes a comparison of observed and computed frequencies.

For a single conformation of the molecule CHX_2COCl, 15 fundamental modes of vibration are possible and, of these, one will involve predominantly a stretching of the carbonyl bond and another a stretching of the carbon-chlorine bond. Table 1.4 shows that considerably more than 15 bands have been observed in the infrared and Raman spectra of both vapour and liquid phases of CHF_2COCl and $CHBr_2COCl$. In particular, two carbonyl stretching bands were observed at around 1800 cm^{-1} for each compound and two carbon-chlorine stretching bands in the region 530-640 cm^{-1}. These results indicate that, like the monohalogen substituted and the dichloro-substituted acetyl halides, both CHF_2COCl and $CHBr_2COCl$ exhibit rotational isomerism, two stable conformations of the molecule co-existing in the vapour and liquid phases of the compounds. No evidence has been found to suggest the presence of more than two rotational isomers.

Several techniques have been used in attempts to obtain one-isomer solid spectra of the two compounds, viz. a) formation of the solid either by cooling a liquid film or by condensing the appropriate vapour onto a pre-cooled KBr disc; b) variation of the rate of cooling of liquid or vapour; and c) 'annealing' the film after its formation. It has, however, only been possible to obtain partial reductions in the intensities of bands due to the less stable isomer. There are two possible explanations for this. Crowder and Northam[40] have attributed a similar effect in 2-bromo-2-methyl propionyl bromide to a lack of crystallinity in the solid sample studied. Woodward and

Jonathan[4] on the other hand attribute the two-isomer solids of $CHCl_2COCl$ and $CHCl_2COBr$ to a very small energy difference between the rotational isomers in the liquid phases of these two compounds. In this case the explanation was supported by a report by Mizushima et al.[3] that the relative intensities of the carbon-carbon stretching bonds of each isomer of $CHCl_2COCl$ remain almost constant throughout the temperature range, room temperature down to -150°C. Although no measurements of this type have been made in the present study of CHF_2COCl and $CHBr_2COCl$ the second explanation is considered more reasonable in these cases.

The intensity changes observed on passing from the liquid to the solid state of $CHBr_2COCl$ have enabled an assignment of each frequency greater than 500 cm^{-1} to one or other of the rotational isomers. Solution spectra were recorded to support the assignments but were somewhat inconclusive due to relatively small intensity changes with variation in solvent polarity. The changes in the relative intensities of the two carbonyl stretching bands from non-polar CCl_4 solution to polar $MeNO_2$ solution were however sufficient to show that, as expected, the more polar isomer of $CHBr_2COCl$ is the more stable in the solid state.

The high frequency conformational assignments of CHF_2COCl have been based on intensity changes in the infrared spectra of solids showing varying degrees of equilibration to the more stable isomer. The data from two of these spectra are given in Table 1.4. Conformational assignments for the skeletal vibrations of both compounds will be

discussed below.

The assignment of frequencies to particular vibrational modes of the isomers has relied on group frequency considerations and the normal coordinate analysis results given in Tables 1.6 and 1.7. The latter indicate a coupling of pure stretching and bending modes in some instances, particularly for the difluoro-compound, and therefore these vibrational assignments are considered approximate. Complete assignments are given in Table 1.4, and important features are now discussed.

Carbonyl Stretching Frequencies

Bellamy and Williams[41,42] have studied the carbonyl frequencies of α-halogenated ketones and found them to be controlled by two factors. Firstly, interaction of the carbon-α-halogen and carbon-oxygen dipoles decreases the polarisation of the C=O bond and consequently increases the carbonyl frequency from its value in the unsubstituted acetyl halide. Secondly, interaction between the α-halogen atom and the carbonyl halogen leads to a reduction in the electronegativity of the carbonyl halogen and a lowering in the carbonyl frequency, since this is primarily governed by the electronegativity of the group attached to it. Table 1.8 makes a comparison of the value of the carbonyl frequency of each rotational isomer with that of the parent acetyl halide and includes the data previously reported for $CHCl_2COCl$ and $CHCl_2COBr$[4]. Although no quantitative significance may be attached to these relatively small frequency shifts the data indicate

that in the eight isomers considered the interaction between α-halogen atoms and the carbonyl halogen is dominant.

The previous investigation of $CHCl_2COCl$ and $CHCl_2COBr$ found in each case a less polar conformation $\theta = 0^\circ$ and a more polar conformation $\theta = 90^\circ - 135^\circ$. The α-halogen-oxygen interaction is greater in these more polar forms than it is in the less polar isomers, while the α-halogen - carbonyl halogen interaction is similar or slightly less (this is confirmed by the results of the potential energy calculations). The above theory therefore correctly predicts that the more polar isomers of these compounds will have the higher carbonyl frequency. The data of Table 1.8 indicate that the rotational isomers of $CHBr_2COCl$ have similar conformations to the corresponding isomers of $CHCl_2COCl$ and $CHCl_2COBr$. The higher carbonyl frequency of the more polar isomer of $CHBr_2COCl$ is therefore explained.

The data for CHF_2COCl are not consistent with those of the other disubstituted acetyl halides, the less polar isomer having the higher carbonyl frequency. Rationalisation of this fact in terms of the interaction effects would require that the α-halogen - carbonyl halogen interaction is predominantly greater in the more polar isomer than it is in the less polar isomer, or that the α-halogen - oxygen interaction is predominantly less in the more polar form. Assuming a less polar conformation $\theta = 0^\circ$ for CHF_2COCl this implies a more polar conformation for which θ is in the region of 60°. In view of the potential energy calculations this is unreasonable.

TABLE 1.6

CHF_2COCl CONFORMATION $\theta = 0^\circ$

COMPUTED POTENTIAL ENERGY DISTRIBUTION AMONG FORCE CONSTANTS[a]

Frequency	Energy Distribution (%)[b]	Force constant
3075	75	K(C-H)
	22	F(F...H)
1769	85	K(C=O)
	5	K(C-C)
1490	50	F(F...H)
	28	K
	11	H(H-C-F)
	6	K(C-F)
1293	29	F(F...H)
	19	H(C-C-H)
	19	K
	18	F(C...H)
	7	H(H-C-F)
1140	79	K(C-F)
	14	F(F...H)
	5	F(F...C)
1127	15	K(C-C)
	14	K(C-F)
	13	H(C-C-Cl)
	10	F(F...C)
	10	F(C...H)
	7	K(C=O)
	6	H(O=C-Cl)
	5	F(F...H)
	5	H(C-C-H)

Table 1.6 contd.

Frequency	Energy Distribution(%)[b]	Force constant
	36	K(C-F)
	30	K(C-C)
1100	13	F(F...H)
	7	H(F-C-F)
	5	F(F...F)
	26	F(F...F)
	17	F(F...C)
709	11	K
	10	K(C-F)
	9	H(H-C-F)
	26	K(C=O)
	10	H(C-C=O)
635	10	H(O=C-Cl)
	6	F(O...C)
	6	F(C...H)
	23	F(Cl...O)
	20	F(F...C)
549	16	K(C=O)
	15	F(F...F)
	11	H(F-C-F)
	71	F(F...C)
498	14	H(C-C-F)
	7	F(F...H)
	20	F(F...C)
	18	F(Cl...O)
	15	H(C-C=O)
415	9	H(F-C-F)
	8	H(O=C-Cl)
	7	K(C=O)
	37	F(Cl...C)
	13	H(C-C-Cl)
211	12	F(F...C)
	11	H(C-C=O)
	6	H(O=C-Cl)

a. Computed distributions for other conformations are similar.

b. Only force constants possessing $\geq$ 5% total energy are shown.

TABLE 1.7

$CHBr_2COCl$ CONFORMATION $\theta = 0^{\circ}$

COMPUTED POTENTIAL ENERGY DISTRIBUTION AMONG FORCE CONSTANTS

Frequency	Energy Distribution (%)	Force constant
2877	86	K(C-H)
	10	F(Br...H)
1749	88	K(C=O)
1133	28	F(C...H)
	27	F(Br...H)
	26	H(C-C-H)
	7	K
1115	63	F(Br...H)
	11	H(H-C-Br)
	8	K
	5	F(C...H)
1076	46	K(C-C)
	9	H(C-C=O)
	9	F(Br...H)
	7	K(C-Cl)
	7	H(O=C-Cl)
741	19	K(C-Br)
	17	H(C-C=O)
	14	F(Br...H)
	12	K(C-C)
	12	F(O...C)
	7	K(C-Cl)
680	61	K(C-Br)
	17	H(C-C-Br)
	10	F(Br...H)
	8	F(Br...C)

Table 1.7 contd.

Frequency	Energy Distribution (%)	Force constant
	25	K(C-Cl)
	22	F(Cl...C)
	8	H(O=C-Cl)
575	6	K(C-Br)
	6	F(Br...H)
	6	H(C-C-Br)
	5	F(C...H)
	42	F(Cl...O)
	18	K(C-Cl)
519	15	H(O=C-Cl)
	9	F(Br...C)
	64	F(Br...C)
352	21	H(C-C-Br)
	14	K(C-Br)
	27	F(Br...C)
	22	K(C-Br)
334	13	H(C-C-H)
	6	F(O...C)
	6	F(Cl...C)
	63	F(Br...Br)
171	14	H(Br-C-Br)
	25	F(Br...C)
	22	F(Cl...C)
138	15	H(C-C-Br)
	8	H(C-C-Cl)

TABLE 1.8

VALUES FOR ν(C=O) IN THE VAPOUR PHASE (cm^{-1})

Molecule	ν (C=O)	$\Delta\nu$
CH_3COCl [a]	1822	-
CHF_2COCl M	1802	-20
CHF_2COCl L	1810	-12
$CHBr_2COCl$ M	1815	-7
$CHBr_2COCl$ L	1786	-36
$CHCl_2COCl$ M [c]	1818	-4
$CHCl_2COCl$ L [c]	1786	-36
CH_3COBr [b]	1821	-
$CHCl_2COBr$ M [c]	1815	-6
$CHCl_2COBr$ L [c]	1786	-35

[a] J. Overend, R.A. Nyquist, J.C. Evans and W.J. Potts, Spectrochim.Acta 17, 1205 (1961).

[b] L.C. Hall and J. Overend, Spectrochim.Acta 23, 2535 (1967).

[c] A.J. Woodward and Neville Jonathan, J.Phys.Chem., 74, 798 (1970).

TABLE 1.9

COMPUTED CARBONYL FREQUENCIES (cm^{-1})

Molecule	$\theta^{(o)}$ 0	45	90	135	180
CHF_2COCl	1769	1768	1765	1758	1751
$CHCl_2COF$	1784	1786	1788	1785	1783
$CHCl_2COCl$	1747	1748	1750	1747	1745
$CHCl_2COBr$	1745	1747	1748	1746	1744
$CHBr_2COCl$	1749	1750	1751	1748	1745

Table 1.9 gives the computed carbonyl frequencies for the series $CHCl_2COX$ and for the two molecules studied here. As mentioned previously, these frequencies have been computed assuming no interactions between the two rotating groups of the molecule so that any variation with azimuthal angle θ is a result of changes in the inverse kinetic matrix G with θ. It can be seen that the computed carbonyl frequencies of $CHCl_2COX$ and $CHBr_2COCl$ are almost invariant with θ but for CHF_2COCl this is not so. If one assumes the same stable conformations for CHF_2COCl as have been considered for the other molecules, the carbonyl frequency computed for the less polar isomer is about 5-10 wave-numbers higher than that of the more polar isomer, in agreement with the experimental data. It would appear therefore that the rotational isomers of CHF_2COCl are such that a) the α-halogen - carbonyl interactions produce similar displacements of their carbonyl frequencies from the acetyl chloride frequency (which could indicate slightly different conformations to those of corresponding isomers of other disubstituted acetyl halides); and b) due to a "kinetic energy effect" the less polar isomer has the higher carbonyl frequency.

Carbon-Halogen Stretching Vibrations

The region 1000 - 1200 cm^{-1} of the difluoroacetyl chloride spectrum is complicated. Not only is there overlap between a (C-H) bending mode, a (C-C) stretching mode, and the symmetric and asymmetric stretching modes of the ($C-F_2$) group, but the calculation of normal

vibrations shows a certain degree of mixing of these "pure" modes. Assignments for this region are therefore tentative.

The assignment of the carbon-halogen stretching modes of $CHBr_2COCl$ given in Table 1.4 may at first sight seem surprising, the ν(C-Cl) vibrations of the two isomers being assigned to lower frequencies than the symmetric and asymmetric $\nu(C-Br_2)$ modes.

The data of Tables 1.6 and 1.7 however show that for both $CHBr_2COCl$ and CHF_2COCl the assignment of observed frequencies to carbon-chlorine stretching modes is very approximate. The normal vibrations of the molecules which have been assigned in this way can be seen to be a combination of (C-Cl) stretch and several other less energetic "pure" modes. For $CHBr_2COCl$ this mixing gives the normal vibration a lower frequency than the vibrations which involve predominantly stretching in the $(C-Br_2)$ group.

Carbon-Hydrogen Vibrations

It has not been possible to assign bands to the lower frequency (C-H) bending mode of difluoroacetyl chloride due to the overlap previously mentioned. The assignments of other caebon-hydrogen modes are however straightforward.

Skeletal Vibrations

Raman spectra were recorded for solutions of $CHBr_2COCl$ in an effort to obtain conformational assignments for these frequencies. However the data obtained were inconclusive. Evidence for the assignments have therefore been sought from the calculated frequencies and

comparison with the Raman spectra of the dichloroacetyl halides. A similar approach has been applied to the analysis of CHF_2COCl skeletal frequencies.

It was mentioned previously that assignments based on a comparison of observed and calculated frequencies must be tentative due to the less than ideal molecular model used for the calculations. However the present assignments have been made with considerable confidence because of the very good agreement between the two sets of data (see Table 1.5). This is particularly true for CHF_2COCl where the observed skeletal frequencies can readily be split into two sets; one agreeing with frequencies computed for $\theta = 0^\circ$ (assumed less polar) and the other with those for $\theta = 135^\circ$. Although the agreement is not so good for the frequencies of $CHBr_2COCl$ (computed frequencies for $\theta = 0^\circ$ and $\theta = 135^\circ$ or 180° giving the most reasonable fit), the assignments are supported by the very great similarity in the Raman spectra of this molecule and the spectra of the dichloroacetyl halides.

An indication of the normal modes of vibration responsible for these low frequencies may be obtained from the data of Tables 1.6 and 1.7.

Certain low frequencies were not observed, namely the torsional bands for each isomer and the frequencies for out-of-plane deformation of the (COCl) group. In the case of $CHBr_2COCl$, bands apparently due to a deformation of the (C-C-Br) bond angles, have also not been observed.

The validity of the complete conformational assignments was tested by application of the Mizushima Sum Rule to the observed frequencies of Table 1.5. This rule equates the sum of the squares of the frequencies of one rotational isomer with that of the other isomer, and its derivation is given in Appendix 1.2. The results are given in Table 1.10, which shows that the agreement is good.

Calculated frequencies

The agreement between computed and observed frequencies greater than 1000 cm^{-1} could be improved by a suitable refinement of the force constants. However, since force constants have been transferred from the analyses of similar molecules in order to determine the stable conformations and to assist the frequency assignments, such refinement is initially not justified. The refinement would in any case require prior knowledge of the conformations. Having obtained evidence that the less polar of the rotational isomers of CHF_2COCl and $CHBr_2COCl$ are the conformations $\theta = 0^\circ$, a refinement of force constants to give agreement between the frequencies computed for $\theta = 0^\circ$ and the observed frequencies of the less polar isomer would be justified. This refined set of force constants could be used to compute frequencies for conformations in the range $\theta = 90^\circ - 180^\circ$ for tentative comparison with observed frequencies of the more polar isomer. Time has not allowed such an analysis.

TABLE 1.10

MIZUSHIMA SUM RULE AGREEMENT FOR CHF_2COCl AND $CHBr_2COCl$

Molecule	More polar $\sum_i \nu_i^2 \times 10^{-7}$	Less polar $\sum_i \nu_i^2 \times 10^{-7}$	Difference (%)
CHF_2COCl	1·925	1·950	1·3
$CHBr_2COCl$	1·770	1·779	0·0

1.5 The Rotational Isomers

The evidence so far obtained for the nature of the stable conformations of CHF_2COCl and $CHBr_2COCl$ is summarised below.

Source of Evidence	Conformations			
	CHF_2COCl		$CHBr_2COCl$	
	L	M	L	M
a. Potential Energy Calculations	0°	90°-180°	0°	90°-180°
b. Carbonyl Frequency Data			0°	90°-135°
c. Computed/Observed Frequency Agreement	0°	90°	0°	90° or 135°

A further indication can be obtained by use of the so-called product rule. The derivation of this rule is given in Appendix 1.3. It may be written:

$$\frac{\Pi \nu_M^2}{\Pi \nu_L^2} \qquad \frac{|G(\theta_M)|}{|G(0^\circ)|} \qquad \ldots \quad (1.30)$$

where G is the inverse kinetic energy matrix which is dependent only on the azimuthal angle θ. It is assumed that the less polar isomer is the conformation $\theta = 0^\circ$ and attempts are then made to determine the conformation θ_M of the more polar isomer. Table 1.11 gives calculated values of the right-hand side of Equation (1.30) for various values of θ_M, together with the experimental values $\Pi \nu_M^2 / \Pi \nu_L^2$ calculated from the observed frequencies of Table 1.5. Although only 12 of the 13 frequencies are known for each isomer of the dibromo-compound, the

TABLE 1.11

VALUES OF $|G(\theta_M)| / |G(0^\circ)|$

θ_M (°)	CHF_2COCl	$CHBr_2COCl$
0	1·00	1·00
45	0·85	0·70
90	0·72	0·44
135	0·94	0.87
180	1·13	1·24
Experimental $\prod \nu_m^2 / \prod \nu_L^2$	0·68	0·91

computed frequencies of these unobserved bands show little variation with azimuthal angle and their neglect will have only a small effect on the value of $\prod \nu_M^2 / \prod \nu_L^2$.

The best fit between experimental and calculated values for difluoroacetyl chloride is for an azimuthal angle $\theta_M \approx 90^\circ$. For dibromoacetyl chloride it is for an angle $\theta_M \approx 135^\circ$.

Bearing in mind the limitations of experiment and calculations it is reasonable only to suggest from the evidence presented above that for both difluoroacetyl chloride and dibromoacetyl chloride, the less polar rotational isomer is that conformation with $\theta \approx 0^\circ$ and for the more polar isomer θ lies in the range $90 - 135^\circ$.

APPENDIX 1.1

For CHX_2COCl the conformation $\theta = 0^\circ$ (see Fig.1.1) is the only one possessing an element of symmetry; this being the plane of symmetry containing the O-C-C-H skeleton. The conformation $\theta = 0^\circ$ therefore belongs to the C_s point group while all others belong to the C_1 point group. The character table for the C_s point group is

C_s	I	$\sigma(xy)$	
A'	+ 1	+ 1	x, y, R_z, α_{xx}, α_{yy}, α_{zz}, α_{xy}
A"	+ 1	- 1	z, R_x, R_y, α_{xz}, α_{yz}

The behaviour of the normal modes with respect to the various symmetry operations is described in terms of characters of which a symmetry operation consists. Thus +1 and -1 characters represent symmetric and anti-symmetric behaviour respectively of a normal mode under a symmetry operation. From the character table it is possible to determine the number of normal modes of a particular symmetry species, and their activity in the infrared and Raman spectra. The total number of normal modes of a symmetry species is given by

$$n_i = \frac{1}{N} \sum_R U_R \, (\pm 1 + 2 \cos \phi_R) \, \chi_i (R)$$

where

N = Order of the group (i.e. the number of symmetry elements in the group)

U_R = Number of atoms that remain unchanged under the symmetry operation R.

$\chi_{i(R)}$ = Character of the symmetry element in the i^{th} species

The plus sign is used if R is a proper rotation through ϕ whereas the minus sign is used for an improper rotation through ϕ. The summation extends over all the symmetry elements.

The identity operation, I, corresponds to a proper rotation through 0° and leaves all the seven atoms of CHX_2COCl unchanged, i.e. $\phi = 0$ and $U_R = 7$. The σ_{xy} operation corresponds to an improper rotation through 0° and leaves five atoms unchanged i.e. $\phi = 0$ and $U_R = 5$. The total number of normal modes in species A' and A" are therefore

$$n(A') = \frac{1}{2}\left[(7)\,(1 + 2\cos 0^\circ)\,(+1) + 5(-1 + 2\cos 0^\circ)(+1)\right]$$

$$= \frac{1}{2}\left[(7)\,(3)\,(+1) + (5)\,(1)\,(+1)\right] = 13$$

$$n(A'') = \frac{1}{2}\left[(7)\,(3)\,(+1) + (5)\,(1)\,(-1)\right] = 8$$

This however includes pure rotations and translations, i.e.

$$\Gamma_{Total} = \Gamma_{Vib} + \Gamma_{Rot} + \Gamma_{Trans}$$

$$= 13A' + 8A''$$

The number of pure translations under a symmetry operation is given by

$$n_i\,(T) = \frac{1}{N}\sum_R\,(\pm 1 + 2\cos\phi_R)\,\chi_i\,(R)$$

Therefore

$$n_{A'}(T) = \frac{1}{2}\left[(3)(+1) + (1)(+1)\right] = 2$$

$$n_{A''}(T) = \frac{1}{2}\left[(3)(+1) + (1)(-1)\right] = 1$$

and

$$\Gamma_{Trans} = 2A' + A''$$

This would give

$$\Gamma_{Rot} = A' + 2A''$$

Therefore

$$\Gamma_{Vib} = 10A' + 5A''$$

That is, ten of the fundamental vibrations of CHX_2COCl are A' and the remaining five are A".

Infrared and Raman activity

If the vibrational modes of a given species are to be infrared active the quantity

$$n_i(\mu) = \frac{1}{N}\sum_R (\pm 1 + 2\cos\phi_R)\chi_i(R)$$

should have a value other than zero. For CHX_2COCl, $n_{A'}(\mu) = 3$ and $n_{A''}(\mu) = 1$ and all fifteen fundamentals are allowed in the infrared.

If the modes are to be Raman active the quantity

$$n_i(\alpha) = \frac{1}{N}\sum_R 2\cos\phi_R (\pm 1 + 2\cos\phi_R)\chi_i(R)$$

associated with the polarisability α should have a value other than zero. The equation gives $n_{A'}(\alpha) = 8$ and $n_{A''}(\alpha) = 4$ for CHX_2COCl hence all fifteen fundamentals are Raman active.

Combinations and Overtones

The overtone of both the species A' and A" and their combinations are allowed both in the infrared and Raman.

APPENDIX 1.2

The Mizushima Sum Rule (43)

If the solutions of the secular equation

$$\left| GF - \lambda E \right| = 0$$

are $\lambda_1, \lambda_2 \ldots \lambda_n$,

then

$$\sum_{i=1}^{n} \lambda_i = \sum_{k,\ell=1}^{n} G_{k\ell} F_{k\ell}$$

Since in the analysis cis interactions are neglected, all the elements $F_{k\ell}$ corresponding to $G_{k\ell}$ containing the azimuthal angle θ vanish and the right-hand side is therefore independent of the degree of internal rotation, i.e.

$$\sum_{i=1}^{n} \nu_i^2 = \text{constant}$$

This is the sum rule which has been used to check the conformational assignments for the observed frequencies of the dihaloacetyl chlorides.

APPENDIX 1.3

The Product Rule (43)

The product of normal frequencies of a molecular configuration can be expressed:

$$4\pi^2 \prod_{i=1}^{n} \nu_i^2 = |G||F|$$

Neglecting cis interactions, the F matrix becomes common to all conformations and therefore,

$$\frac{\prod_{i=1}^{n} \nu_i'^2}{\prod_{i=1}^{n} \nu_i^2} = \frac{|G'|}{|G|}$$

REFERENCES : PART 1

1. R.A. Pethrick and E. Wyn-Jones, Quart.Revs. 3(23),301 (1969).

2. S. Mizushima, "Structure of Molecules and Internal Rotation", Academic Press, New York (1954).

3. S. Mizushima et al., Spectrochim.Acta, 13, 161 (1958).

4. A.J. Woodward and Neville Jonathan, J.Phys.Chem., 74, 798 (1970).

5. J.B. Hendrickson, J.Am.Chem.Soc., 83, 4537 (1961); 84, 3355 (1962); 86, 4854 (1964); 89, 7036, 7043, 7047 (1967).

6. R.L. McCullough and P.E. McMahon, J.Phys.Chem., 69, 1747 (1965).
   R.A. Scott and H.A. Scheraga, J.Chem.Phys., 44, 3054 (1966).

7. R.A. Scott and H.A. Scheraga, J.Chem.Phys., 42, 2209 (1965).

8. M. Cignitti and T.L. Allen, J.Phys.Chem., 68, 1292 (1964).

9. L. Pauling, "The Nature of the Chemical Bond", Cornell University Press, New York, 3rd ed., p.130 (1960).

10. W.L. Bade, J.Amer.Phys., 27, 1280, 1284 (1957).

11. N.R. Kestner and O. Sinanoglu, ibid., 45, 194 (1966).

12. Tables of inter-atomic distance and configuration in molecules and ions (The Chemical Society, London).

13. K.S. Pitzer, Advan.Chem.Phys., 2, 59 (1959).

14. J.A.A. Ketalaav, "Chemical Constitution", Elsevier Publishing Co., Amsterdam (1958).

15. I.Amdur and A.L. Harkness, J.Chem.Phys., 22, 664 (1954).
    I. Amdur and E.A. Mason, ibid., 23, 415 (1915).

16. M.S. Newman (Ed.) Steric Effects in Organic Chemistry, John Wiley and Sons, Inc., New York (1956). Chap.12 by F.H. Westheimer.

17. J.B. Hendrickson, J.Am.Chem.Soc., 83, 4537 (1961).

18. A. Bondi, J.Phys.Chem., 68, 441 (1964).

19. A. Veillard, Chem.Phys.Lett., 3(3), 128 (1969).
R.J. Abraham and K. Parry, J.Chem.Soc.(B), 539 (1970).

20. J.W. Smith, "Electric Dipole Moments", Butterworths Sci.Pub. (1955).

21. E.B. Wilson Jr., J.C. Decius and P.C. Cross, "Molecular Vibrations" McGraw Hill Book Co. (1955).

22. Mansel Davies (Ed.), "Infrared Spectroscopy and Molecular Structure", Chap.V by I.Mills.

23. E.B. Wilson, J.Chem.Phys., 7, 1047 (1939).

24. E.B. Wilson, ibid., 9, 76 (1941).

25. See ref. 22.

26. H.C. Urey and C.A. Bradley, Phys.Rev., 38, 1969 (1931).

27. T. Shimanonchi, J.Chem.Phys., 17, 245 (1949).

28. J. Overend and J.R. Scherer, J.Chem.Phys., 32, 1296 (1960).

29. Refs.27 and 28.

30. A.Y. Khan, Ph.D. thesis, Southampton University (1969).

31. I. Nakagawa et al., J.Chem.Phys., 20, 1720 (1952).

32. J.H. Schachtschneider, "Vibrational Analysis of Polyatomic Molecules", Shell Development Co., Emeryville, California.

33. M. Prober, J.Am.Chem.Soc., 75, 970 (1953).

34. A.B.Sen and K.C. Joshi, J.Indian Chem.Soc., 25, 483 (1948).

35. Manual of the Grubb-Parsons G.S.2A Ir Spectrometer.

36. Manual of the Perkin-Elmer 225 Ir Spectrometer.

37. Manual of the Spex Raman Spectrometer (Model 1401).

38. C.R. Wellman, Anal.Chem., 36, 697 (1964).

39. N. Sheppard, Advan.Spectr., 1, 288 (1959).

40. G.A. Crowder and F. Northam, J.Mol.Spec., 26(1), 98 (1968).

41. L.J. Bellamy and R.L. Williams, J.Chem.Soc., London, 4295 (1957).

42. L.J. Bellamy and R.L. Williams, ibid., 3465 (1958).

43. S. Mizushima et al., J.Chem.Phys., 21, 215 (1953).

PART 2

INFRARED SPECTRA OF NO ADSORBED ON ALKALI HALIDE FILMS

2.1 INTRODUCTION

Almost every experimental technique available to the chemist has at some stage been applied to the study of the solid-gas interface, and it is generally recognised that, to date, the application of infrared spectroscopy has been the most valuable. The success is due to the superior sensitivity of the technique in this field. This is a result of the somewhat fortuitous circumstance that the extinction coefficient of a molecular vibration is considerably enhanced when the parent molecule is in the adsorbed state. In some instances this increase has been by a factor of two orders of magnitude[1]. The absorption spectra obtained (reflection spectra have been recorded only in very few instances) have usually been compared with the known absorptions of the adsorbate in the gas, liquid and solid phases. From the shape of the absorption bands, shifts in frequencies and their intensities, conclusions have been drawn about the chemical and physical properties of the adsorbate, type of surface bonding and surface site, orientation of the adsorbate and possible changes in its structure.

Because of their catalytic importance, the vast majority of these studies have employed various forms of silica or alumina either as the adsorbent or as a support for highly dispersed metal adsorbents. A large number of scientific papers and detailed review articles have been published on these systems. Of particular importance are the recent monographs of L.H. Little and M.L. Hair[2,3].

There are two basic requirements for any i.r./adsorption system. Firstly, the adsorbent must be, to some extent, transparent to infrared radiation. Incident energy may be reduced as a result of scattering and absorption by the adsorbent. Secondly, despite the advantage of enhanced extinction coefficients, it is still necessary to have a large number of adsorbent-adsorbate interfaces in the infrared beam to produce a measurable absorption of radiation by the adsorbed species (or the surface active species if these are being investigated, e.g. the surface hydroxyl groups of silica gel). An adsorbent of high specific surface is therefore required. Furthermore, the surface area must be sufficiently large to allow spectra to be recorded for low surface coverages of adsorbate. At high surface coverages, interactions between adsorbed species adjacent on the surface may become significant,making the interpretation of spectra difficult. Whenever possible, it has been found advisable to measure the surface coverage for which spectra are obtained[4].

Studies of the classical adsorbents (silica, alumina etc.) have been restricted to rather limited spectral regions due to strong absorption of radiation by the adsorbent. It has only been possible to investigate a few high frequency stretching modes of the adsorbate-adsorbent system. Moreover, the surfaces of these adsorbents are not always well-defined from the chemical point of view and usually manifest large energetic heterogeneity which introduces serious difficulties into any attempt to treat the results quantitatively.

In 1964, Y. Kozirovski and M. Folman[5] pioneered the production of high-surface-area alkali halide films suitable for spectroscopic studies of adsorption. The films are transparent down to 200 cm^{-1} or further (depending on the salt used) and the difficulties arising from surface heterogeneity are markedly diminished. Several studies of small molecules adsorbed on different alkali-halide films have since been reported, and in some instances, energies of adsorption and spectral shifts have been calculated for comparison with experimental data. This work will be discussed briefly in a later section.

The present work has used a similar i.r./adsorption system to study the adsorption of nitric oxide on various alkali halide surfaces. The interest in NO arises from its odd electron structure and the possibility that it might exist in a dimerised form in the adsorbed state.

2.2 EXPERIMENTAL

2.2.1 Development of the infrared/adsorption system

A low temperature infrared/adsorption cell was developed for the in situ preparation of high-surface-area alkali halide films. Figure 2.1 shows the initial design of this apparatus which followed that reported by Kozirovski and Folman[6]. Made of stainless steel, the cell consisted of a Dewar and two demountable jackets. The inner compartment formed by jacket A and the Dewar served as an adsorption cell which could be evacuated via tube C. Since this part of the apparatus was to be used at low temperatures, vacuum seals could not be maintained with O-rings: consequently a Teflon gasket was used between the flange of A and the Dewar. KBr windows were attached to A by the method of Kozirovski and Folman. Rings of copper foil were soldered to brass rings attached to A, and the windows were then sealed with Araldite to the copper foil.

The outer compartment formed by jacket B could be evacuated via port E and was rendered vacuum-tight by a standard rubber O-ring. Its purpose was to prevent condensation of water vapour on the windows of the adsorption cell. Windows were attached to this jacket with Hysol Epoxi-Patch (The Dexter Corporation, London) - an epoxy adhesive-sealant.

The high surface area films were deposited on a cooled central window ($-196^{\circ}C$) by evaporating the alkali halides from a small tantalum furnace positioned opposite to the window during deposition. The window was held in a copper block soldered to the base of the Dewar. Copper foil was used to ensure good thermal contact between the window and the

block. Vertical movement of the furnace was possible within tube D; a vacuum seal being maintained by two rubber O-rings.

Although built to this design the apparatus was never used in this form. Tube C was considered to be of too narrow a bore to provide efficient pumping of the adsorption cell. An additional flange section, fitted with a $\frac{1}{2}$" i.d. pumping port, was therefore introduced between the Dewar and the two jackets. This design is shown in Figure 2.2. Iron-constantan thermocouples, for measuring the temperature of the central window and the copper block, were admitted via the new port. Gas was still to be admitted to the adsorption cell through Tube C. The method of connecting the cell to the Pyrex vacuum line, shown in Figure 2.2, enabled the apparatus to be dismantled fairly readily.

The cell was soon found to have two further inadequacies. Firstly, the method of attachment of windows to the inner jacket was unsatisfactory for a) it was difficult to obtain a good vacuum seal, and b) windows would often crack on cooling, even though the arrangement was intended to reduce thermal strains in them. It was therefore decided to omit the inner jacket, for since the dead space of the adsorption cell was in any case too large to permit measurement of the films' surface areas, its omission could not affect the amount of data which might be obtained. Secondly, the construction of the Dewar was unsatisfactory. Its base had been made by welding a plate of stainless steel across the bottom of a stainless steel tube. On cooling with liquid nitrogen, immense thermal strains were produced in the weld due to the contraction of the

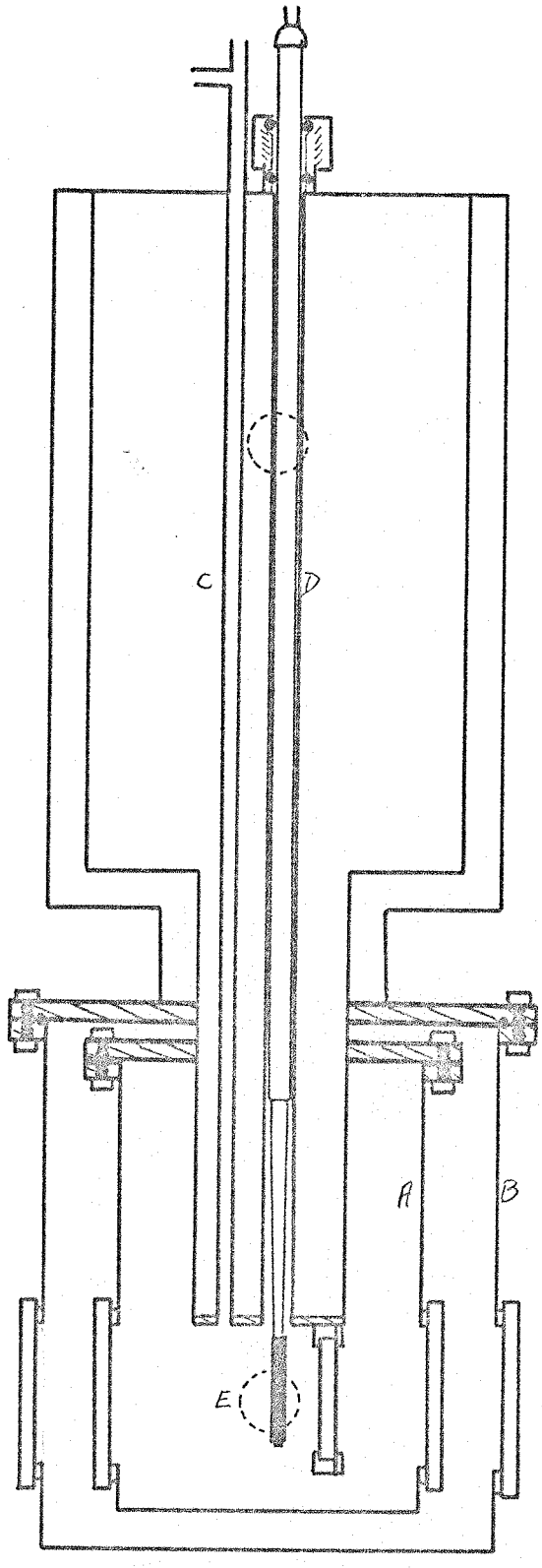

FIG. 2·1 The Initial Design of the I.r. Adsorption System

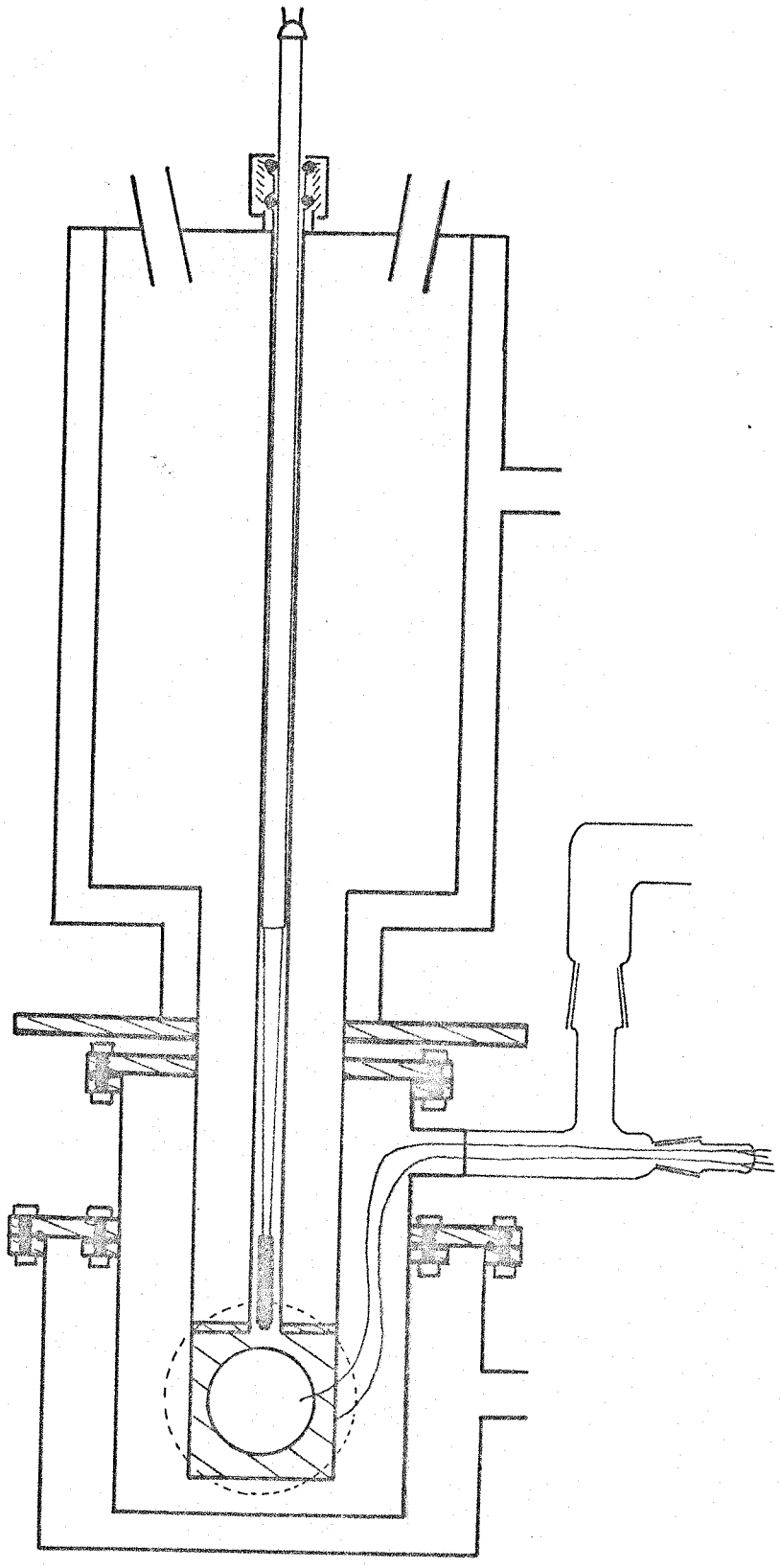

FIG. 2·2 First Modification of the I.r./Adsorption System

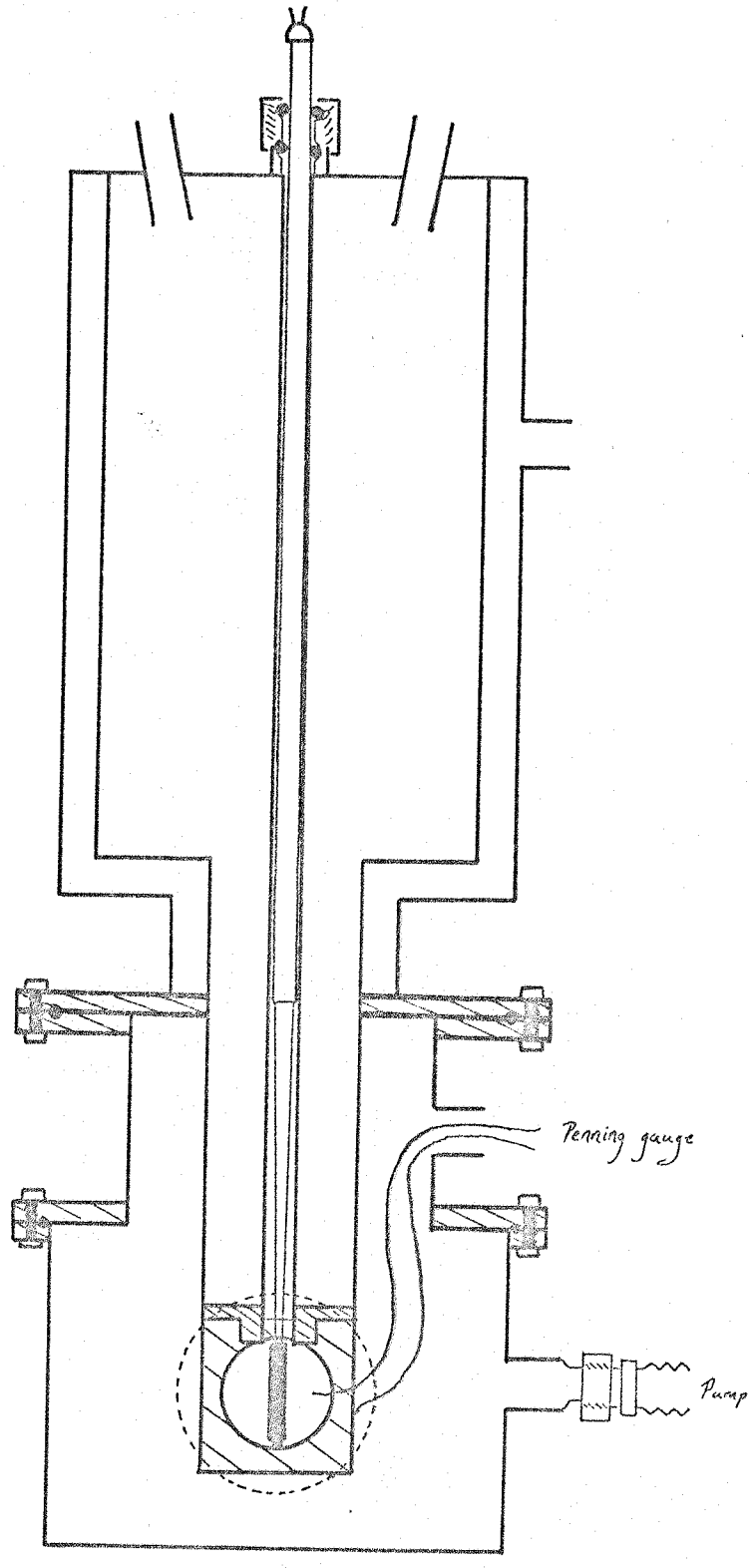

FIG. 2.3 The Final Design of the I.r. / Adsorption System

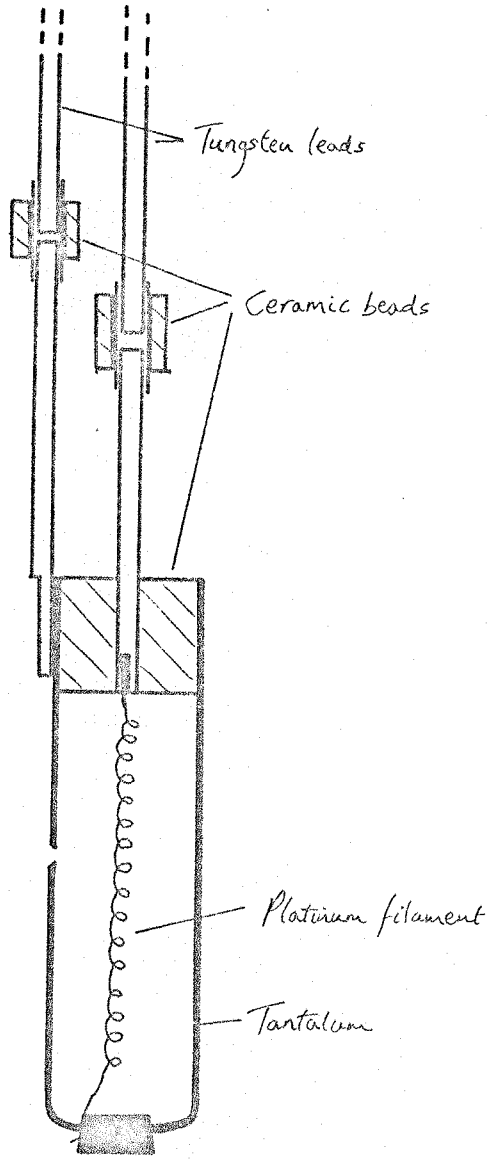

FIG. 2·4 The Tantalum Furnace

two pieces of metal in different directions. Many attempts were made to seal the resulting leaks, but eventually it was decided to have the lower section of the Dewar remade from a solid block of stainless steel. The final arrangement is shown in Figure 2.3. The pumping was switched to the port in jacket B while the port in the flange section was used to mount a Penning gauge.

Several designs for the tantalum furnace were tested. Its limiting dimensions were 1 cm in diameter and 3 cm in length, and it had to maintain a 0·1g. sample of alkali halide at a temperature just below the melting point for at least one hour, i.e. the maximum temperature required was about 800°C. Figure 2·4 shows the final design. The furnace was machined from tantalum rod (0·45 mm. diam.) and was heated by means of the platinum coil. A current of 6 amps (12 watts) was sufficient to deposit a 0·1 g. sample of NaCl in about one hour.

Kozirovski and Folman found that to ensure reproducible results it is necessary to anneal the alkali halide films at -78°C for a period of about 24 hours. The final problem was therefore to maintain the film at this temperature overnight. A unit was first developed for pumping methanol around a closed system involving the cell Dewar. External to the cell the methanol was pumped through a metal box cooled by dry ice/acetone. With this arrangement the central window of the cell could be kept at $\sim$ -70°C overnight. The system was somewhat inflexible, however; in particular it prevented a rapid change to liquid nitrogen coolant. This problem was overcome by using cold

nitrogen gas as the coolant. A coil of nichrome wire wound on a suitable former was used to boil liquid nitrogen in a 25 litre Dewar; the cold gas being led into the cell Dewar. The efficiency of the system was increased by passing the outflowing gas from the cell around the outside of the inlet tube. It was found that the central window could be maintained at -80°C for ten hours with 25 litres of liquid nitrogen. By simply increasing the rate of boiling of the liquid nitrogen, any temperature from -80°C down to almost liquid nitrogen temperature could be obtained, and this proved ideal for recording spectra at varied temperatures.

The complete vacuum system was mounted on a trolley to allow routine use of the spectrometer while adsorption studies were not in progress. The stainless steel cell was supported in a position overhanging the end of the trolley to enable it to be positioned in the i.r. beam of the spectrometer. It was connected to the Pyrex vacuum line by a $\frac{1}{2}$" flexible metal coupling. A two-stage mercury diffusion pump, fitted with suitable cold traps and backed by a rotary pump was used for evacuating the system. The cell could be isolated from the diffusion pump by a $\frac{1}{2}$" bore glass tap situated on the pump side of the flexible metal coupling. The diffusion pump was also used to pump a simple gas handling line consisting of two gas storage bulbs and a mercury manometer. This line could be linked via a needle valve to the i.r./adsorption system and/or an i.r. gas cell positioned in the

reference beam of the spectrometer. The gas cell provided compensation for reflection losses from the windows of the adsorption cell and for the gas spectrum should a high gas pressure be used in the adsorption system. It was also used for calibration of the spectrometer using the Q branch of the NO absorption.

The infrared spectrometer used in this work was the Grubb-Parsons GS2A instrument previously described in Section 1.4, Part 1 of this thesis. For adsorption studies this spectrometer has an advantage over many other commercially available instruments in that the infrared beam is brought to a focus in the sample region. By positioning the adsorbent at this external focus, one reduces the possible scattering of radiation by the adsorbent to a minimum.

2.2.2 Materials

The salts used were of analytical grade. Nitric oxide was supplied by the British Oxygen Company, and purified from trace N_2O by fractional sublimation from liquid argon to liquid nitrogen.

2.2.3 Procedure

The tantalum furnace was loaded with the required alkali halide and positioned opposite the central window of the cell. The cell was then assembled and connected to the vacuum line. 24-48 hours of evacuation reduced the pressure in the cell to between 10^{-4} and 10^{-5} mm. Hg at which stage the salt was heated to about $400^{\circ}C$ and held at this temperature for 2 hours to remove traces of water and other volatile

impurities. When this process was complete, liquid nitrogen was slowly introduced into the Dewar so that the central window was cooled gradually to prevent possible cracking. The window cooled to $\sim -170^{\circ}C$. The alkali halide was evaporated by heating the furnace to a temperature at which deposition of the sample could be completed in about one hour. During this time the pressure in the cell was less than 10^{-5} mm.Hg and the temperature of the central window $\sim -160^{\circ}C$ (previous workers report that the alkali halide was condensed onto a window kept at $-196^{\circ}C$). The initial stages of the condensation process could be followed by viewing the interference fringes produced by the film in reflected light, but after about 15 minutes the film became colourless.

With deposition of the film complete the furnace was raised from the path of the infrared beam and the cooling system was connected into the top of the cell. The film was warmed slowly to $-80^{\circ}C$ and finally annealed at this temperature for 12-24 hours before adsorption studies were made.

To record infrared spectra of adsorbed species, the adsorption cell was recooled with liquid nitrogen, detached from the cooling system, and positioned in the sample beam of the spectrometer. After reconnecting the cooling system, the film was brought to the required adsorption temperature and background spectra were recorded. Radiation losses, due to reflection from windows and scattering by the film, reduced the incident energy by only 20-30%, leaving ample energy to obtain good spectra.

The gas under investigation was admitted to the adsorption cell in small doses, a spectrum being recorded after each dose. Having

obtained sufficient data on adsorption, the adsorbate was pumped from the surface in small doses and spectra were measured for desorption.

2.2.4 The properties of the films

The experimental procedure outlined above follows very closely that of Kozirovski and Folman and it is assumed that the films produced in the two studies were very similar. The assumption is supported by the fact that spectra recorded for N_2O adsorbed on NaCl were identical to those published previously[7]. It is unfortunate that the apparatus design is not suitable for the determination of film surface areas. A more direct comparison of the films would then be possible.

Ron and Folman have studied alkali halide surfaces produced under similar conditions in an adsorption cell having a small dead space[8]. They report that the films have specific surface areas of $\sim$ 300 $m.^2/g.$, depending on the particular halide, the rate of condensation, and the total amount of salt used. When the film is heated to a temperature above $-196^{\circ}C$, partial sintering occurs. Warming to $-80^{\circ}C$ results in a 20-30% reduction in surface area and when kept at this temperature sintering continues at a much slower rate. Films kept for weeks at $-80^{\circ}C$ apparently show little change in transparency and surface area[6].

The annealing process increases the stability of the film and markedly reduces the surface heterogeneity. This was inferred from the heats of adsorption of inert gases measured by Ron and Folman. The homogenization plays an important role in determining the shape of spectral bands of the adsorbate, in reducing their width and in giving better resolution.

2.3 PREVIOUS DATA

In this section a brief review will be given of previous work relevant to the understanding of the present data. For convenience the review is divided into three sections, viz.

a) Present knowledge of the alkali halide surfaces

b) Spectra of NO in the gas, solid and adsorbed states

c) Previous data on the NO/alkali halide systems.

2.3.1 The alkali halide surfaces

The most reliable source of information on the nature of these surfaces and the adsorption sites must be the work of Kozirovski and Folman; this being the only significant study of alkali halide films prepared in this manner. Most of their published spectra for small adsorbate molecules show multiplet absorptions shifted from the corresponding gas phase frequencies. The following explanations for the appearance of these multiplets have been considered.

a) The molecules are adsorbed on sites of different energies.

b) The molecules are adsorbed with more than one orientation with respect to the surface.

c) The orientation of the adsorbate is such as to remove degeneracy of vibrational modes, assuming such degeneracy occurs in the gas phase.

In the case of N_2O adsorption on NaX[7] and CsX[9], where X = Cl, Br or I, the first of these explanations was considered the most appropriate.

With a NaCl adsorbent the ν_1 and ν_2 modes of N_2O appeared as doublets shifted downwards from the gas phase frequency. The low frequency component of each doublet appeared first and ceased to grow in intensity from a certain coverage onwards. These bands were attributed to adsorbate on high energy sites of limited number. When these sites eventually become saturated, adsorption continues on sites of lower energy, giving rise to the second adsorption bands. On desorption, the less energetic sites are vacated first causing a disappearance of the high frequency bands of the doublets. The strong ν_3 adsorption and its attendant shoulder showed a parallel behaviour.

The ν_2 mode of N_2O is doubly degenerate in the gas phase and there is the possibility that the doublet absorption arises from the removal of this degeneracy in the adsorbed state. Such an effect would be anticipated if the orientation of the adsorbate is other than perpendicular to the surface. This explanation was discounted since the two components of the doublet did not appear simultaneously, and on desorption the rates of their disappearance were different. It was therefore assumed that the N_2O was adsorbed perpendicular to the surface. With this orientation a large contribution from electrostatic interaction of the quadrupole-surface field type is obtained (the quadrupole moment of N_2O being large, $4{\cdot}4 \times 10^{-26}$ e.s.u.), and the permanent dipole moment of N_2O (0·16D) although not large also adds some contribution to the electrostatic interaction.

Considering the site for this perpendicular adsorption, it was argued that if the total dipole moment of the molecule were to control

its orientation, attachment to the surface Na^+ ion through the oxygen would be preferred over that of nitrogen to Cl^- since in the former the adsorbate is able to approach the surface more closely. If bond moment were the decisive factor the same orientation would be obtained. Adsorption in the centre of the lattice or midway between the anion and cation was not considered since in both cases the field gradient vanishes. It was suggested that Na^+ ions located at the edges act as the more energetic sites, as compared with those located in the faces of the small crystallites. The electrostatic field above such edge-located ions is much larger than above in-plane ions and this may compensate for the lower contribution from dispersion energy. Their fraction must of course depend on the absolute size of the crystallites, and becomes smaller with increasing dimensions of the adsorbent particles. K. and F. claim that there is some evidence that for strongly sintered films (larger crystallites) the intensities of the absorption bands ascribed to molecules located on the edges become smaller. This is said to be even more evident with CO_2 and COS adsorbates[7].

The spectra obtained with a NaBr adsorbent were more complicated. The ν_1 mode gave rise to three absorptions which appeared in sequence with increasing amounts adsorbed, and showed decreasing downward shifts from the gas phase frequency. The intensity of the band at lowest frequency was always very low and was assigned to sites which are few in number but very energetic. As the third ν_1 band increased in intensity, only one band of the ν_2 doublet increased in intensity.

If two of these absorptions are produced by N_2O molecules adsorbed on sodium ions at edges and in (100) planes (as was suggested for NaCl), the third absorption must be assigned to molecules adsorbed with a different orientation or on new sites. Considering the possibility of a different orientation of the N_2O molecule, K. and F. returned to the idea of a perpendicular adsorption above Cl^-. It was argued that the energy of this adsorption would be lower than in the previous two cases because the bond moment of N≡N is lower than that of N=O and the contribution from the dipole-field interaction would therefore be lower. Resulting absorption bands would therefore show a smaller shift from the gas phase frequency than those due to adsorption over Na^+. However this was not observed and the idea was discounted. Kozirovski and Folman then suggested that the band might be due to adsorption on different crystal planes. If planes other than the (100) are exposed, the electric field above the surface planes will be different, giving rise to different interaction energies and spectral shifts. This seems an acceptable explanation. They do however quote work by Schulz[10] as evidence that different surface planes are exposed in NaBr films. Schulz used several techniques, namely, electron and X-ray diffraction, electron microscopy and optical methods to investigate alkali halide films formed by condensation onto a substrate at room temperature. The results indicated that some films showed a preferred crystal orientation e.g. for thick films of NaCl a strongly preferred /110/ orientation

was found, i.e. the individual crystals tended to be orientated with the (110) plane in the plane of the film, the orientation about this preferred direction being random. For thick NaBr films a random orientation was found. No information was obtained concerning the nature of the surface planes.

The published spectra for N_2O adsorption on caesium halides[9] was similar to those previously described for N_2O/NaCl. Three possible explanations were considered. Firstly, although a perpendicular orientation above a cation was thought most likely, it was stated that other orientations of the adsorbate cannot be ruled out if the difference in energy of adsorption for the two orientations is not large and of the order of kT. Secondly, following the interpretations for N_2O/NaX, adsorption at edge and in-plane sites of the caesium halide crystallites was considered plausible. Finally, for the N_2O/CsCl system adsorption in different lattice planes was considered. All the caesium salts crystallise under normal conditions in a body-centred cubic structure, but at high temperatures transitions to face-centred cubic lattices occur. For CsCl this transition occurs at 470°C, while for the other two salts it occurs near their melting points[11]. When the vapours are rapidly condensed on substrates a mixture of small f.c.c. and b.c.c.crystals is obtained. On heating, the films undergo transitions to the more stable b.c.c. form. In the case of CsCl this transition is completed under 120°C, but in the case of CsBr in the region of -150°C. For CsI the transition most probably occurs in the same region[12].

In view of the very great similarity in the spectra reported for CsCl, CsBr and CsI, it seems unreasonable to assign absorption bands of N_2O/CsCl to adsorbate on different crystal planes while using a different explanation for the N_2O/CsBr and N_2O/CsI data, i.e. either one considers that for each halide adsorption occurs at edge and in-plane sites of a single type of crystallite, or that two types of crystallite coexist for each halide at the working temperature, and adsorption occurs on the surface planes of each crystallite type. If two crystallites are present it is surprising that bands due to adsorption at edge sites were not observed in the same manner as for the N_2O/NaX systems (assuming the assignment for the sodium halide systems to be correct).

A similarity in the surfaces of CsCl and CsI films was also indicated by an earlier study of CO_2 adsorption[13]. The ν_2 region of these spectra indicated two orientations of the CO_2. A perpendicular orientation producing a singlet absorption at low coverage, and at higher coverages a parallel orientation of the CO_2 which produced an overlapping doublet absorption as a result of loss of degeneracy of the ν_2 mode. In this work, K. and F. considered two crystal structures to be present for both CsCl and CsI, and assumed one orientation of the adsorbate on each structure. The possibility of adsorption at edge and in-plane sites of a crystal lattice was not considered. Spectra for CO_2 adsorption on NaCl, NaI and CsF (which always crystallises in a simple cubic lattice) indicated a single parallel orientation. No evidence was found for adsorption on sites of differing energies as in the case

of N_2O adsorption, although the reference to CO_2 and COS adsorption made in the later paper on N_2O/NaI suggests that absorption bands due to higher energy sites were observed on weakly sintered films.

In discussing the orientation of the CO_2, K. and F. state the following: "Since the molecule has no permanent dipole but it possesses a substantial quadrupole moment the largest contribution to the energy of adsorption from electrostatic interaction of the quadrupole-surface field would be obtained for a normal to the surface or tilted by an angle of 45° orientation. (Comment: This statement would appear to be based on the work of Hayakawa and is inaccurate - see below). On the other hand, a parallel orientation of the molecule to the surface would give the largest contribution to the energy of adsorption from the dispersion potential. It is believed that the second possibility is the preferred one on a NaCl substrate."

It is surprising that K. and F. did not consider Hayakawa's theoretical treatment of the system. Hayakawa[14] calculated the adsorption potential of a carbon dioxide molecule (and argon and nitrogen) isolated on the (100) faces of various alkali halide crystals. The potential function was composed of a) the van der Waal's (dispersion) potential, b) the electrostatic potential, c) the repulsive potential, and d) the quadrupole potential and the correction due to the potential barrier hindering the turning over of the molecular axis. Four representative positions on the (100) plane were considered, namely,

A. above the centre of a lattice cell

B. above the mid-point of a lattice edge

C. above an alkali ion

D. above a halogen ion.

It was found that at the position of site A or site D the orientation for maximum quadrupole interaction is with the molecular axis parallel to the surface while at positions of type B and C the maximum quadrupole energies are obtained from the orientations in which the molecular axis makes an angle of 45° and 90° with the surface respectively.

From the complete potential functions, Hayakawa obtained values for the isosteric heats of adsorption at zero coverage for each of the four sites and compared them with his experimental results. The data are given in Table 2.1. It can be seen that for the three gases studied the interaction is greatest over Na^{+} with NaCl, but that the interaction is greatest over the centre of a lattice cell for argon and nitrogen on KCl and KBr. For carbon dioxide the greatest interaction always occurs over the alkali metal ion. Hayakawa attributed the difference in sites A and C for argon and nitrogen between NaCl and the others to the small radius and repulsive constants of Na^{+} as compared with K^{+}. The fact that carbon dioxide was predicted to have a maximum interaction always with site C was attributed to the large quadrupole interaction of carbon dioxide with the lattice.

In view of these calculations the parallel orientation of CO_2 on NaCl observed by Kozirovski and Folman is unexpected. There appears to be no straightforward explanation of the discrepancy.

TABLE 2.1

Hayakawa's calculated and experimental heats of adsorption (taken from refs.14,29)

System	$-\Delta H_o$ cals./mole				
	Site A	Site B	Site C	Site D	Experimental
Ar/NaCl	1,875	1,624	<u>1,978</u>	1,510	2,190
N_2/NaCl	1,901	1,532	<u>2,398</u>	1,376	2,670
CO_2/NaCl	3,572	3,181	<u>5,419</u>	2,567	6,070
Ar/KCl	<u>1,898</u>	1,615	1,637	1,473	2,080
N_2/KCl	<u>2,117</u>	1,737	2,010	1,483	3,010
CO_2/KCl	4,148	3,871	<u>4,970</u>	2,806	6,400
Ar/KBr	<u>2,325</u>	1,867	1,854	1,614	2,440
N_2/KBr	<u>2,482</u>	1,954	2,348	1,555	3,280
CO_2/KBr	4,927	4,131	<u>5,298</u>	2,923	6,780

(The site giving the greatest interaction is underlined in each case.)

Kozirovski and Folman computed the adsorption potential for several orientations of CO on the (100) surface plane of NaCl using a similar potential function to that of Hayakawa[15]. The calculated heat of adsorption for perpendicular CO adsorption above Na^+ was 4200 cals./mole giving far better agreement with the experimental value of $\sim$ 4500 cals./mole (determined for a powdered NaCl sample) than any other orientation considered. The shift in vibrational frequency from the gas phase of CO to the adsorbed state with this orientation was calculated by a perturbation method and gave good agreement with experiment. The spectra for CO adsorbed on NaCl, NaBr and NaI all showed a strong band in the region 2152-7 cm^{-1} with a weak shoulder on the high frequency side. The shoulders were ascribed to molecules adsorbed on some energetic sites.

The final studies to be discussed are those of the HCN/NaCl/NaI/CsCl systems[6]. The heats of these adsorptions are considerably greater than those of the systems described so far, the adsorbate not being removed from the surface by prolonged pumping. The experimental heat for HCN adsorption on NaCl at room temperature is about 10-11 kcal./mole[6] and the bonding to the surface is probably best considered as a hydrogen bond. Evidence was found for both perpendicular and parallel orientations on NaCl. This was thought to be reasonably acceptable. The shortest distance between centres of the positive and negative ions in the (100) plane is 2·81Å and the distance between the centres of the H and N atoms in HCN is 2·22Å. The HCN molecule probably lies nearly parallel to the surface with the hydrogen atom above Cl^- and the other end of the

molecule pointing towards the surface Na^+. The maximum possible contribution from dispersion interaction would be obtained from this orientation. On the other hand, since the permanent dipole moment of HCN is 2·94D, a perpendicular orientation above the Cl^- ion (the spectra indicating considerable perturbation of the basically (C-H) stretching ν_3 mode) would give a high contribution to the total energy from dipole-ion and induced-dipole-ion type interactions. The possibility of adsorption above edge-located Cl^- ions was not considered.

A lack of splitting of bands in the spectrum of HCN on NaI suggested only one orientation of the molecule on this surface. In the case of CsCl however, splitting was observed in the ν_3 and ν_1 regions and was attributed to adsorbate on two crystallite structures. Although no structure was observed in the ν_2 region, Kozirovski and Folman were not certain that the parallel orientation was absent. However, it was thought that the larger distance between oppositely charged ions (3·56Å) compared with the NaCl case may not create favourable conditions for such an orientation.

It will be seen from the above that the available data on these alkali halide surfaces is somewhat confusing. The present data for NO must therefore be examined not only to determine the nature of the adsorbed NO but also to explore further the characteristics of these surfaces.

2.3.2 Nitric Oxide

The infrared vibration-rotation spectrum of gaseous nitric oxide is well-known, consisting of P, Q and R branches with the band centre at 1876 cm^{-1} [16,17]. In the condensed phases NO is almost completely dimerised. In an attempt to deduce the structure of this dimer, Smith, Keeler and Johnston[17] recorded infrared and Raman spectra of the liquid and solid and of solutions of NO in liquid krypton and liquid nitrogen. Further condensed phase spectra were recorded by Fateley, Bent and Crawford[18] using a matrix isolation technique. Relevant data from these two studies are given in Table 2.2.

TABLE 2.2

Infrared spectral data for condensed NO(cm^{-1})
taken from ref.17 and 18

Molecule	ref.18		ref.17	
	In NO	In CO_2	In argon	
NO (monomer)	...	1883	1875	1872 (in krypton)
cis-$(NO)_2$ asym.	1768	1768	1776	1770 (liquid NO)
sym.	1862	1862	1866	1865 (liquid NO)
trans-$(NO)_2$ asym.	...	1740	...	...

The band at 1768 cm^{-1} was assigned to an asymmetric stretch in a non-centrosymmetric dimer on the basis of polarisation and Raman data. Similarly the band at 1862 cm^{-1} was assigned to a symmetric stretch. In the relatively rigid CO_2 matrix the small and presumably unstable nitric oxide monomer was isolated and found to have a vibrational frequency of

1883 cm^{-1}. The band observed at 1740 cm^{-1} in the CO_2 matrix study was assigned to the asymmetric stretch of the trans-dimer; this form being clearly less stable than the cis-dimer.

An extensive X-ray crystallographic study of N_2O_2 has been made by Lipscomb and co-workers[19,20]. They conclude that their data clearly favours an equilateral trapezoidal structure in which the N...N distance is about 2·18Å and O...O is 2·62Å. This unusually long distance between the NO groups is consistent with the low value of 3710 cals./mole for the heat of dissociation of the dimer[21].

In 1961 Coulson[22] gave the following molecular orbital description of bonding in nitric oxide; (i) two inner 1s-orbitals exist, one on each atom and which take no part in molecular bonding, (ii) the valence electrons enter the following molecular orbitals, $2s_O^2$, $2s_N^2$, $\sigma 2p_x^2$, $\pi 2p_y^2$, $\pi 2p_z^2$ and $\pi^* 2p_z$. Two electrons in both $\sigma 2p_x$ and $\pi 2p_y$ provide a σ- and a π-bond, while the remaining three electrons constitute a three electron π-bond. Removal of the $\pi^* 2p_z$ antibonding electron results in increased bond strength and vibrational frequency. The nitrosonium ion (NO^+) absorbs at 2300-2200 cm^{-1} in ionic salts[23]. Addition of a further electron to the $\pi^* 2p_z$ orbital reduces bond strength and the vibrational frequency. The nitrosyl ion (NO^-) absorbs at 1100-1000 cm^{-1} [24].

Spectroscopic studies of nitric oxide in the adsorbed state have been confined to adsorption on metals, metal oxides and salts. The spectra were reported by Terenin and Roev in 1959[25]. Several bands were

observed in each case, their assignments varying from an ionic species $- \vert NO^+$ (the vertical line representing the catalyst surface) for the highest frequencies (2000-2100 cm^{-1}) to species with essentially nitrogen-oxygen double-bond character, $- \vert =\overset{+}{N}=O$, $\vert -N=O$ for the lower frequencies (1800-1850 cm^{-1} and 1730-1740 cm^{-1} respectively). Of particular note are two weak bands at 1865 and 1770 cm^{-1} which were observed for NO adsorbed on a ferric oxide gel and assigned to capillary condensed NO dimer.

2.3.3 Studies of NO/Alkali Halide Systems

Three previous studies of this type are known.

In 1936, Tompkins[26] reported an adsorption isotherm for NO on a NaCl powder at -183°C. The shape of this isotherm indicated appreciable attractive forces between the adsorbed molecules, and these were attributed to induced dipoles of opposite sign adjacent on the surface.

More recently (1966) Granville and Hall[27] determined isotherms for NO adsorption on KCl films evaporated onto a substrate kept at 0°C. Since the available data[28] suggested that the quadrupole moments of NO and N_2 were similar, these workers thought it interesting to determine whether a large quadrupole interaction with the surface was present in NO/KCl, as had been observed by Hayakawa for N_2/NaCl and N_2/KCl. The isotherms were determined at -197 , -185 and -160°C and all were concave to the pressure axis, and thus similar to those reported for argon, nitrogen and oxygen on cubic NaCl, and cubic KCl. This contrasted

the convex shape reported by Tompkins for NO/NaCl. The low coverage heat was of the order of 4 kcal./mole, i.e. about 1 kcal./mole higher than the experimental zero-coverage heat for nitrogen on cubic KCl and about 2 kcal./mole higher than that for argon. A comparison between the experimental value for nitric oxide and the calculated heat of 1·9 kcal./mole for argon[29] was made on an approximate basis using intermolecular energy parameters for these adsorbates. With the simplified function

$$\phi = Ar^{-9} - Br^{-6} \qquad (2.1)$$

for the interaction energy between like atoms or molecules and using the equilibrium separation energies of $2{\cdot}71 \times 10^{-14}$ and $1{\cdot}46 \times 10^{-14}$ ergs for NO and argon respectively[30], it is apparent that the heat for nitric oxide, excluding quadrupole interaction should be about 1·8 times that for argon. This factor is largely due to the relatively small size of NO, since the polarisabilities and repulsion constants are about the same. The difference of about 0.8 kcal./mole between the heat of 3·4 kcal./mole estimated on this basis and the experimental value was attributed mainly to surface heterogeneity arising from both surface imperfections and the presence of different crystal faces. Detailed investigations with argon on octahedral KCl and with various non-polar gases on cubic KCl indicate that the heterogeneity effect is generally of this order. It was concluded that the quadrupole interaction term for nitric oxide on KCl is not significant compared with the marked effect shown by nitrogen. No explanation was given, it being suggested that this would require more definite proof of the quadrupole moment of NO and perhaps more detailed

calculations on the lines of Hayakawa. No evidence was found either for dimerisation or for the strong lateral interactions reported with NaCl. In view of Hayakawa's calculations for argon and nitrogen, it was thought that the difference between KCl and NaCl was probably due to the most favourable adsorption sites being respectively above the centre of a lattice square and above a sodium ion.

More extensive work by Granville and Hall investigated the adsorption of nitric oxide and krypton on evaporated films of LiCl, NaCl, KCl and CsCl[31]. A fact of particular importance from this work was that no significant convex curvature to the pressure axis was found for NaCl, or in fact any of these chlorides. Heats of adsorption were again calculated by means of the potential function of equation (2.1) and compared with the experimental data. For both krypton and nitric oxide the experimental heats were close to those calculated for the (100) face of KCl, while the results for CsCl indicated that the films had crystallised more in the (110) form than the (100) form. (CsCl has been found to crystallise from solution as rhombic dodecahedra exposing the (110) face of the b.c.c. structure rather than the (100) face[32].

The calculated heats for both gases on NaCl (100) were about 1·0 kcal./mole lower than the experimental values. However, the fact that the ratio of the experimental heats, $\Delta H(NO)/\Delta H(Kr)$, for NaCl was in good agreement with the ratio of the equilibrium separation energies of NO and krypton, suggested that the discrepancy was not due to the 9:6 potential method being invalid, but was probably due to the

crystallisation of the NaCl adsorbent in some form other than purely (100). Finally it was concluded that the quadrupole moment of nitric oxide is not of sufficient magnitude to have any effect on the heats of adsorption of nitric oxide on NaCl, KCl and CsCl but it does seem to have an appreciable effect where the much smaller cation of LiCl is concerned.

This interpretation of Granville and Hall has been based on the parameters given by Moelwyn-Hughes for the potential function of equation (2.1). Relevant data from this text are given in Table 2.3 It has not been possible to trace the method of calculation of the parameters A and B for NO, but it will be appreciated that if they originate from data for the condensed phases the potential function will represent an average of interactions between the NO molecules in a dimer and interactions between NO molecules in adjacent dimers. This seems quite probable since the parameters A and B for NO are somewhat different to those for O_2 and N_2 and the resultant equilibrium separation r_e for NO (3·58Å) is significantly shorter than the separation for O_2 (4·01Å) and N_2(4·21Å). The heats of adsorption which Granville and Hall have calculated for NO, will therefore have an implicit contribution from dimerisation which might well conceal the effects of quadrupole interaction.

TABLE 2.3

Parameters for the function $\phi = Ar^{-9} - Br^{-6}$ (taken from ref.30)

Molecule	A x 10^{81} (erg-cm^9)	B x 10^{60} (erg-cm^6)	r_e x 10^8 (cm)	$-\phi_e$ x 10^{14} (ergs)
A	6.02	151	3.91	1.41
O_2	7.70	179	4.01	1.44
N_2	9.90	199	4.21	1.19
CO	10.6	217	4.18	1.36
NO	5.23	171	3.58	2.71

2.4 RESULTS

Films of NaCl, NaBr, NaI, KCl, CsCl have been studied. The background spectra of these films showed no absorption bands in the region 2·5 - 25μ immediately after their deposition. However, after annealing at -80°C, a band was always observed in the region 2·9 - 3·0μ, its intensity being dependent on the length of the annealing period. The band arises from traces of water which desorb slowly from the walls of the cell and become adsorbed on the film. There was no way of overcoming this difficulty since the cell could not be evacuated at higher temperatures. Kozirovski and Folman have reported the same effect with their apparatus[6] and from the low intensity of the band they considered the amount of water vapour adsorbed to be very small, only a small fraction of the surface being affected. Nevertheless, it has been the tendency in this work to anneal the films for somewhat shorter periods than K. and F., in order to keep the water coverage as low as possible. Most of the spectra reported here were obtained from films annealed for 10-15 hours as opposed to 24 hours. With this reduction in the annealing period it has of course been necessary to ensure that there is no resultant effect on the surface adsorption sites. K. and F. reported that the rate of annealing is very slow at -80°C. This has been verified by recording spectra for NO adsorbed on films annealed for different periods. For example there was no noticeable difference between the spectrum of NO adsorbed on a KCl film which had been annealed for 3 hours and that for a film annealed for 10 hours or between films of NaBr annealed for 10 and 16 hours. A dependence on the annealing time has only been observed for

a NaI surface. This will be discussed below.

Figure 2.5 shows the water band recorded for a NaCl film annealed for 15 hours. Its frequency of $\sim$ 3400 cm^{-1} is greatly shifted from the gas phase frequency (3756 and 3652 cm^{-1}) indicating a strong perturbation by the surface field. This strength of adsorption was also indicated by the fact that the water was not removed by prolonged pumping of the system at the working temperature. A band of similar intensity was observed for all films excepting those of CsCl for which a strong absorption was always recorded.

The spectra of adsorbed NO are displayed in Figures 2.6 to 2.11. Each figure gives data for a particular surface and is divided into two parts - part a showing a series of spectra recorded at different surface coverages on the adsorption cycle, part b showing similar data for the desorption cycle. Two sets of spectra are included for the NaI surface. The first set (Fig.2.8) was obtained with a NaI film annealed for 10 hours, the second (Fig.2.9) for a film annealed for 18 hours. All spectra were recorded for a central window temperature in the range -145 to 150°C (b.p. of NO -151·8°C). The observed frequencies and their variation with surface coverage are summarised in Table 2.4.

2.4.1 NO/NaCl

Four bands were observed in the absorption spectrum of NO adsorbed on a NaCl surface, and from their intensity variation with surface coverage these are readily divided into two pairs with low-coverage frequencies of 1893, 1809 cm^{-1} and 1860, 1751 cm^{-1}. As more gas was admitted to the

TABLE 2.4

Frequencies observed for the NO/alkali halide systems (cm^{-1})

Surface	ν low coverage		ν high coverage	
NaCl	1893	→	1889	
	1860	→	1863	
	1809	→	1809	
	1751	→	1761	
NaBr	1893	→	1889	
	1857	→	1863	
	1807	→	1807	
	1746	→	1761	
NaI	1889	→	1886	1876 } set A[a]
	1861	→	1861	1852 } set A[a]
	1815	→	1817	1785 } set A[a]
	1757	→	1757	1737 } set A[a]
KCl	1889	→	1883	
	1860	→	1862	
	1790	→	1795	
	1757	→	1757	
CsCl	~1877	→	~1868	
	~1858	→	~1858	
	~1778	→	~1772	
	~1753	→	~1743	

a. see text.

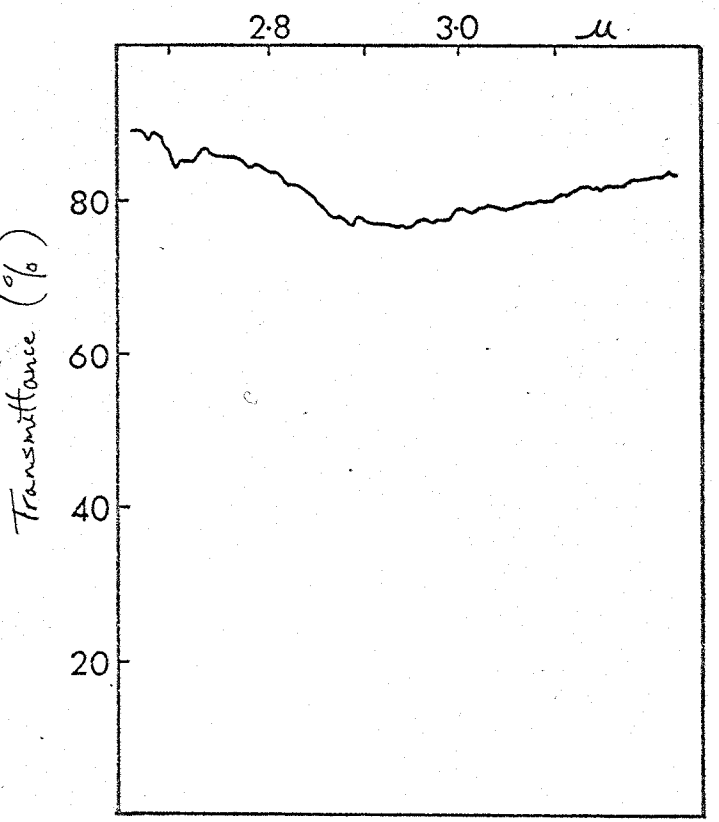

FIG 2·5 I.r. band of water adsorbed on an NaCl film

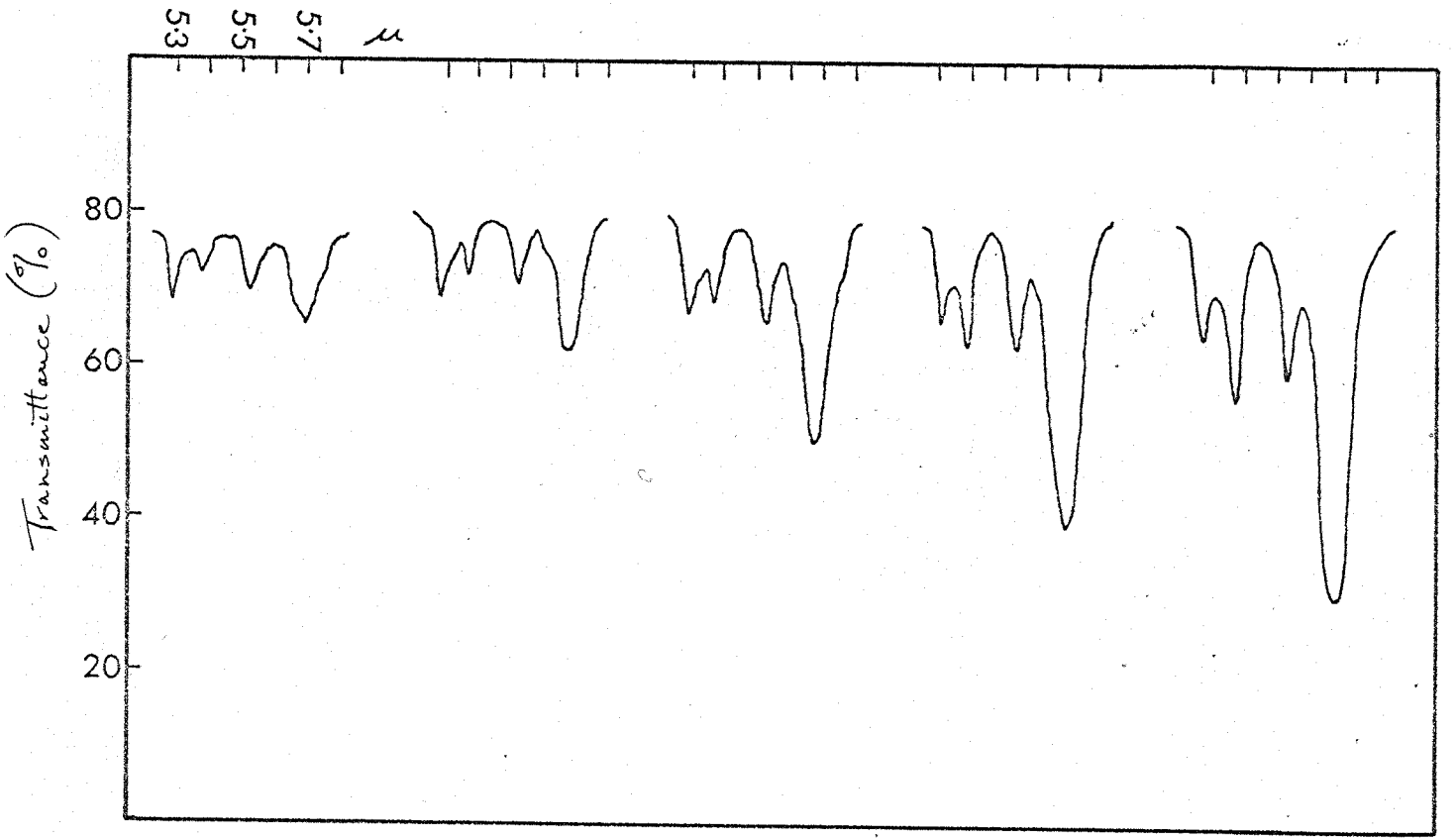

FIG. 2·6a I.r. data for NO adsorption on NaCl

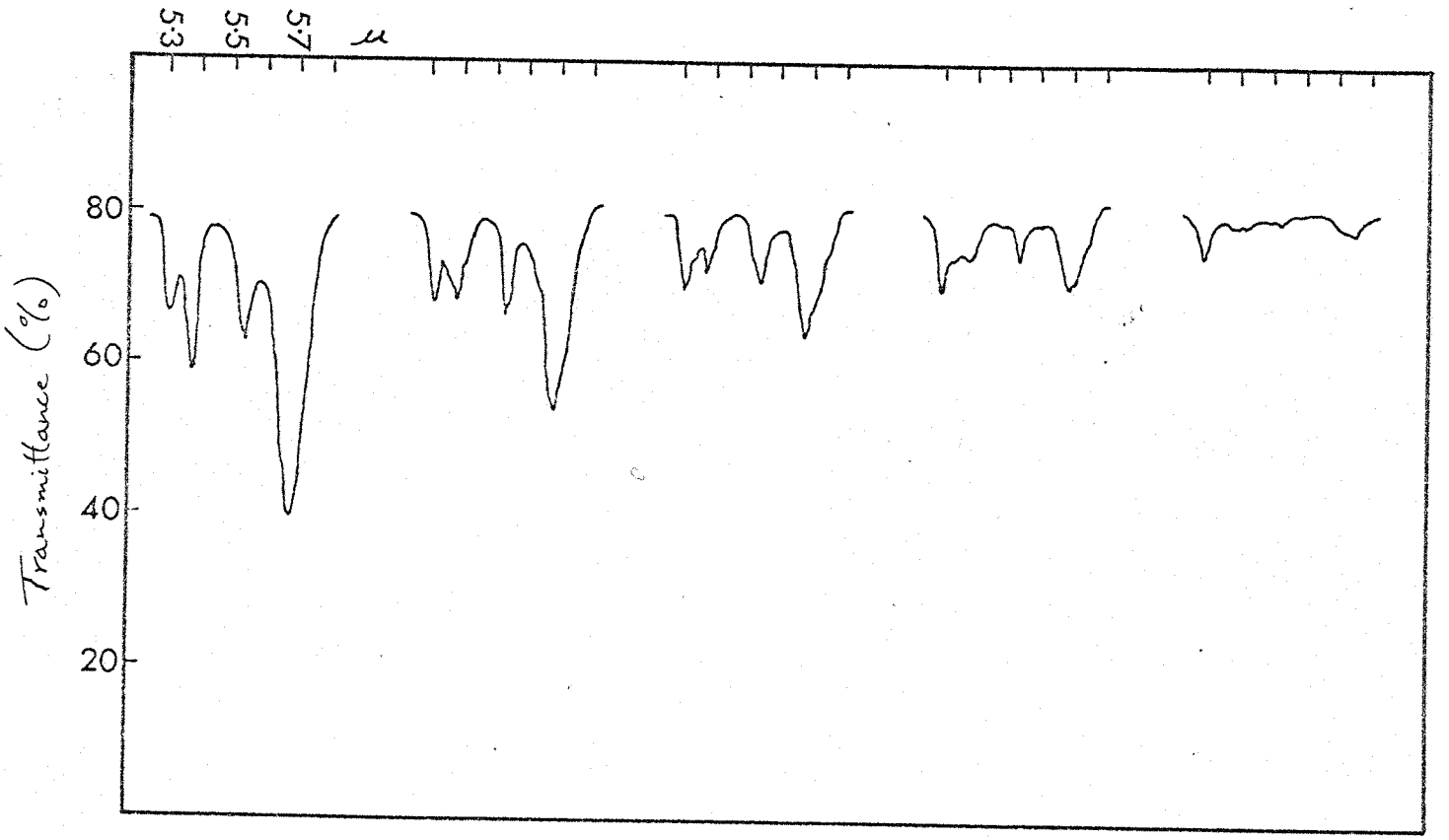

FIG. 2·6b I.r. data for NO desorption from NaCl

surface, all four bands increased in intensity, the rate of increase being greatest for the second pair. Then, from a certain coverage onwards, the first pair of bands ceased to grow, all the intensity increase occurring in the low frequency pair. The band of lowest frequency showed the greatest variation in frequency with surface coverage, shifting from 1751 cm^{-1} to 1761 cm^{-1} at the highest coverage studied. Its partner showed a slight frequency increase to 1863 cm^{-1}, while the 1893 cm^{-1} band decreased to 1889 cm^{-1}. No significant shift was noted for the 1809 cm^{-1} band. On desorption the bands always disappeared in the reverse order of their appearance.

2.4.2 NO/NaBr

The bands recorded for a NaBr film showed a parallel behaviour to that described for NaCl. The low-coverage frequencies being 1893, 1807 cm^{-1} and 1857, 1746 cm^{-1}.

2.4.3 NO/NaI

The data for the NaI surfaces were more complicated. With the film annealed for 18 hours, four bands were observed at 1886, 1815 cm^{-1} and 1861, 1757 cm^{-1} whose behaviour with coverage was again similar to that of the NO/NaCl bands. But, additional shoulders were observed on the low frequency side of the 1861 and 1757 cm^{-1} bands. The frequencies of these shoulders were approximately 1853 and 1735 cm^{-1} and they appeared to stop growing from a certain coverage onwards. More pronounced bands of similar frequencies to these shoulder absorptions were observed on the film annealed for 10 hours, and these also ceased to grow from a certain coverage onwards.

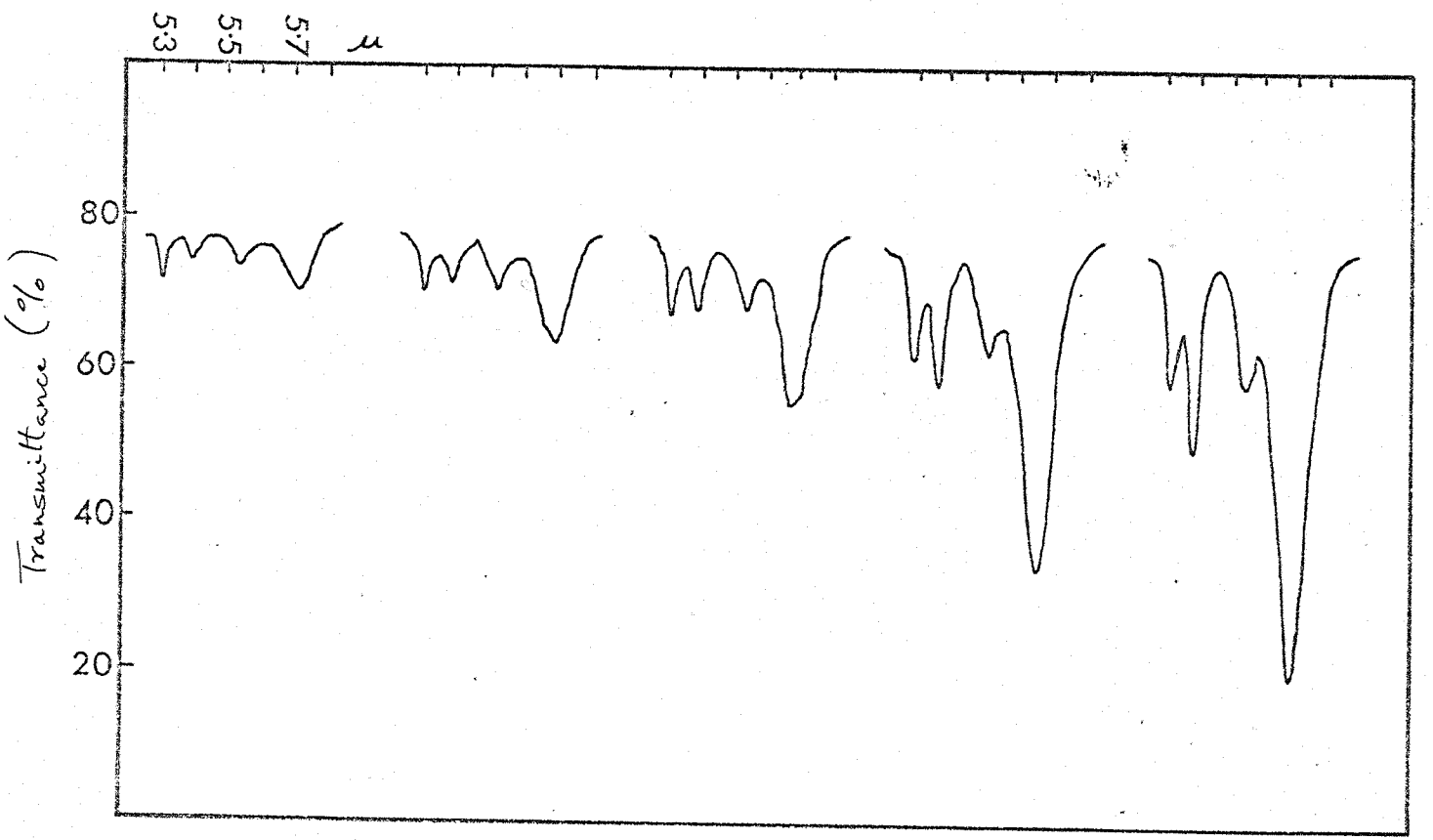

FIG 2·7a I.r. data for NO adsorption on NaBr

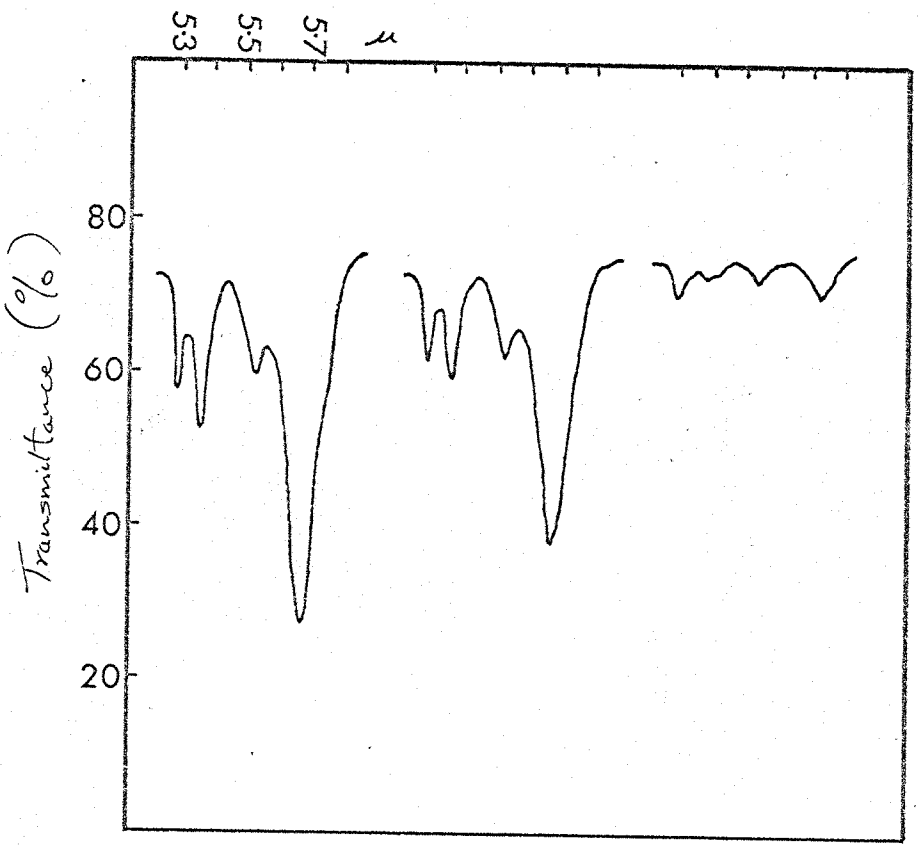

FIG. 2·7.b. I.r. data for NO desorption from NaBr

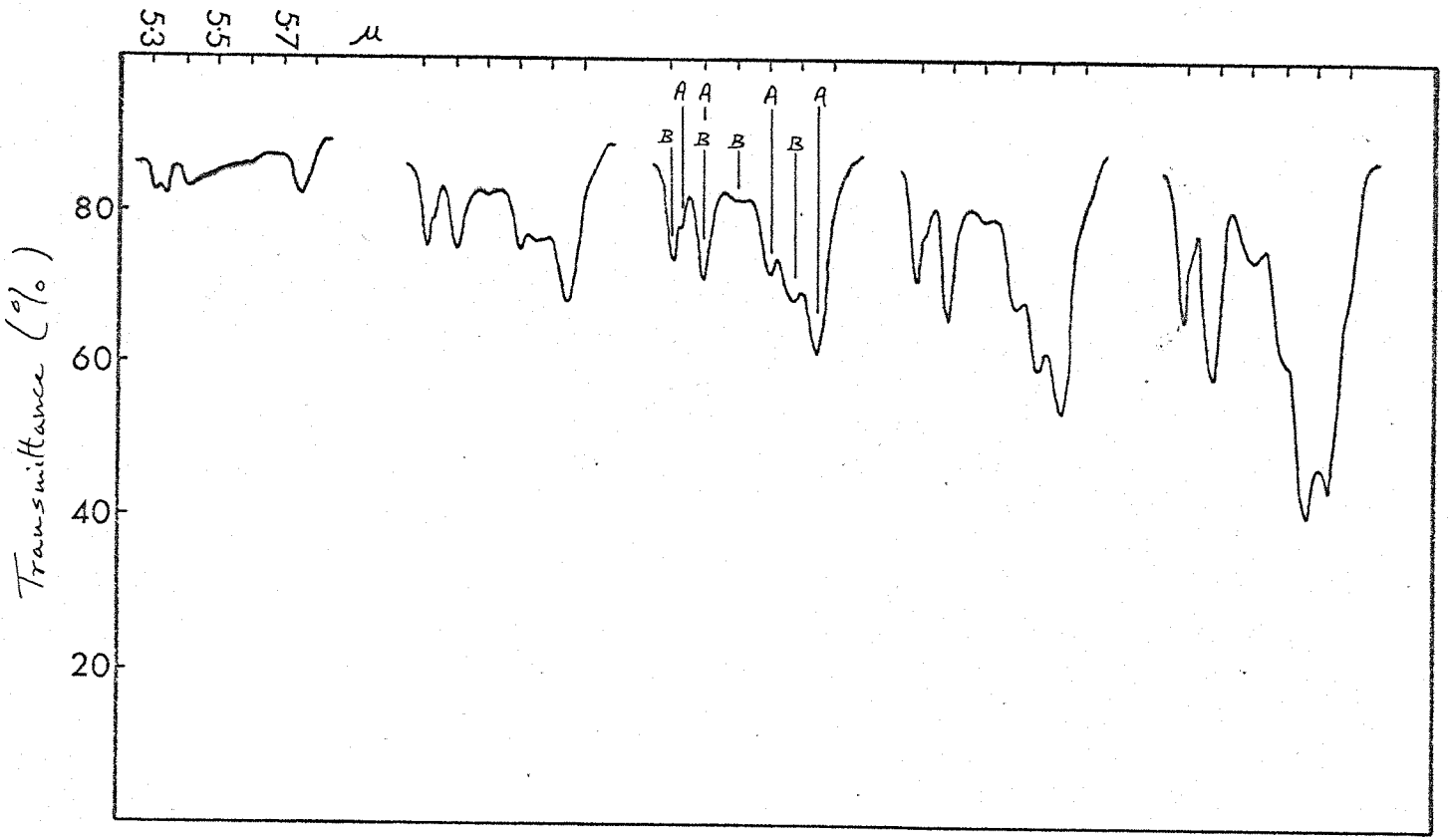

FIG. 2.8a. I.r data for NO adsorption on a NaI film annealed for 10 hours

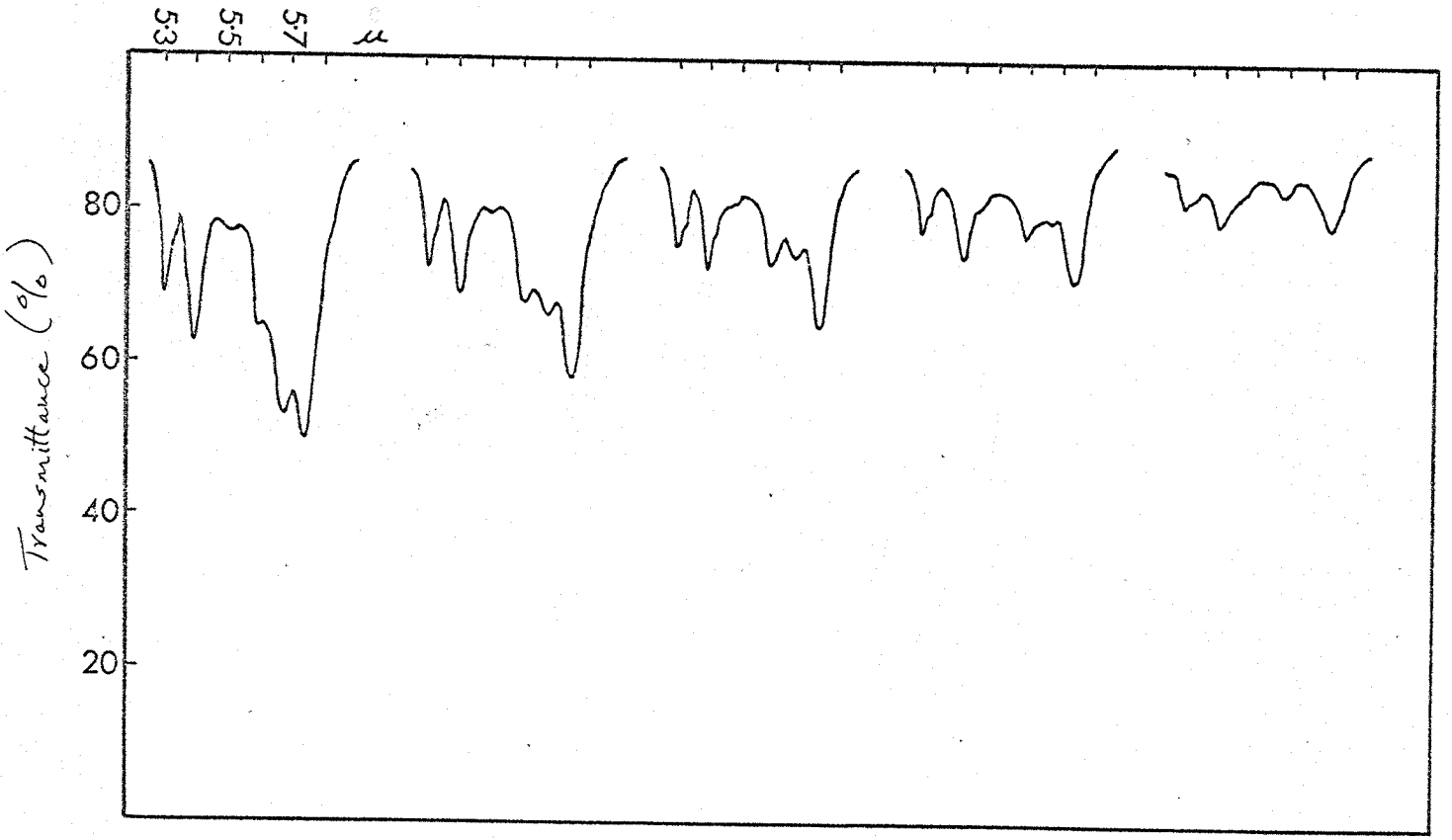

FIG. 2·8b. I·r. data for NO desorption from a NaI film annealed for 10 hours.

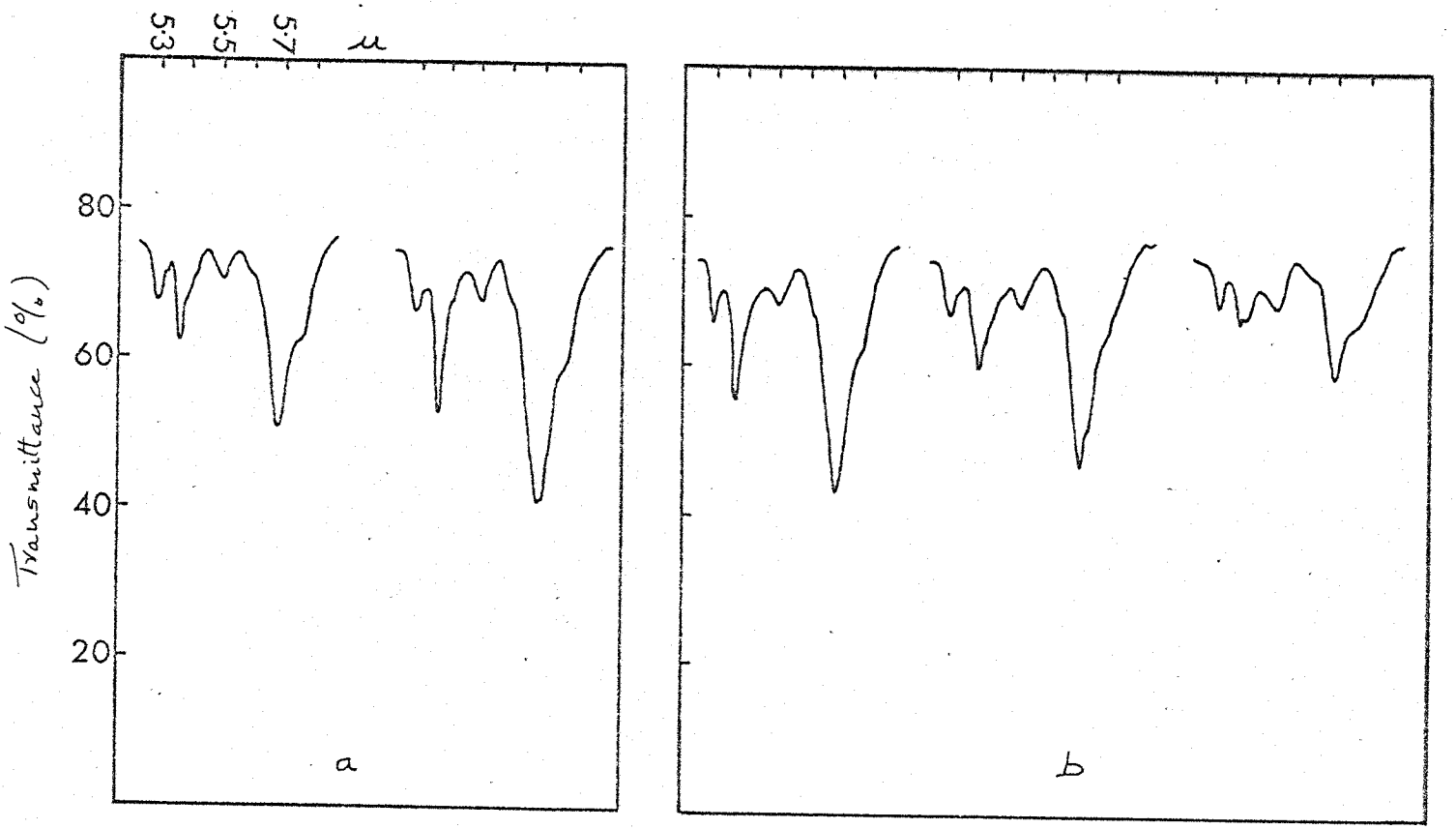

FIG. 2.9 I.r. data for NO adsorbed on a NaI film annealed for 18 hours

a — adsorption cycle b — desorption cycle

This latter film showed additional features of a weak shoulder on the low frequency side of the 1886 cm^{-1} band (frequency $\sim$ 1876 cm^{-1}) which seemed to appear and cease to grow at the same time as a weak absorption at 1785 cm^{-1}.

2.4.4 NO/KCl

The spectra for this system differed slightly from the NO/NaCl data in that only one pair of bands was observed at low coverage (1860, 1757 cm^{-1}); the higher frequency pair only becoming apparent from a certain coverage onwards (1889, 1790 cm^{-1}). The variation in the relative intensities of the four bands resembled that of NO/NaCl, but the band of lowest frequency showed no frequency shift with increasing coverage.

2.4.5 NO/CsCl

The overlapping of bands in the spectra of this system has made it difficult to study variations in intensity with coverage. There appeared to be at least four absorptions at $\sim$ 1873, $\sim$ 1861, $\sim$ 1776, and $\sim$ 1749 cm^{-1}, and there was a weak indication of a fifth absorption $\sim$ 1765 cm^{-1}.

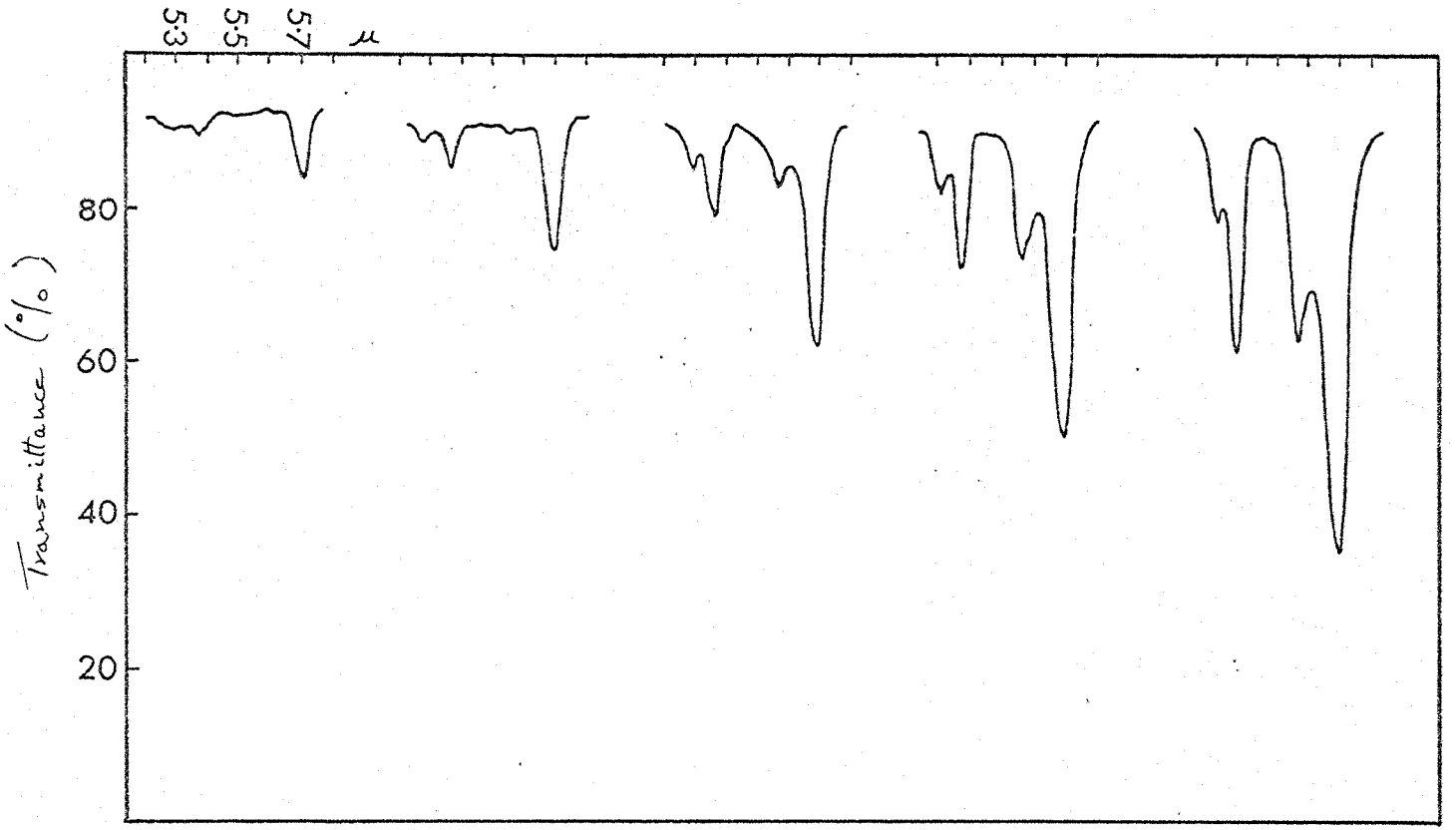

FIG. 2·10a. I.r. data for NO adsorption on KCl

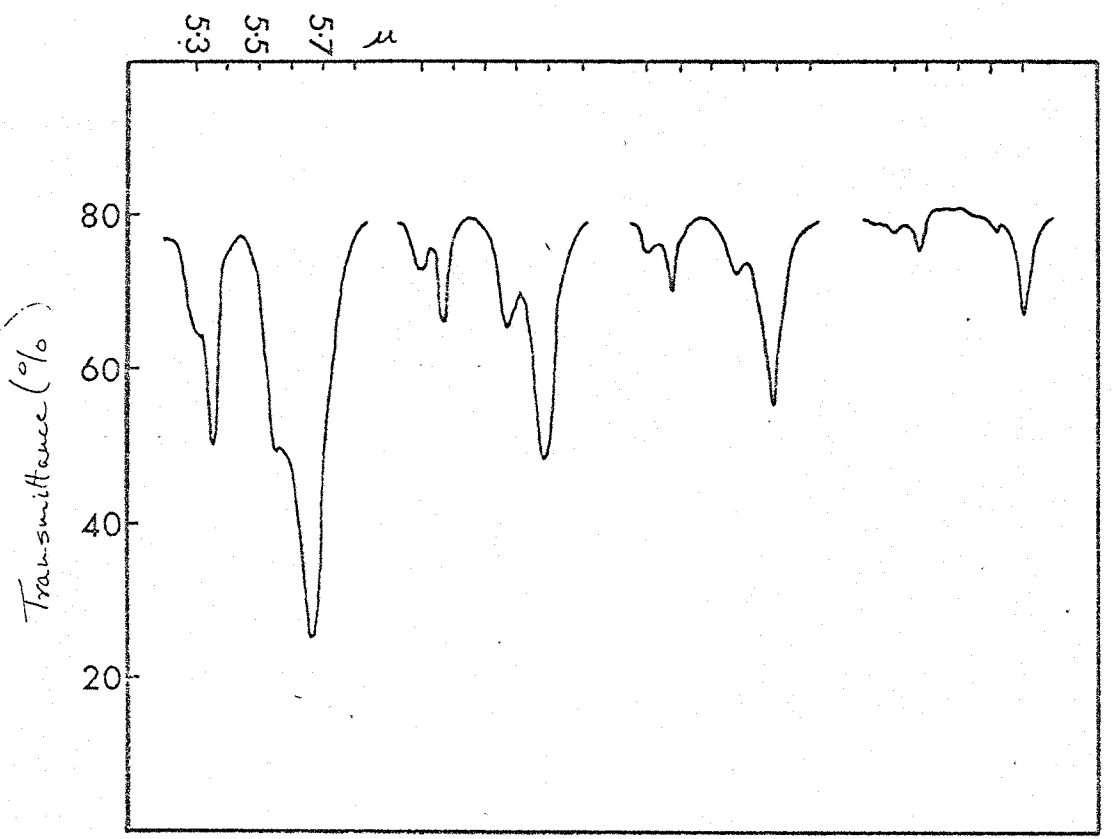

FIG 2·10 b. I.r. data for NO desorption from KCl

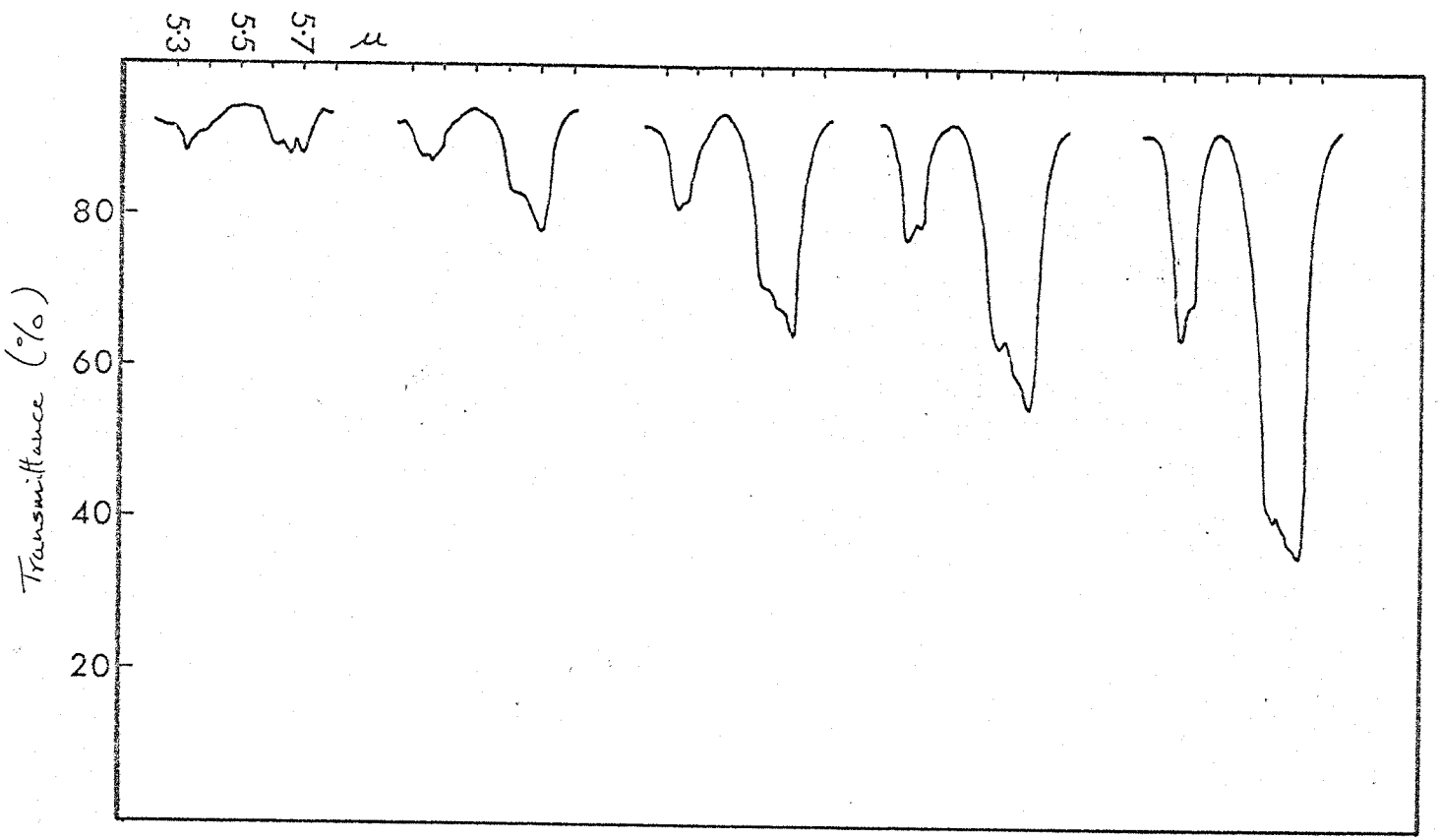

FIG. 2·11a. Ir data for NO adsorption on CsCl

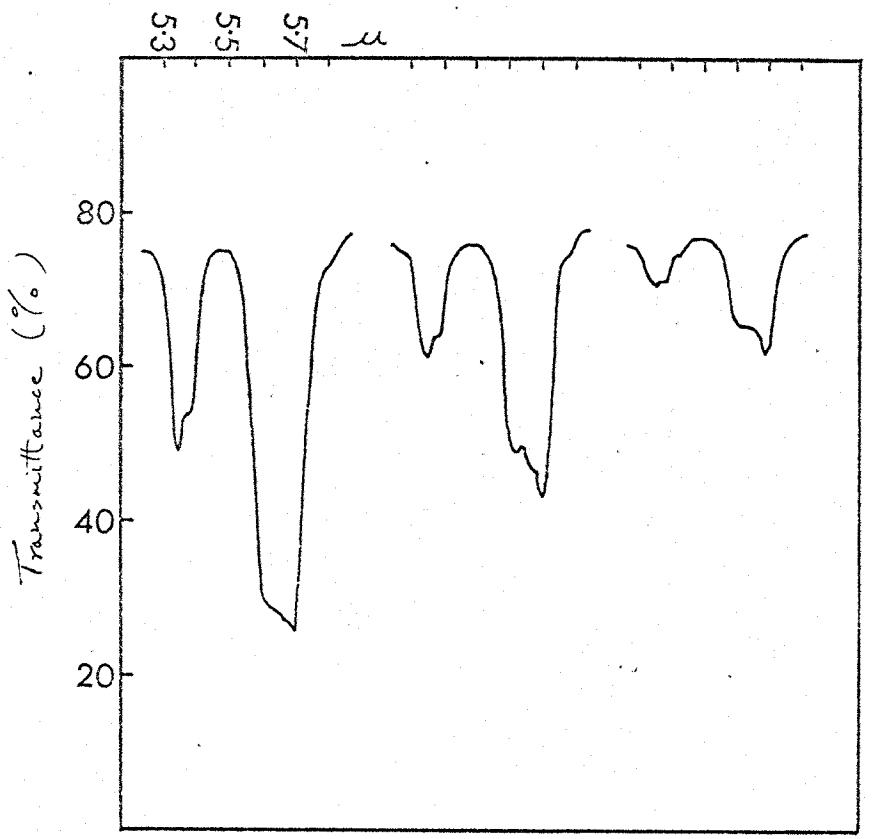

FIG. 11b. I.r. data for NO desorption from CsCl

2.5 DISCUSSION

It has been mentioned previously that the i.r./adsorption system is inadequate in two important respects. Firstly, it was not possible to degas the metal of the system at high temperature and thereby considerably reduce the problem of water adsorption on the films. Secondly, no suitable method was available for determining the surface area of the films; the extent of the water coverage; or the extent of the nitric oxide coverage. The following interpretation of the spectral data is therefore made bearing in mind the possibility that the spectra might arise, in part, from a) NO adsorbed on sites adjacent to adsorbed water; b) NO adsorbed on pre-adsorbed water; and at higher coverages; c) NO adsorbed above a monolayer.

2.5.1 Adsorption on Sodium Salts

The following conclusions seem acceptable from the data for the NaCl surfaces.

For the 1893 and 1809 cm^{-1} absorptions:

a) The sites producing the absorptions are limited in number. This is inferred from the fact that the absorptions ceased to grow in intensity from a certain coverage onwards.

b) Each band arises from a nitric oxide monomer adsorbed on a particular type of site.

The two frequencies bear no resemblance to those previously reported for dimeric $(NO)_2$ while the 1893 cm^{-1} frequency is similar to

that observed for the nitric oxide monomer isolated in a CO_2 matrix.

c) Some relationship between the two sites is suggested by the similar intensity variations of the two bands with surface coverage.

d) There is little energetic heterogeneity amongst sites of the same type. This is indicated by the fact that the absorption bands are sharp and show little variation in frequency with surface coverage.

For the 1860 and 1751 cm^{-1} absorptions:

a) The bands arise from the symmetric and asymmetric stretching modes of a cis-dimeric species at the surface. This is inferred from the fact that the intensities of the bands increase at a similar rate with increasing coverage, and their frequencies resemble closely those reported for the condensed phases.

b) A certain degree of energetic heterogeneity of the surface sites involved would seem to be indicated by the shift in frequency of the bands with coverage, although there is the possibility that at the later stages in the adsorption cycle the bands might arise from cis-dimeric NO adsorbed above a monolayer. It is thought unlikely that all the intensity in the dimer bands may be assigned in this manner.

The above two sets of evidence point to an assignment of bands to adsorption on sites located at the edges and in the surface planes of the edges and in the surface planes of the crystallites, as was previously suggested for the N_2O/NaX systems. Schulz[10] observed crystallites of $\sim 50\text{Å}$ on an edge in films condensed onto a substrate at room temperature. The ratio of in-plane to edge sites for a crystallite

of this size is about 8:1, which would account for the relative intensities of the absorption bands at the higher coverages studied. If the 1893 and 1809 cm^{-1} absorptions do arise from NO adsorbed at crystallite edges, the NO must in one case be associated with the cation and in the other case with the anion. Adsorption in this manner would explain the limited number of sites; their lack of energetic heterogeneity; and also the similar intensity variation of the absorption bands with coverage.

The 1893 cm^{-1} absorption was the only band to show an upward shift from the gas phase frequency of 1876 cm^{-1}. At low coverage the shift was 17 cm^{-1}. Such a shift must be the result of a partial reduction in electron density in the 3-electron π bond. This can only be the result of the NO molecule being closely associated with a Na^{+} ion. Since the frequency is very high and shows only a very slight shift with a change in anion for Cl^{-} to I^{-}, a perpendicular orientation above the sodium ion seems probable. With such an orientation a maximum contribution to the electrostatic potential is obtained from interaction of the NO quadrupole with the surface field (see section 2.3.1) and also from interaction of the dipole with the surface field, although the dipole moment of NO is small (0·16D[33]).

The absorption band at 1809 cm^{-1} is shifted downwards by 67 cm^{-1} from the gas phase frequency. The shift is indicative of an increase in electron density in the π -system of NO on adsorption and suggests that in this case the molecule is associated with the anion. A slight increase

in frequency was observed for a change in anion from Cl^- to I^- while a somewhat greater shift was noted for the change NaCl to KCl. This indicates the probability of a non-perpendicular edge adsorption with the nitrogen atom almost above the anion and the oxygen directed towards the cation.

The fact that a dimer is not formed at the edge sites suggests that on the surface plane the dimer is probably formed by the adsorption of NO molecules on adjacent sites of the same type. This necessitates the two components of the dimer being aligned in a parallel manner, as observed in the solid state. With this information and a knowledge of the dimensions of the solid-state dimer, the possible adsorption sites can be considered.

a) A parallel orientation above anion or cation. Adjacent adsorption in this manner would not be favourable to dimerisation since the separation of similar ions in NaCl is 3·97Å and the solid-state dimer has dimensions

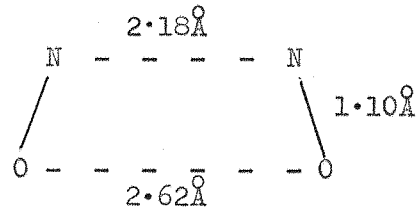

b) Adsorption above the mid-point of a lattice edge. Dimerisation would not be expected to occur from adjacent adsorption on these sites since the site separation is 2·81Å and the adjacent adsorbate molecules would not be parallel.

c) Perpendicular adsorption above adjacent cations. Although the separation of these sites is 3·97Å, a slight deviation from perpendicularity would allow formation of a dimer with similar dimensions to the solid state dimer

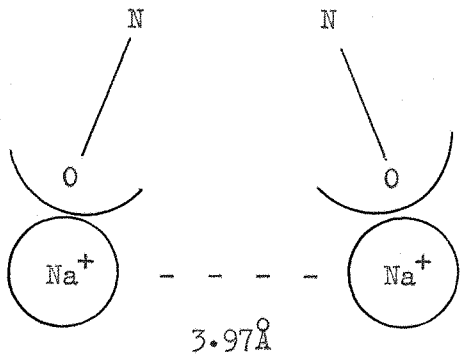

If quadrupole interaction with the surface is large, this is the most favourable site for adsorption even in the absence of dimerisation. The reduction in electron density in the π system of NO resulting from adsorption above the cation might well prevent dimerisation however, or should at least cause the vibrational frequencies to be significantly different from those of the solid state dimer. This was not observed. Furthermore, although the cation-cation separation is perhaps theoretically suitable in the case of NaCl, the separation in NaBr (4·33Å) and NaI (4·47Å) would be expected to be too great to allow dimerisation by this means. Dimer has been observed on these surfaces.

d) A perpendicular adsorption above the centre of the lattice square. Since the field gradient perpendicular to this site is zero, there can be nc

quadrupole interaction with the surface. In the absence of dimerisation, therefore, only dispersion interactions can contribute to the energy of adsorption. However, if dimerisation can accompany the adsorption, the sites may be stabilised to the extent that they become the most favourable in the surface plane. The separation of such sites for all the surfaces studied would appear suitable for dimerisation and the vibrational frequencies should be similar to those of the solid state dimer. The site is probably not in fact exactly above the lattice square centre but displaced towards the Na^+ ion. Some interaction between adjacent dimers might therefore be anticipated at higher coverages, and this could account for the quite large shift in the frequency of the asymmetric stretching mode with coverage, although the shift could equally well be the result of energetic heterogeneity of the surface sites.

It is difficult to draw definite conclusions about the relative energies of the adsorption sites. In view of the relative numbers of edge and in-plane sites the fact that all four absorptions appear at the same time suggests that the edge sites are the most energetic. However this argument assumes that the extinction coefficients of the various absorptions are not significantly different. A higher energy for the edge sites is also suggested by the fact that these sites are quickly saturated and that the dimer is removed most rapidly in the early stages of desorption. A knowledge of the surface coverage is necessary to confirm this argument.

Finally, it must be noted that there is no evidence to suggest that more than one crystal plane is exposed at the film surface.

The data for NaBr are almost identical to those described above and the absorptions are assigned in a similar manner, i.e. the bands with low coverage frequencies of 1893 and 1807 cm^{-1} are attributed to anion and cation sites located at crystallite edges and the 1857, 1746 cm^{-1} bands to dimeric adsorption approximately above the centres of adjacent lattice squares. Although K. and F.'s data for N_2O/NaBr indicated that more than one crystal plane might be exposed at the surface of NaBr films, no evidence for this has been found in the present study.

Having interpreted the data for NaCl and NaBr, it is now possible to attempt an assignment of the more complicated NO/NaI data.

The dependence of the NO/NaI spectra on the annealing time is believed to be due to the size of the anion. Measurements of the dielectric properties of alkali halide films[34] have shown pronounced aging effects which were attributed to high defect concentrations. The annealing rate was found to be dependent on the anion mobility, which is highest for a small anion and/or large cation and vice versa.

Eight absorptions were distinguished in the spectra of NO adsorbed on the NaI film annealed for 10 hours. These could be divided into two sets of four bands, each set behaving in an analogous way to the four bands described for NO/NaCl and NO/NaBr. The sets are labelled A and B in Figure 2.8. At the lowest coverage studied only the bands

of set A and the high frequency band of set B were observed. As the coverage was increased, the A bands quickly ceased to grow in intensity while the B bands increased continuously. From the relative intensities of the bands they may be further split into pairs in the manner used for NaCl and NaBr. The approximate frequencies of the bands are: for set A, 1876, 1785 cm^{-1} and 1852, 1737 cm^{-1}; for set B, 1888, 1814 cm^{-1} and 1852, 1761 cm^{-1}. The absorption at $\sim$ 1852 cm^{-1} was clearly due to two overlapping bands at the higher coverages. The spectra recorded for the NaI film annealed for 18 hours resembled the NaCl data. Two pairs of bands were observed at 1886, 1815 cm^{-1} and 1861, 1757 cm^{-1} corresponding to set B of the 10 hour film. The strong bands of set A were observed as weak shoulders at approximately 1852 and 1737 cm^{-1} on the low frequency sides of the strong bands of set B.

In view of these observations, it is concluded that two crystal forms were present in the NaI films. Firstly, a somewhat unstable high energy form whose concentration decreased with the time of annealing. Adsorption on crystallites of this form occurred at edge sites giving rise to absorptions at $\sim$ 1876 and $\sim$ 1785 cm^{-1}, and surface sites giving absorptions at $\sim$ 1852 and 1737 cm^{-1} (set A). Secondly, a more stable form (presumably (100)) possessing similar sites to the NaCl crystallites, i.e. cation and anion edge sites giving 1888 and 1814 cm^{-1} absorptions and sites at the centre of lattice squares on which dimeric adsorption occurs producing bands at 1852 and 1761 cm^{-1}. The differences in the observed frequencies for the two forms are attributed to the different arrangement

of ions in the surface and underlying planes. This different arrangement could mean that the adsorption sites are somewhat different for the high energy form. The similarity between the 1737 cm^{-1} frequency and the frequency observed for the asymmetric stretching mode of the trans-dimer isolated in a CO_2 matrix might suggest a similar assignment for the surface species. A cis-dimer is considered more likely.

This analysis of NO/NaI gives support to K. and F.'s study of N_2O adsorption on NaI in which bands were assigned to adsorption on a second surface plane. In that and the present study the concentration of this second crystal form in strongly sintered films was not sufficient to allow observation of bands due to adsorption at the edges of these crystallites.

2.5.2 Adsorption on Potassium Chloride

The four bands observed for NO/KCl are assigned in the same manner as for NO/NaCl. The bands due to the dimer (1860, 1757 cm^{-1}) are observed from the lowest coverage, but the edge adsorptions (1889, 1790 cm^{-1}) only become apparent from a certain coverage onwards. There appear to be two acceptable reasons for this behaviour. Firstly, the extent of the annealing may be somewhat greater in KCl due to the somewhat larger cation. This being so, the crystallites would be larger than those in the sodium halide films and as a result the ratio of edge sites to in-plane sites would be smaller. Providing that the two types of site are not too dissimilar in energy, this would explain the order of appearance and also the relative intensities of the two pairs of bands.

More extensive annealing might also be expected to result in less energetic heterogeneity amongst the in-plane sites. This could account for the lack of frequency shift in the dimer bands with increasing coverage.

The second possible explanation is that the heat of adsorption of NO on sites in the surface plane of KCl is somewhat greater than that for adsorption at edge sites, and the in-plane sites are therefore occupied preferentially. The calculations of Hayakawa for the N_2/NaCl and N_2/KCl systems have shown that on the (100) surface planes the most favourable mode of adsorption changes from a perpendicular adsorption above the cation for NaCl to a parallel adsorption above the centre of the lattice square for KCl. This is partly due to a decrease in the energy of interaction with the cation from Na^+ to K^+ and partly to an increase in quadrupole interaction for the parallel orientation on going from NaCl to KCl. In the case of a near perpendicular orientation of NO above the centre of a lattice square only the former effect is applicable, but this would act to stabilise the dimeric in-plane adsorption with respect to perpendicular adsorption on edge located cation. The correct explanation is probably a combination of these two effects.

2.5.3 Adsorption on Caesium Chloride

Two regions of absorption were found in the spectra for NO/CsCl; one from 1850 to 1880 cm^{-1} and the other from 1740 to 1780 cm^{-1}. At the higher coverages studied the high frequency region appeared to be composed of two overlapping bands having approximate frequencies of

1868 and 1858 cm^{-1}, while the second region comprised two overlapping bands at $\sim$ 1774 and $\sim$ 1746 cm^{-1}. In view of the above assignments for the other alkali halide surfaces one might consider an assignment of the $\sim$ 1868, $\sim$ 1774 cm^{-1} absorptions to NO adsorbed at the edges of the CsCl crystallites and the $\sim$ 1858, $\sim$ 1746 cm^{-1} bands to adsorption on the crystallite surface planes. Such an assignment is considered unsatisfactory for the following reasons. Firstly, the intensities of the two pairs of bands appear to be somewhat similar. This would not be expected for adsorption at edge and in-plane sites. Secondly, all four frequencies are shifted down from the NO gas phase frequency, whereas if the higher frequency pair were due to edge adsorptions one of the bands would be expected to show an upward shift as a result of association with the cation. Thirdly, both pairs of frequencies resemble to some extent those reported for the cis-dimer in the solid state.

Previous i.r. studies of adsorption on these films have considered the possibility that spectra arise from adsorption on two different crystal faces. The available data (see Section 2.3.1) indicate that films of CsCl produced in this manner are almost certainly a mixture of b.c.c. crystallites exposing the (110) face and f.c.c. crystallites exposing the (100) face. It seems reasonable therefore to assign one of these pairs of bands to adsorption as a dimer on one crystallite surface, and the other pair to a similar dimeric adsorption on the surface of crystallites of the second type; the difference in frequencies being attributed to the different arrangement of ions in the surface and

underlying planes. However, since the absorption due to adsorbed water was of high intensity for all the CsCl films studied, this assignment must be tentative, since there is the very real possibility that one of the dimers at least may be closely associated with adsorbed water. The similarity of the $\sim$1858, $\sim$ 1746 cm^{-1} frequencies with those observed for the sodium halides and potassium chloride suggests that they are probably associated with the f.c.c. structure.

If the above assignment is correct, one might expect to observe edge adsorptions on the two crystallite structures. At the lowest coverage studied there is some slight evidence for a third absorption at about 1767 cm^{-1} in the lower frequency region and the initial absorption at 1877 cm^{-1} in the high frequency region might be due to an edge adsorption. It seems likely, however, that either the crystallites are too large to allow detection of NO adsorbed on these sites, or the water coverage at the edge sites reduces the number of NO/edge adsorptions below the detectable level. The fact that bands due to edge sites have not been observed in previous i.r. studies of adsorption on CsCl (assuming the assignment to coexisting crystallites to be the correct one), supports the idea of relatively large crystallites in these films. This is considered to be due to the influence of the large cation producing more extensive annealing compared to the NaX and KCl films.

2.6 CONCLUSIONS

The present infrared spectroscopic study of nitric oxide adsorption on high surface area alkali halide films (prepared by condensation on a surface at -196°C and sintering at -80°C) has found evidence that a dimeric species is formed at these surfaces. This contradicts a previous interpretation of isotherms measured for NO adsorption on similar films deposited on a substrate at 0°C[31]. The dimer has the cis-configuration and is believed to be formed by the adsorption of NO molecules at the centres of adjacent lattice squares.

Further bands in the spectra of NO adsorbed on NaCl, NaBr, NaI and KCl have been attributed to two types of monomeric adsorption at the edges of the small crystallites present in the films. One is thought to be a perpendicular adsorption through oxygen above an edge-located cation; the other, an orientation with the nitrogen atom almost above an edge-located anion and the oxygen atom directed towards the cation.

The spectra provide support for the surface structures suggested by previous spectroscopic investigations. Two types of crystallite were thought to exist in CsCl films, one a b.c.c. structure exposing (110) faces and the other a f.c.c. structure exposing (100) faces. The spectra of adsorbed NO indicate two dimeric species and one is assigned to each surface plane. Evidence has again been found for a single crystallite type in NaCl films and two crystallite types in NaI films (one being

somewhat unstable at -80°C) but contrary to the previous study of N_2O/NaBr only one crystallite was apparent in NaBr films.

Finally, there are indications that the extent of annealing in the films (and hence the crystallite size) is dependent on the size of the anion and cation; being greatest for a large cation and/or a small anion, and vice versa. This is suggested by the intensities of bands attributed to edge adsorptions.

REFERENCES : PART 2

1. G.B.B.M. Sutherland and W. Tutte, Nature, 144, 707 (1939).
2. L.H. Little, Infrared Spectra of Adsorbed Species, Academic Press, London (1966).
3. M.L. Hair, Infrared Spectroscopy in Surface Chemistry, Marcel Dekker Inc., New York (1967).
4. D.J.C. Yates, Trans.Brit.Ceram.Soc., 54, 272.
5. Y. Kozirovski and M. Folman, J.Chem.Phys., 41, 1509 (1964).
6. Y. Kozirovski and M. Folman, Trans.Farad.Soc., 62, 808 (1966).
7. Y. Kozirovski and M. Folman, ibid., 65, 244 (1969).
8. I. Ron and M. Folman, Israel J.Chem., 3, 18 (1965).
9. Y. Kozirovski and M. Folman, ibid., 7, 595 (1969).
10. L.G. Schulz, J.Chem.Phys., 17, 1153 (1949).
11. J.W. Johnson, P.A. Argon and M.A. Bredig, J.Am.Chem.Soc., 77, 2734 (1955).
12. M. Blackman and I.H. Khan, Proc.Phys.Soc. (London), 77, 471 (1961).
13. Y. Kozirovski and M. Folman, Trans.Farad.Soc., 62, 1431 (1966).
14. T. Hayakawa, Bull.Chem.Soc. Japan, 30, 236 (1957).
15. Y. Kozirovski and M. Folman, Trans.Farad.Soc., 65, 2206 (1969).
16. Nielsen and Gordy, Phys.Rev., 56, 781 (1939).
17. A. Lee Smith, W.E. Keeler and H.L. Johnston, J.Chem.Phys., 19, 189 (1951).
18. W.G. Fateley, H.A. Bent and Bryce Crawford Jr., J.Chem.Phys., 31, 204 (1959).
19. W.J. Dulmage, E.A. Meyers and W.N. Lipscomb, Acta.Cryst., 6, 760 (1953).
20. W.J. Dulmage et al., Acta Cryst., 14, 1100 (1961).

21. A. Lee Smith and H.L. Johnston, J.Am.Chem.Soc., 74, 4696 (1952).

22. C.A. Coulson, "Valence" 2nd Ed., p.222, 159, Oxford University Press, London (1961).

23. D.J. Millen and D. Watson, J.Chem.Soc., 1369 (1957).

24. W.P. Griffith, J. Lewis and G. Wilkinson, J.Inorg.Nuc.Chem., 7, 38 (1958).

25. A.N. Terenin and L.M. Roev, Spectrochim.Acta 15, 274, 946 (1959).

26. F.C. Tompkins, Trans.Farad.Soc., 32, 643 (1936).

27. A. Granville and P.G. Hall, J.Phys.Chem., 70, 937 (1966).

28. R.M. Hill and W.V. Smith, Phys.Rev., 82, 451 (1951).

29. T. Hayakawa, Bull.Chem.Soc. Japan, 30, 332 (1957).

30. E.A. Moelwyn-Hughes, "Physical Chemistry", Pergamon Press Ltd., London, 335 (1961).

31. A. Granville and P.G. Hall, Trans.Farad.Soc., 63, 701 (1967).

32. F.C. Tompkins and D.M. Young, Trans.Farad.Soc., 47, 77 (1951).

33. Watson, Rao and Ramanswamy, Proc.Roy.Soc.A., 143, 558.

34. C. Weaver and S. Lorenzoni, J.Vac.Sci.Tech., 6, 597 (1969).